

**P1 ParB: The Structural and Functional Domains of the P1 Plasmid
Centromere-Binding Protein**

Jennifer A. Surtees

Thesis submitted in conformity with the requirements
for the Degree of Doctor of Philosophy,
Graduate Department of Molecular and Medical Genetics
in the University of Toronto.

© by Jennifer Anne Surtees 2001



National Library
of Canada

Acquisitions and
Bibliographic Services

395 Wellington Street
Ottawa ON K1A 0N4
Canada

Bibliothèque nationale
du Canada

Acquisitions et
services bibliographiques

395, rue Wellington
Ottawa ON K1A 0N4
Canada

Your file Votre référence

Our file Notre référence

The author has granted a non-exclusive licence allowing the National Library of Canada to reproduce, loan, distribute or sell copies of this thesis in microform, paper or electronic formats.

The author retains ownership of the copyright in this thesis. Neither the thesis nor substantial extracts from it may be printed or otherwise reproduced without the author's permission.

L'auteur a accordé une licence non exclusive permettant à la Bibliothèque nationale du Canada de reproduire, prêter, distribuer ou vendre des copies de cette thèse sous la forme de microfiche/film, de reproduction sur papier ou sur format électronique.

L'auteur conserve la propriété du droit d'auteur qui protège cette thèse. Ni la thèse ni des extraits substantiels de celle-ci ne doivent être imprimés ou autrement reproduits sans son autorisation.

0-612-59026-7

Canada

P1 ParB: The structural and functional domains of the P1 plasmid centromere-binding protein.

Doctor of Philosophy, 2001

Jennifer Anne Surtees

Department of Molecular and Medical Genetics, University of Toronto

The P1 prophage plasmid is stably maintained as a unit-copy plasmid in *Escherichia coli*.

Faithful maintenance of P1 requires an active partition system, *par*, that is encoded by the plasmid. The *par* operon consists of two *trans*-acting factors, *parA* and *parB*, and a centromere-like site called *parS*. ParB is a multifunctional protein. It interacts with and stimulates the biochemical activities of ParA. ParB is a dimer in solution. Finally, ParB binds specifically to *parS*, along with the *E. coli* integration host factor (IHF) to form a high affinity nucleoprotein complex called the partition complex, which mediates partition. ParB and IHF stimulate each other's DNA binding activity. In this thesis I examine the structural and functional domains of ParB. Using protein fragments, I show that ParB contains two independent multimerization domains, one at its C-terminus and one at its N-terminus. I also show that the extreme N-terminus of ParB is required for ParA-ParB interactions. By limited proteolytic digestion, I show that ParB has a distinct domain structure, with the C-terminal dimerization domain at its core. I have examined the architecture of the partition complex by investigating the DNA binding activity of various ParB fragments. A single dimer of ParB is sufficient for partition complex formation. The first 141 residues of ParB are dispensable for the formation of the partition complex. A fragment missing only the last 16 amino acids of ParB binds specifically to *parS*, but binding is weak and no longer stimulated by IHF. The ability of IHF to stimulate ParB binding to *parS* correlates with C-terminal dimerization. Using full and partial *parS* sites, I have found that two regions of ParB, one in the centre and the other near the C-terminus, interact with distinct sequences within *parS*. I propose a model of how the ParB dimer binds *parS* to form the minimal partition complex.

ACKNOWLEDGEMENTS

I am grateful for the support of many people throughout my time as a graduate student. First, I would like to thank my supervisor, Barbara Funnell, for her mentorship and her friendship over the past few years. Past and present members of the lab have also contributed to a challenging yet enjoyable working environment. In particular, I would like to thank Megan Davey, for her intellectual input and personal perspectives, Jean-Yves Bouet, for many lively debates and a successful collaboration, Emma Fung, for much discussion and Natalie Erdmann, for many interesting conversations, both scientific and non-scientific. And the current members of the lab, Zhen Zhang and Rachel Rumley, greatly enhance the atmosphere in the lab. I would also like to thank my supervisory committee members, Dr. Andrew Spence and Dr. Jack Greenblatt, for their considerable input. I would also like to thank Dr. Don Awrey for his help with the MALDI-TOF. I acknowledge financial support from University of Toronto Open Fellowships.

I would also like to acknowledge some people outside of the lab. Tara Beattie has been a wonderful friend who has been there for me throughout. I thank her for her support and for numerous coffee breaks. I would like to thank my sisters for their pride and pleasure in my successes. The support of my parents, in its many facets, has been a tremendous help in my completion of this degree. I thank them for that support, for their love and their confidence.

Finally, I would like to thank my husband, Andrew Bukata. He is my best friend, my sounding board and my staunchest supporter. I thank him for his confidence in me, for his constant encouragement and support and his understanding of both my frustrations and my triumphs. And I share this particular triumph with him.

TABLE OF CONTENTS

	page
PREFACE	
Thesis abstract	ii
Acknowledgements	iii
Table of Contents	iv
List of Tables	viii
List of Figures	ix
List of Abbreviations	xii
CHAPTER 1: GENERAL INTRODUCTION	1
I: PLASMID PARTITION	3
I-1: P1 Plasmid partition	3
I-2: P1 ParA	5
I-2.1: Gene Regulation	5
I-2.2: Partition Role	7
I-3: P1 ParB and the partition complex	8
I-3.1: The <i>parS</i> site	8
I-3.1.1: P1 vs. P7 <i>par</i>	13
I-3.2: Physical properties of ParB	13
I-3.3: ParB's DNA binding activity	14
I-3.3.1: Gene silencing	18
I-3.4: ParB homologues	19
I-4: Other plasmid partition systems	20
I-4.1: F	20
I-4.2: P7	23
I-4.3: pMT1	23
I-4.4: R1	23
I-5: Partition models	24
I-6: Plasmid localization	27
I-6.1: P1	27
I-6.2: F	28
I-6.3: R1	30
I-7: Importance of the cell $\frac{1}{4}$ and $\frac{3}{4}$ positions	31
II: ADDITIONAL FACTORS IN PLASMID STABILITY	33
II-1: Plasmid copy number control	33
II-1.1: Replication control	33
II-1.2: Multimer resolution	34
II-2: Post-segregational killing	34
III: BACTERIAL CHROMOSOME SEGREGATION	36
III-1: Chromosome positioning	36
III-1.1: Chromosome localization	36
III-2: Chromosome partition systems	38

III-2.1: <i>Streptomyces coelicolor</i>	
TABLE OF CONTENTS (cont.)	page
III-2.2: <i>Caulobacter crescentus</i>	38
III-2.3: <i>Bacillus subtilis</i>	39
III-3: Model of chromosome segregation	42
III-4: Chromosome condensation	43
III-4.1: <i>E. coli</i> Muk proteins	43
III-4.2: SMC proteins	44
III-5: Chromosome separation	46
III-5.1: Chromosome decatenation	46
III-5.2: Multimer resolution	47
IV: THESIS RATIONALE	47
CHAPTER 2: THE P1 ParB DOMAIN STRUCTURE INCLUDES TWO INDEPENDENT MULTIMERIZATION DOMAINS	49
INTRODUCTION	50
EXPERIMENTAL PROCEDURES	52
Bacterial and yeast strains	52
Media and antibiotics	52
Reagents and buffers	52
Plasmid construction	53
Yeast two-hybrid analysis	60
Protein purification	60
DSP cross-linking	62
Proteolysis	62
Protein sequencing	62
RESULTS	64
Proteolytic digestion of ParB	64
Definition of dimerization domains by yeast two-hybrid and <i>in vitro</i> cross-linking	72
A second self-association domain of ParB	74
ParA-ParB interactions	80
DISCUSSION	81
ParB's dimerization domains	81
A C-terminal region of ParB inhibits cross-linking in the absence of the C-terminus	83
Possible roles for dimerization in ParB activity in partition	84
CHAPTER 3: STOICHIOMETRY OF P1 ParB IN THE PLASMID PARTITION COMPLEX	87

INTRODUCTION	88
TABLE OF CONTENTS (cont.)	
	page
EXPERIMENTAL PROCEDURES	90
Reagents and enzymes	90
DNA and proteins	90
Gel mobility shift assays	90
RESULTS	92
Characterization of two forms of the partition complex	92
Relative stoichiometry between the two partition complexes	92
The I+B1 complex contains one ParB dimer	94
DISCUSSION	100
CHAPTER 4: THE DNA BINDING DOMAINS OF P1 ParB AND THE ARCHITECTURE OF THE P1 PLASMID PARTITION COMPLEX	104
INTRODUCTION	105
EXPERIMENTAL PROCEDURES	109
Bacterial strains, growth media, reagents and buffers	109
Plasmid construction	109
DNA substrates	110
Electrophoretic mobility shift assays	111
DNaseI protection assays	111
RESULTS	112
The region between residues 142 and 325 contains all information required for binding to the full <i>parS</i> site	116
C-terminal dimerization is required for high-affinity <i>parS</i> binding	121
Binding to isolated box A or box B sequences	125
The putative helix-turn-helix domain can function as a monomer	132
DISCUSSION	136
The putative helix-turn-helix domain	138
Higher order partition complexes	139
CHAPTER 5: INFLUENCE OF DELETIONS AND DNA ON ParB'S STRUCTURAL DOMAINS & FUTURE DIRECTIONS	141
INTRODUCTION	142

TABLE OF CONTENTS (cont.)

	page
EXPERIMENTAL PROCEDURES	144
Proteins	144
DNA fragments	144
Proteolysis	144
Protein sequencing	144
RESULTS AND DISCUSSION	145
Disruption of the C-terminal dimerization domain destabilizes ParB's domain structure	145
DNA binding alters the conformation of His-ParB	151
THESIS SUMMARY	155
FUTURE DIRECTIONS	160
Structural studies	160
ParA-ParB interactions	160
Immunofluorescence microscopy	162
REFERENCES	164

LIST OF TABLES

	page
CHAPTER 2	
Table 2-1: Vectors and P1 plasmids	54
Table 2-2: Plasmids used for yeast two-hybrid analysis	56
Table 2-3: Plasmids constructed for protein expression	57
Table 2-4: N-terminal sequences of proteolytic fragments generated by trypsin and chymotrypsin	68
CHAPTER 4	
Table 4-1: Quantification of synthetic substrate binding activity	131
CHAPTER 5	
Table 5-1: N-terminal sequences of proteolytic fragments generated by trypsin	150

LIST OF FIGURES

	page
CHAPTER 1	
Figure 1-1: The P1 plasmid partition operon	4
Figure 1-2: The P1 <i>parS</i> site	9
Figure 1-3: Summary of ParB fragment interactions with 30-333 ParB	15
Figure 1-4: Putative domains of P1 ParB	17
Figure 1-5: Partition operons of several different plasmids	21
Figure 1-6: Models for P1 plasmid partition	26
Figure 1-7: Model of the P1 partition cycle	32
CHAPTER 2	
Figure 2-1: Sequences of N-terminal tags of purified fusion proteins used in this chapter	59
Figure 2-2: Tryptic digestion of ParB and His-ParB	65
Figure 2-3: Chymotrypsin and trypsin digestion of His-ParB	67
Figure 2-4: Tryptic digestion of His-ParB, two C-terminal fragments (His-47-333 ParB and His-67-333 ParB) and two N-terminal fragments (His-1-293 ParB and His-1-274 ParB)	71
Figure 2-5: Examples of filter tests to determine β -galactosidase activity in the yeast two-hybrid system	73
Figure 2-6: Summary of dimerization assays with C-terminal fragments of ParB	75
Figure 2-7: Cross-linking of His-ParB and His-ParB fragments with DSP	77
Figure 2-8: Summary of dimerization assays with N-terminal fragments of ParB	79
Figure 2-9: Model of ParB's functional and structural domains	82

	page
CHAPTER 3	
Figure 3-1: The P1 <i>parS</i> site	89
Figure 3-2: Multiple partition complexes form at <i>parS</i> with increasing ParB	93
Figure 3-3: Competition analysis of ParB binding to <i>parS</i>	95
Figure 3-4: Mobility of ParB and His-ParB homodimers and heterodimers bound to <i>parS</i> DNA	98
 CHAPTER 4	
Figure 4-1: The P1 <i>parS</i> site	106
Figure 4-2: The structural and functional domains of ParB	114
Figure 4-3: Cross-linking of His-ParB and of ParB fragments	115
Figure 4-4: DNA binding activity of several ParB fragments in the presence and absence of IHF, measured in gel mobility shift assays	118
Figure 4-5: DNaseI footprinting of His-ParB and ParB fragments at <i>parS</i>	123
Figure 4-6: Competition analysis of His-1-317 ParB binding to <i>parS</i>	126
Figure 4-7: DNA binding activity of ParB fragments to oligomeric DNA substrates	129
Figure 4-8: ParB/His-275-333 ParB heterodimers bind to <i>parS</i>	135
Figure 4-9: Model of the minimal partition complex	137
 CHAPTER 5	
Figure 5-1: Tryptic digestion of His-ParB and ParB fragments	147
Figure 5-2: Tryptic digestion of His-ParB in the absence and presence of <i>parS</i> or non-specific DNA fragments	152
Figure 5-3: Comparison of tryptic digestions of His-ParB +/- <i>parS</i> in the presence and absence of IHF	154

Figure 5-4: Model of ParB DNA binding	page 156
Figure 5-5: A model of P1 plasmid partition at the level of the partition complex	159

LIST OF ABBREVIATIONS

3-AT: 3-amino-1,2,3-triazole

ATP γ S: adenosine-5'-*O*-(3-thiotriphosphate)

bp: base pair(s)

BSA: bovine serum albumin

DNaseI: bovine pancreatic deoxyribonuclease I

DRS: discriminator recognition sequence

DSP: dithiobis[succinimidyl propionate]

FISH: fluorescent *in situ* hybridization

GFP: green fluorescence protein

HTH: helix-turn-helix

IHF: integration host factor

IPTG: isopropyl- β -D-thiogalactopyranoside

kDa: kilodaltons

lacO: *lac* operator region

OP-Cu: 1,10-phenanthroline-copper

parOP: P1 *par* operator.promoter region

PCR: polymerase chain reaction

PVDF: polyvinylidene difluoride

X-Gal: 5-bromo-4-chloro-3-indolyl β -D-galactopyranoside

CHAPTER 1
GENERAL INTRODUCTION

The P1 prophage is maintained as a unit-copy-number plasmid in *Escherichia coli*; that is, there is one copy of the plasmid per copy of the host chromosome (Prentki *et al.*, 1977). Despite its very low copy number, P1 is extremely stable within a cell population (Austin *et al.*, 1981). Its stability is dependent on an active partition mechanism encoded by the plasmid. Other low-copy-number plasmids have also been identified, e.g. F, R1. These plasmids also encode an active partition system that is functionally analogous to that of P1.

The mechanism of plasmid partition is not well understood, but can be thought of as a positioning reaction. As such, two newly replicated sister plasmids are positioned within the cell such that septum formation and subsequent cell division occurs between the two plasmids. Because plasmids must “know” where they are in the cell, host components have been implicated in partition, although few have been identified. It is thought that the plasmids use at least some component(s) of the cellular machinery that the host chromosome uses for segregation. This machinery has not yet been fully identified and therefore P1 partition is a good model system for chromosome segregation. Both P1 and the chromosome are maintained at the same copy number, but P1 is not essential for cell growth and therefore it is easier to study defects in the P1 system. Similarly, studying P1 partition will elucidate the partition mechanism of other low-copy-number plasmids. In addition, understanding how plasmids are maintained is an important clinical problem because antibiotic resistance and virulence genes are often encoded by extrachromosomal episomes in bacterial pathogens (such as pMT1 of *Yersinia pestis*; Hu *et al.*, 1998; Youngren *et al.*, 2000).

All partition systems identified to date, in both bacterial and plasmid genomes, encode a *cis*-acting, or centromere-like, site to which a *trans*-acting protein binds. In P1, the site is *parS* and the protein is ParB. In this thesis I investigate the structural and functional domains of ParB. Specifically, I demonstrate the regions of ParB that are involved in self-association and in DNA

binding and I discuss the implications of these properties for the architecture of the “partition complex” that assembles at *parS*.

I. Plasmid Partition

I-1 P1 Plasmid Partition

The P1 prophage exists as a unit-copy plasmid in *E. coli* (Prentki *et al.*, 1977) and is lost in fewer than one in every 10^5 cell divisions (Austin *et al.*, 1981). This stable maintenance is absolutely dependent upon its partition system, *par*, encoded by a 2.5 kilobase region of the plasmid (Austin and Abeles, 1983a). The *par* region encodes two *trans*-acting factors, *parA* and *parB*, transcribed from a promoter upstream of *parA* and a *cis*-acting site, *parS*, located immediately downstream of *parB* (Abeles *et al.*, 1985) (Figure I-1). All three elements are essential for partition, although only *parS* is required in *cis* (Austin and Abeles, 1983a; Austin and Abeles, 1983b; Abeles *et al.*, 1985; Friedman and Austin, 1988).

ParA is required for two distinct functions in P1 partition: 1) regulation of *par* gene expression (Abeles *et al.*, 1985; Friedman and Austin, 1988; Hayes *et al.*, 1994) and 2) physical segregation of the plasmids (Davis *et al.*, 1996; Youngren and Austin, 1997; Radnedge *et al.*, 1998; Bouet and Funnell, 1999). ParA’s regulatory role is fairly well understood, while its role in partition is less clear. Recent reports, however, have suggested some intriguing possibilities (see section I-2.2).

ParB and the *E. coli*-encoded integration host factor (IHF) bind to *parS* to form a nucleoprotein structure called the partition complex (Davis and Austin, 1988; Funnell, 1988b; Davis *et al.*, 1990; Funnell, 1991; Funnell and Gagnier, 1993). Formation of this complex is one of the earliest steps in partition. The partition complex mediates localization of the plasmid (Erdmann *et al.*, 1999), presumably through ParB-ParB and ParB-ParA interactions as well as

P1 *par*

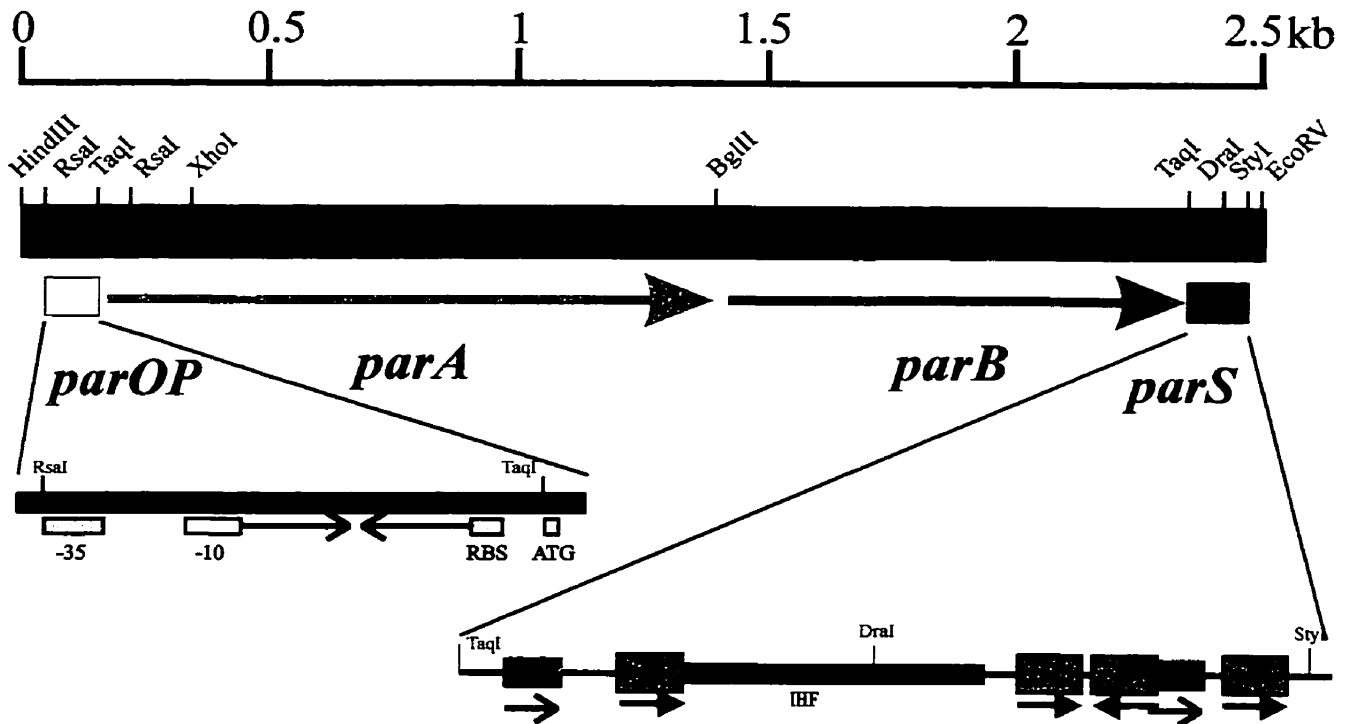


Figure 1-1. The P1 plasmid partition operon. The genes encoding ParA and ParB are indicated by the arrows, *parS* (the centromere-like site) is denoted by the blue box and *parOP* (the operator-promoter region) by the yellow box (Abeles et al, 1985). The scale (in kilobases) is shown above the diagram. The *parS* and *parOP* regions are extended below the operon. The -35 and -10 transcription signals, the ribosome binding site (RBS) and the *parA* start codon (ATG) are indicated. The inverted arrows represent the 20 bp imperfect inverted repeat to which ParA is thought to bind (Davis et al, 1992; Davey and Funnell, 1994). In *parS*, the specific box A and box B sequences (Davis et al, 1988; 1990; Hayes and Austin, 1994; Funnell and Gagnier, 1993; 1994) are indicated in blue and magenta, respectively. The IHF binding site (Funnell, 1991) is indicated in green.

interactions with specific host-encoded factors. ParB also stimulates ParA's biochemical activities (Davis *et al.*, 1992; Davey and Funnell, 1997).

I-2 P1 ParA

I-2.1 Gene regulation: Regulation of *parA* and *parB* gene expression is crucial. Excessive amounts of either or both gene product(s) disrupt partition (Abeles *et al.*, 1985; Funnell, 1988a; Hayes *et al.*, 1994). ParA is a site-specific DNA binding protein; it regulates gene expression by binding to the operator region, *parOP*, thereby repressing the *parAB* operon (Friedman and Austin, 1988; Davis *et al.*, 1992; Davey and Funnell, 1994). DNaseI footprinting has shown that ParA binding is centred over an inverted repeat within the operator (Davis *et al.*, 1992; Davey and Funnell, 1994). ParA is thought to bind the DNA as a dimer, and since protection from DNaseI can extend to 150 base pairs, several ParA dimers likely bind cooperatively to the operator region (Davey and Funnell, 1997). ParA binding probably interferes with the ability of RNA polymerase to interact with the promoter. ParB acts as a co-repressor by stimulating repression by ParA, but has no repressor activity on its own (Friedman and Austin, 1988). *In vitro*, ParB stimulates ParA's site-specific DNA binding activity (Davey and Funnell, 1997).

ParA belongs to a superfamily of proteins that have a unique version of the Walker A motif and two potential Walker B motifs (Motallebi-Veshareh *et al.*, 1990), motifs that are involved in nucleotide binding (Walker *et al.*, 1982). Consistent with the presence of these conserved sequences, ParA has a weak ATPase activity that is stimulated by ParB and by DNA of no particular sequence, length or topology (Davis *et al.*, 1992). The stimulatory effects of ParB and DNA are additive (Davis *et al.*, 1992).

Nucleotide binding and hydrolysis by ParA modulate its site-specific DNA binding activity in a complex manner (Davey and Funnell, 1994; Davey and Funnell, 1997; Bouet and

Funnell, 1999). First, ATP stimulates ParA binding to the operator region 5- to 10-fold, as determined by DNaseI footprinting (Davey and Funnell, 1994). ADP and non-hydrolyzable analogues of ATP stimulate DNA binding an additional 5- to 10-fold. Therefore binding of ParA to adenine nucleotides stimulates its DNA binding, while the act of hydrolysis is inhibitory (Davey and Funnell, 1994). Second, nucleotide binding affects the oligomeric state of ParA, pushing the monomer-dimer equilibrium toward dimer formation (Davey and Funnell, 1994). These observations led to the proposal that the more active DNA-binding form of ParA is a dimer (Davey and Funnell, 1994).

Nucleotide binding also alters the conformation of ParA, increasing its percent helicity as determined by circular dichroism (Davey and Funnell, 1997). These studies also showed small but distinct differences in the conformational changes induced by adenosine di- and tri-phosphates and by hydrolyzable and non-hydrolyzable adenosine triphosphates (Davey and Funnell, 1997). The conformational changes presumably affect ParA's various activities.

ParB stimulates ParA's DNA-binding activity in the presence of ATP (Davey and Funnell, 1997) but not in the absence of nucleotide or in the presence of ADP or ATP γ S, suggesting that ATP hydrolysis was required for stimulation by ParB. Interestingly, stimulation by ParB and ATP resulted in the same level of *parOP* binding as observed with ADP and non-hydrolyzable analogues of ATP, suggesting that ParB negated the inhibitory effects of ATP hydrolysis on DNA binding.

Deletion of the Walker A motif, or mutation of the conserved lysine within the motif (K122), disrupts ParA's ATPase activity and causes significant defects in both autoregulation and partition (Davis *et al.*, 1996). More recently, a series of point mutations was introduced into the Walker A motif and the Walker B motifs (Fung, 2000). All of the mutant proteins had reduced ATPase activity and were defective in partition but were able to repress transcription to

varying degrees. In fact, one class of mutants were “super”-repressors, repressing transcription *in vivo* to a much greater extent than the wild-type protein represses. Therefore *parOP* binding and subsequent repression do not require ATP hydrolysis, although it may be required to modulate repression. Together, the different effects of different nucleotides suggested that ATP binding and hydrolysis have separable functions in repression, and perhaps also in partition (Davis *et al.*, 1996; Davey and Funnell, 1997; Fung, 2000).

I-2.2 Partition role: The transcriptional regulatory role of ParA is dispensable for plasmid stability. Certain point mutations in the *parOP* region lead to low-level, constitutive expression of *parA* and *parB*. The resulting protein levels support partition (Davis *et al.*, 1996). However, even in the presence of these mutations, ParA is required for P1 stability. Therefore ParA is directly required for the positioning reaction.

One class of *parA* mutants is called “propagation-defective”, or PD (Youngren and Austin, 1997). P1 plasmids encoding these mutants can not be established or maintained in a cell unless they are complemented with a copy of the wild-type *parA* gene, even when autoregulation has been bypassed. This is in direct contrast to plasmids carrying *parA* null mutations or other point mutations that are established and then slowly lost from a cell population by random diffusion (Abeles *et al.*, 1985; Friedman and Austin, 1988). The dramatic phenotype of the propagation-defective *parA* mutants is only observed in the presence of ParB, indicating that ParA interacts with the ParB-*parS* complex (Youngren and Austin, 1997). Thus it was suggested that ParA is involved in partition complex pairing and that the mutant ParA proteins formed paired complexes that could not be separated.

Interestingly, propagation-defective *parA* mutants caused a phenotype very much like that observed upon overexpression of *parB* (Funnell, 1988a). A large excess of ParB has a strong destabilizing effect on plasmids that contain *parS*, preventing their establishment in *E.*

coli. The excess ParB likely binds the plasmids and other ParB molecules, leading to sequestration of large aggregates of ParB-*parS* complexes (Funnell, 1988a). Similarly, propagation-defective ParA proteins may have a defect in their ability to dissociate or separate paired plasmids.

In vitro, ParA interacts directly with the ParB-*parS* partition complex (Bouet and Funnell, 1999). The interaction is absolutely dependent on both ATP and ParB. ATP γ S also supports the interaction indicating that ATP hydrolysis is not required. The effect of the interaction varies with ParB concentration. At high ParB concentration ParA is recruited to the partition complex, whereas at low concentration, ParA causes disassembly of the partition complex (Bouet and Funnell, 1999). It is tempting to suggest that the latter effect is a result of the role that ParA plays in dissociating paired partition complexes.

ADP does not support a ParA-partition complex interaction, but does allow stable ParA binding to *parOP* (Bouet and Funnell, 1999). This interaction is not stable in the presence of ATP, however. The data suggest that nucleotide binding by ParA acts as a molecular switch in which ParA-ADP is the repressor form of the protein while ParA-ATP has a direct role in partition (Bouet and Funnell, 1999).

I-3 P1 ParB and the partition complex

I-3.1 The *parS* site: *parS* is the centromere-like site of P1 and consists of several distinct DNA sequences that are specifically bound by either ParB or IHF (Davis and Austin, 1988; Funnell, 1988a; Funnell, 1988b; Davis *et al.*, 1990; Funnell, 1991; Funnell and Gagnier, 1993; Funnell and Gagnier, 1994). The wild-type *parS* site is 84 bp long and can be divided into three main sections: left, central and right (Fig. 1-2). The right 34 bp region contains a 13 bp palindrome with a 3 bp spacer. The significance of this inverted repeat is not clear, however, because further deletion analyses narrowed the minimal region down to the leftmost 22 bp of this

P1 *parS*

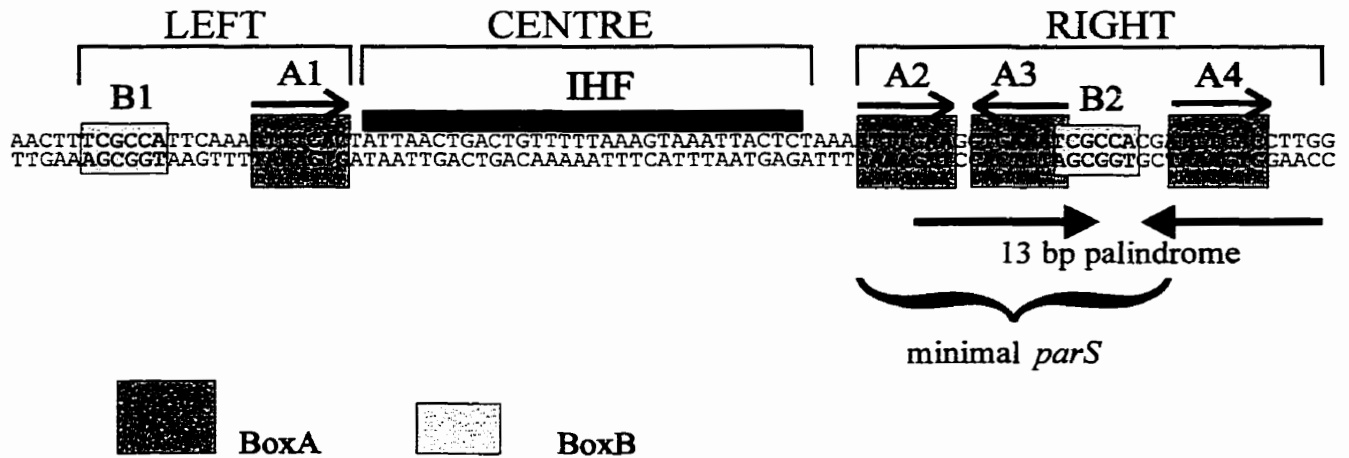


Figure 1-2. The P1 *parS* site. The *parS* site is divided into three sections, LEFT, RIGHT and CENTRE, as described in the text. The box A and box B sequences are drawn in blue and pink boxes, respectively. The inverted arrows below the sequence represent the 13 bp palindrome on the right side of *parS* (Martin et al, 1987; Davis et al., 1990). The bracket indicates the minimal region of *parS* required for partition (in the absence of IHF) (Martin et al, 1991).

region, indicating that only the left half of this palindrome was important for function (Martin *et al.*, 1991; Funnell and Gagnier, 1994; Hayes and Austin, 1994). Within this smaller region is an inverted repeat of a heptameric sequence, ATTTAC/A, called the box A sequence (Fig. 1-2). The right half of the larger palindrome contains an additional copy of this heptameric sequence. A second specific sequence, called the box B sequence (TCGCCA), is also present in single copy in the right section of *parS*. The left portion of *parS* contains a single copy each of the box A and the box B sequence and ParB exhibits some specificity for this region when isolated from the rest of *parS* (Davis *et al.*, 1990).

The left and right regions of *parS* flank an IHF (Integration Host Factor) binding site (Funnell, 1988b; Davis *et al.*, 1990; Funnell, 1991). IHF is a small, architectural protein of *E. coli* with site-specific DNA binding activity. It is involved in a number of cellular processes, including λ site-specific recombination (Friedman, 1988). IHF is a DNA bending protein (Robertson and Nash, 1988; Thompson and Landy, 1988; Rice *et al.*, 1996). IHF binds its recognition site within *parS* and creates a large bend in the DNA (Funnell, 1991). DNA-bending by IHF can be partially replaced by intrinsically bent DNA (Hayes and Austin, 1994), arguing that the role of IHF is primarily to bend the DNA rather than to mediate protein-protein interactions. The IHF-induced bend brings the left and right sides of *parS* into close proximity (Funnell, 1991; Funnell and Gagnier, 1993).

In wild-type *E. coli* cells, IHF forms part of the partition complex (Funnell, 1988b; Funnell, 1991) and increases ParB's affinity for *parS* approximately 10,000-fold (Funnell, 1991). In the presence of IHF, both the right and left sides of *parS* are occupied simultaneously (Funnell and Gagnier, 1993), indicating that the bend facilitates simultaneous interactions of ParB with both sides of *parS*. IHF is not, however, absolutely required for P1 partition. In its absence, ParB binds the right side of *parS* with higher affinity than the left side, although at higher ParB

concentrations, both sides of *parS* become occupied (Funnell and Gagnier, 1993). The right half of *parS* is sufficient for partition (Martin *et al.*, 1987; Funnell, 1991; Martin *et al.*, 1991) and ParB is able to interact specifically with this portion of the site (Davis *et al.*, 1990). However, partition in the absence of the IHF site or the left side of *parS* (IHF-independent partition) is slightly less efficient because the affinity of ParB for the minimal *parS* site (i.e. the right side) is lower than for the intact site, causing less efficient complex formation (Funnell, 1991; Funnell and Gagnier, 1993).

parS contains four copies of box A and two copies of box B. These sequences are arranged non-symmetrically throughout the site and are directly contacted by ParB, as determined by DNaseI footprinting and methylation protection and interference experiments (Davis and Austin, 1988; Davis *et al.*, 1990; Funnell and Gagnier, 1993). In several different studies, different regions of *parS* were mutated to determine which of these boxes is required for partition. Plasmids containing these versions of *parS* were then tested for plasmid stability or for incompatibility phenotypes (the latter is the ability to displace another plasmid that is maintained with the same *par* system; see section I-5). These analyses showed that box A4 was not required for partition or incompatibility in the presence or absence of IHF (Funnell and Gagnier, 1994; Hayes and Austin, 1994). Deletion of box A3, on the other hand, showed that it was absolutely essential for partition (Martin *et al.*, 1987; Martin *et al.*, 1991; Hayes and Austin, 1994). A single point mutation (T to A) in either box A2 or box A3 did not affect partition with or without IHF, as determined by incompatibility experiments (Funnell and Gagnier, 1994). But when the same point mutation was present in both box A2 and box A3, the mutant *parS* was significantly reduced in its ability to exert incompatibility (Funnell and Gagnier, 1994). When the entire box A3 sequence was changed, the plasmid exerted no incompatibility (Davis *et al.*, 1990). When the same changes were introduced into box A1, partition was unaffected (Davis *et al.*, 1990). In

fact, in the presence of IHF and ParB, the mutated box A1 region was still protected from DNase I digestion, indicating that the box A1 sequence is completely dispensable for partition and for organizing the wild-type partition complex (Davis *et al.*, 1990).

The importance of the box B sequences has also been examined. Deletion of either box B1 or box B2 disrupts partition in the presence of IHF (Davis *et al.*, 1990; Hayes and Austin, 1994). Deleting or mutating box B1 does not, however, interfere with IHF-independent partition (Martin *et al.*, 1987; Martin *et al.*, 1991; Funnell and Gagnier, 1993), indicating that the left side of *parS* is unimportant in the absence of a bent complex. In contrast, box B2 is absolutely required for partition in the absence (or presence) of IHF (Martin *et al.*, 1991) and mutations within box B2 are particularly destabilizing in IHF-independent partition (Martin *et al.*, 1991; Funnell and Gagnier, 1993).

Therefore, the data indicate that boxes B1, A2, A3 and B2 are essential for wild-type partition complex formation, i.e. in the presence of IHF. Boxes A1 and A4 appear to be redundant in complex formation, although they may stabilize additional protein-DNA interactions *in vivo* (see section I-3.3.1). In the absence of IHF, the left side of *parS*, i.e. box B1 is also dispensable. Therefore the minimal binding site in the absence of IHF consists of the box A2-A3 inverted repeat and the overlapping box B2 sequence.

The spacing and helical phasing of the box A and boxB sequences is also critical for IHF-stimulated partition complex formation (Funnell and Gagnier, 1993; Hayes and Austin, 1994). Specific faces of the left and right side of *parS* must be oriented toward each other to allow high-affinity ParB binding (Funnell and Gagnier, 1993; Hayes and Austin, 1994). Furthermore, if the left side of *parS* is extended but still correctly oriented with respect to the right arm, the resulting site does not support partition unless the right side is similarly extended (Hayes and Austin, 1994). The right side is apparently more flexible than the left side, so that when it is extended by

an integral number of helical turns it can still align itself with the wild-type left side (Hayes and Austin, 1994). The additional flexibility of the right arm may be related to the AT-rich region adjacent to the IHF binding site (Hayes and Austin, 1994). These observations support a model in which ParB makes simultaneous contacts with both sides of *parS* in the presence of an IHF-induced bend. In order for the “cross-bend” interactions to be made and stabilized, the two arms of *parS* and the ParB binding sites within these arms must be properly aligned.

I-3.1.1 P1 vs. P7 *par*: The P7 prophage encodes a *par* system that is very similar to that of P1 (see section I-4.2) (Ludtke *et al.*, 1989). In particular, the *parS* sites of the two plasmids are strikingly similar. P7 *parS* contains a central IHF binding site that is flanked by “box A” (heptameric) and “box B” (hexameric) sequences. The box A sequences of P1 and P7 differ only in the seventh residue of the heptameric sequences (Hayes and Austin, 1993; Hayes *et al.*, 1993) and are functionally interchangeable (Hayes and Austin, 1993). The box B sequences are more divergent and cannot substitute for one another (Hayes and Austin, 1993). In fact, exchanging the box B sequences is sufficient to change the specificity of ParB binding. P1 ParB binds a *parS* site with P1 box B sequences and P7 ParB binds a *parS* site with P7 box B sequences (Hayes and Austin, 1993). Within the P1 box B hexameric sequence, a single dinucleotide (CG) is sufficient to maintain P1 ParB specificity (Hayes and Austin, 1993).

I-3.2 Physical properties of ParB: The ParB polypeptide is 333 amino acids in length. ParB is very basic, containing 55 lysine + arginine residues. It has a molecular mass of approximately 38 kDa, although it migrates with 45 kDa proteins on SDS-polyacrylamide gels. Gel filtration analyses suggested a native molecular mass of approximately 140 kDa (Funnell, 1991), while sedimentation analyses indicated a smaller size of approximately 60 kDa (Funnell, 1991). Since both of these techniques are sensitive to the shape as well as to the size of a protein, the simplest interpretation was that ParB exists as an asymmetric dimer in solution

(Funnell, 1991). This prediction was supported by *in vitro* cross-linking reactions with dithiobis[succinimidyl propionate] (DSP), a 12Å cross-linker that reacts primarily with lysines. In the presence of DSP, ParB migrated as a dimer-sized smear on denaturing polyacrylamide gels (Funnell, 1991).

Sequence analysis of ParB does not provide any clues regarding the region of ParB required for its dimerization activity. Lobočka and Yarmolinsky (1996) isolated a series of point mutations within *parB*, and found that certain amino acid substitutions near the C-terminus of ParB disrupted dimerization activity of the mutant proteins in cell lysates (Lobočka and Yarmolinsky, 1996). As part of my Master's thesis, I found that a dimerization activity was contained within the C-terminal 59 amino acids of ParB. This region was sufficient to interact with a version of ParB lacking only the first 29 amino acids, in the yeast two-hybrid system (see Fig.1-3; Surtees, 1996). This small C-terminal fragment (275-333 ParB) was not, however, able to self-associate in this assay. I concluded that either the assay was not sufficiently sensitive to detect such interactions, or that a more N-terminal region of ParB was required to mediate self-association (Surtees, 1996). In this thesis I present evidence that there are in fact two self-association domains within ParB, one at its C-terminus and a second at its N-terminus (Chapter 2).

I-3.3 ParB's DNA binding activity: Since ParB interacts specifically with both box A and box B sequences, it is reasonable to expect that two different regions of ParB are involved in the site-specific DNA binding activities. Indeed single amino acid substitutions in two different regions of ParB have been observed to disrupt its DNA-binding activity (Lobočka and Yarmolinsky, 1996). Substitutions in the centre of ParB, on either side of a putative helix-turn-helix domain (see below), prevent *parS* binding. Similarly, substitutions within the C-terminus of ParB resulted in proteins that were unable to bind *parS*. Since these C-terminal point mutants

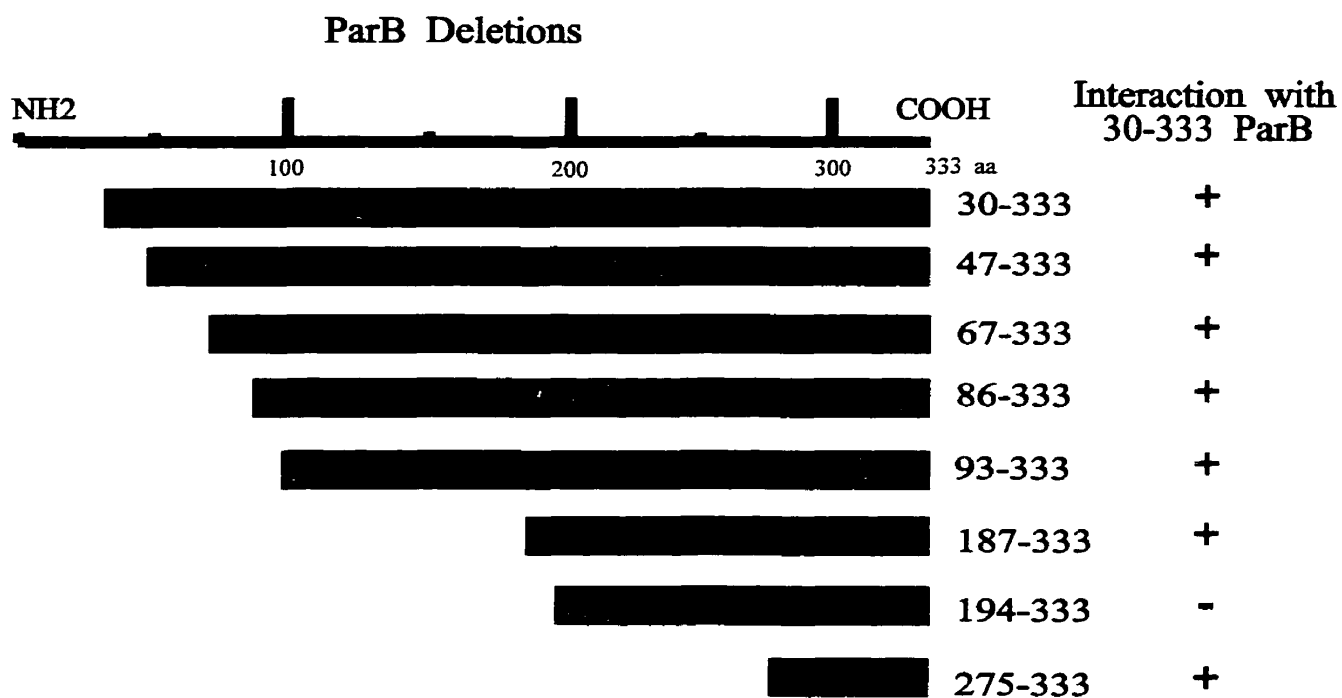


Figure 1-3. Summary of ParB fragment interactions with 30-333 ParB. This is a schematic of some of the work from my Master's thesis. It is a summary of my yeast two-hybrid analysis of ParB-ParB interactions. The ParB fragments drawn on the left were fused to the GAL4 activation domain and were tested for an interaction with 30-333 ParB fused to the GAL4 DNA binding domain (Surtees, 1996).

were also unable to dimerize (see section I-3.2), it was suggested that the defect in self-association weakened or eliminated ParB's DNA-binding activity (Lobocka and Yarmolinsky, 1996). Alternatively, the C-terminus could form part of a second, independent DNA binding domain of ParB.

To identify the region of ParB required for box B binding (and therefore for P1 *parS* specificity; Hayes and Austin, 1993), Radnedge *et al* (1996) constructed a series of P1:P7 hybrid ParB proteins. Homologous domains were identified and swapped (Radnedge *et al.*, 1996). The resulting proteins were tested for their ability to support either P1 or P7 *parS* partition *in vivo*. The authors found that when the region corresponding to P1 ParB residues 281-302 was exchanged for that of P7 ParB, the species specificity was swapped (Radnedge *et al.*, 1996). Since the box B sequence determines this species-specificity (see section I-3.2.1), this C-terminal region of P1 ParB is the minimal region of ParB required for P1 box B binding (Radnedge *et al.*, 1996). This region is called the “discriminator recognition sequence”, or DRS (Radnedge *et al.*, 1996). It is not clear whether the DRS directly interacts with the box B DNA or is involved in promoting a ParB conformation that allows another region of the protein to interact with the box B sequence.

A putative helix-turn-helix motif was identified by sequence alignment near the centre of ParB (Dodd and Egan, 1990) (Fig. 1-4). Secondary structure predictions by PHD (Rost and Sander, 1993; Rost and Sander, 1994) support this prediction (see Chapter 4). The helix-turn-helix (HTH) structure was the first DNA-recognition motif to be discovered. The first structures were of the λ Cro repressor, the *E. coli* CAP protein and the DNA-binding domain of the λ repressor. The conserved recognition motif for these proteins consisted of an α -helix, followed by a short turn and then a second α -helix. It is important to note, however, that regions of the protein outside the HTH often have significant roles in DNA recognition. For instance, the

P1 ParB

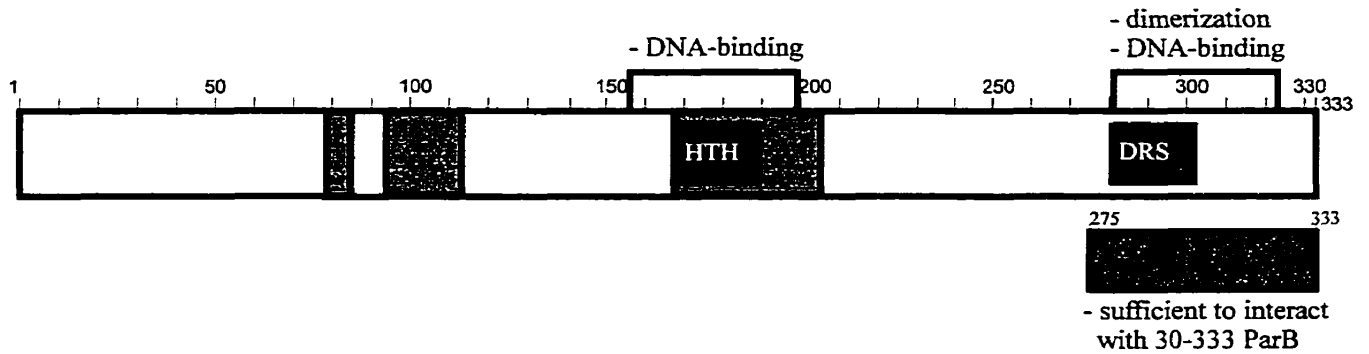


Figure 1-4. Putative domains of P1 ParB. The orange boxes indicate conserved regions of ParB (Williams and Thomas, 1992; Lobočka and Yarmolinsky, 1996; Hanai et al, 1996). The blue HTH box indicates a putative helix-turn-helix domain that has been predicted by sequence alignment (Dodd and Egan, 1990). The pink DRS box represents the “discriminator recognition sequence”, involved in box B recognition (Radnedge et al, 1996). The brackets above ParB indicate regions in which mutations affecting dimerization and/or DNA-binding activities of ParB were mapped (Lobočka and Yarmolinsky, 1996). The blue box below ParB indicates a region (residues 275-333) that is able to interact with 30-333 ParB in the yeast two-hybrid system (Surtees, 1996).

extended N-terminal arm of the λ repressor makes essential contacts with the major groove and wraps around the operator site (Pabo and Sauer, 1992).

Co-crystals of typical HTH proteins bound to their DNA sites have revealed common features (reviewed in (Pabo and Sauer, 1992). First, dimeric HTH proteins bind DNA sites containing inverted repeats. Each monomer binds a half site. Second, one helix of the HTH domain makes contacts with the major groove. Since boxes A2 and A3 on the right side of *parS* form an almost perfect inverted repeat, it has been proposed that the ParB putative HTH directly contacts this repeat in *parS*.

I-3.3.1 Gene silencing: In contrast to its activity in partition, which stabilizes plasmids with *parS*, ParB binding can destabilize certain *parS*-containing plasmids, depending on the location of *parS* on the plasmid (Lobocka and Yarmolinsky, 1996; Rodionov *et al.*, 1999). Destabilization occurs as a result of ParB-dependent gene silencing, i.e. repression of genes linked to *parS* (Rodionov *et al.*, 1999). *In vivo* chromatin immunoprecipitation experiments suggested a mechanism for silencing (Rodionov *et al.*, 1999). In these experiments, ParB bound DNA up to several kilobases away from *parS*. The results therefore indicate that ParB polymerizes along the DNA, in either direction away from its nucleation site, *parS* (Rodionov *et al.*, 1999). The extent of ParB polymerization was reduced in the absence of IHF (Rodionov *et al.*, 1999), indicating less efficient complex formation. Extensive ParB polymerization is presumably mediated by protein-protein (dimer-dimer) interactions and largely non-specific protein-DNA interactions. The biological relevance of ParB gene silencing is not clear, but these observations support a model in which ParB and IHF binding to *parS* stimulates the formation of a substantial nucleoprotein complex (see Chapter 3).

Additional evidence supporting the formation of a large nucleoprotein structure is provided by immuno-localization of ParB in fixed bacterial cells (Erdmann *et al.*, 1999) (see

section I-6.1). Immunofluorescence microscopy revealed the *parS*-dependent formation of large, bright ParB foci. These experiments indicate that the majority of ParB in the cell (approximately 7000 dimers (Funnell, 1991; Funnell and Gagnier, 1994) converges into only a few foci (Erdmann *et al.*, 1999), implying large nucleoprotein structures.

I-3.4 ParB homologues: Partition operons analogous to that of P1 have been identified in a large number of plasmids as well as in the chromosomes of many bacterial species (Gerdes *et al.*, 2000) (see sections III-2.2 and III-2.3). All of these systems encode a ParB-like protein that, where studied, binds a specific DNA site. However, the sequences of these proteins are of limited similarity and are best compared within closely related groups (e.g. *sop/par*, section I-4) (Motallebi-Veshareh *et al.*, 1990; Williams and Thomas, 1992; Hanai *et al.*, 1996; Gerdes *et al.*, 2000). ParB-like proteins do share two regions of reasonable conservation. The first extends from about residues 168-205 (P1 ParB numbering), and a helix-turn-helix motif is predicted in at least several of these proteins (Dodd and Egan, 1990; Hanai *et al.*, 1996; Lobočka and Yarmolinsky, 1996). A second region of similarity lies between ParB residues 78 and 136, particularly from residues 93-97 and from residues 102-112 (Motallebi-Veshareh *et al.*, 1990; Williams and Thomas, 1992; Hanai *et al.*, 1996; Lobočka and Yarmolinsky, 1996). No functional role for these “motifs” has been identified. There is little or no conservation in the C-terminal half of ParB homologues (Hanai *et al.*, 1996).

The chromosome-encoded ParB-like proteins exhibit more similarity with each other than with the plasmid-encoded proteins. Nonetheless, there is some similarity between the chromosomal proteins and P1 ParB in the central regions of these proteins, the region that contains a putative HTH motif (sections III-2.2 and III-2.3) (Mohl and Gober, 1997).

I-4 Other plasmid partition systems

The numerous partition systems encoded by other plasmids are analogous, although not always homologous, to the P1 partition system (Figure 1-5). There are two major families of partition systems, the *sop/par* family and the IncFII family. Plasmids in both families encode a *cis*-acting site and a protein that binds that site. Typically, a protein with putative ATPase activity is also involved, although the role of ATP binding and hydrolysis is not clear.

I-4.1 F: The partition system of F is called *sop* (stability of plasmid) and is related to the P1 *par* system. It encodes two proteins, SopA and SopB, that are similar in sequence to ParA and ParB, respectively. The *cis*-acting site is called *sopC* and is located downstream of *sopB*. *sopC* is very different in sequence from *parS* and consists of 12 tandem direct repeats of a 43 bp sequence (Mori *et al.*, 1986; Motallebi-Veshareh *et al.*, 1990; Williams and Thomas, 1992). Each sequence contains a short inverted repeat to which SopB binds (Hayakawa *et al.*, 1985; Mori *et al.*, 1986; Mori *et al.*, 1989). The SopB-*sopC* complexes form a nucleoprotein structure that is analogous to the P1 partition complex and is presumably the substrate for plasmid localization. Unlike P1 however, no host factor is thought to be involved in partition complex formation.

Like P1 ParA, SopA has ATPase activity that is stimulated by SopB (Watanabe *et al.*, 1992). SopA binds the *sop* promoter region and regulates transcription from the operon (Mori *et al.*, 1989; Hirano *et al.*, 1998). *In vitro*, SopB stimulates the interaction between SopA and the promoter, indicating that SopB also plays a role in *sop* gene regulation (Mori *et al.*, 1989; Biek and Strings, 1995). The stimulation of SopA activity by SopB suggested that the two proteins interact. Subsequently SopA and SopB have been shown to interact directly (Hirano *et al.*, 1998; Kim and Shim, 1999).

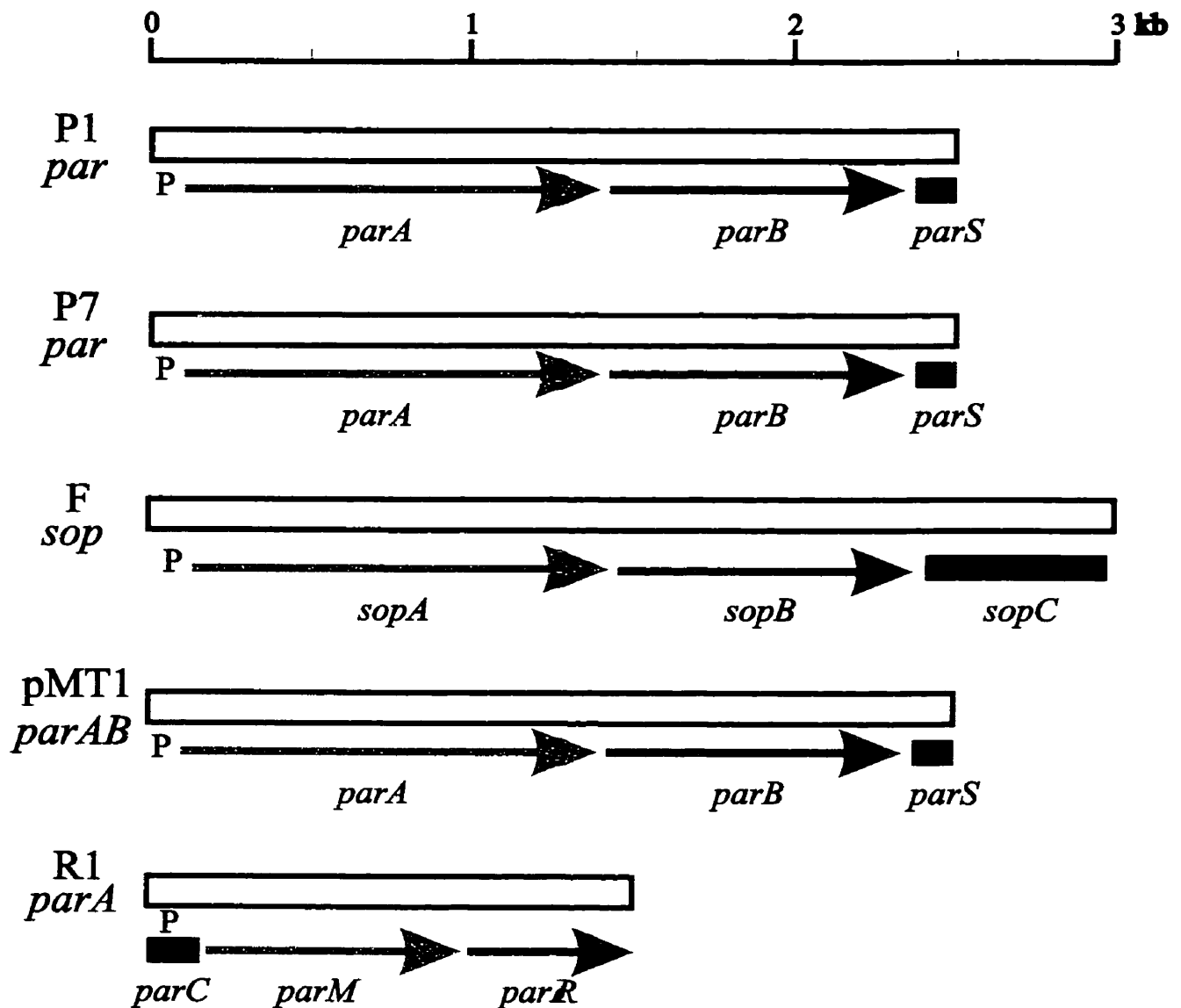


Figure 1-5. Partition operons of several different plasmids. The orange arrows indicate the genes encoding the ParA homologues (the ATPase protein) and the blue arrows indicate the genes encoding the ParB homologues (the centromere-binding protein). There is limited homology among these Par proteins. The *cis*-acting sites are represented by the blue boxes and are very different. P denotes the promoter region. The scale is indicated above the maps in kilobases. The maps are derived from several sources (Abeles et al, 1985; Ludtke et al, 1989, Mori et al, 1986; Gerdes et al, 1986; Youngren. et al, 2000).

Both P1 ParB (section I-3.3.3) and F SopB are able to silence, or repress, genes that are on either side of their DNA sites (*parS* or *sopC*, respectively) (Lynch and Wang, 1995; Lobočka and Yarmolinsky, 1996; Kim and Wang, 1999; Rodionov *et al.*, 1999). In both cases, the silencing can extend up to several kilobases. Furthermore, genes silenced by SopB are apparently inaccessible to *dam* methylase and DNA gyrase (Lynch and Wang, 1995). Two models have been proposed to explain the silencing effects. In the first, binding the *cis*-acting site recruits more protein to the DNA, resulting in a large complex that occludes RNA polymerase (see section I-3.3.1) (Rodionov *et al.*, 1999). The second model suggests that the protein-DNA complex is localized to a specific region in the cell and is therefore sequestered from the transcriptional machinery (Kim and Wang, 1999). The data for P1 support the first model. ParB has been shown, by chromatin immunoprecipitation assays, to directly interact with DNA up to 10 kb away from *parS* (Rodionov *et al.*, 1999).

SopB binding to *sopC* reduces the negative superhelicity (i.e. increases the linking number) of the DNA, indicating that the DNA is wrapped around the protein core (Biek and Shi, 1994; Lynch and Wang, 1994; Biek and Strings, 1995). Increased SopB expression results in increased linking numbers, even in the presence of a single copy of the 43 bp *sopC* repeat (Biek and Shi, 1994; Lynch and Wang, 1994; Biek and Strings, 1995). This suggests that SopB bound to its site can recruit other SopB molecules and promotes wrapping of the adjacent non-specific DNA, resulting in a large partition complex (Biek and Shi, 1994; Lynch and Wang, 1994; Biek and Strings, 1995). On the other hand, the N-terminal 82 residues of F SopB fused to a heterologous DNA-binding domain were sufficient to promote gene silencing in DNA adjacent to the specific site recognized by the heterologous protein (Kim and Wang, 1999). The authors found that these N-terminal residues were also sufficient to localize SopB within the cell (see section I-6.2) (Kim and Wang, 1998), suggesting that these residues direct the protein-DNA

complex to a specific cellular location. However, there have been conflicting reports of SopB localization (see section I-6.2) (Hirano *et al.*, 1998; Kim and Wang, 1998) and the nature of silencing remains to be elucidated.

I-4.2 P7: The P7 prophage partition system is very similar to the P1 system. The organization of the *par* operon is virtually identical and the Par proteins are highly homologous. Despite the similarities, however, the P1 and P7 *par* components are not interchangeable, and each system is specific for its own site. This system has been useful for defining the functional requirements within P1 *par* through swapping experiments (see section I-3.2.1).

I-4.3 pMT1: Recently, the pMT1 virulence plasmid of *Y. pestis* has been found to encode a partition system that is very similar to that of P7 (and, slightly less so, but still similar to that of P1) (Hu *et al.*, 1998; Youngren *et al.*, 2000). The operons are organized the same way, including the presence of a *parS* site downstream of the *parB* gene. pMT1 *parS* contains heptameric box A and hexameric box B sequences, although the box B sequences of pMT1 are different than those of P1 and of P7 (Youngren *et al.*, 2000). Interestingly, the pMT1 *par* locus is fully functional in *E. coli* and does not compete with either the P1 or P7 plasmid (Youngren *et al.*, 2000). The pMT1 plasmid from *Y. pestis* must be able to interact with whatever *E. coli* host factors are involved in partition.

I-4.4 R1: The R1 plasmid is a member of a different plasmid family, called IncFII, that also includes NRI (R100). The organization of the IncFII partition systems is superficially like those of the *par/sop* partition systems, but there is very little sequence homology (Williams and Thomas, 1992). The *par* region of R1 consists of a *cis*-acting site, *parC*, located upstream of the *parM* and *parR* genes that encode the two *trans*-acting factors (Fig. 1-5) (Dam and Gerdes, 1994). The *parC* site is the centromere-like site of R1 and also contains the operon promoter (Jensen *et al.*, 1994; Breuner *et al.*, 1996). ParR binds to *parC* and autoregulates transcription of

both *parR* and *parM* (Jensen *et al.*, 1994). This protein-DNA complex also serves as the centromere-like complex that is the substrate for partition (Dam and Gerdes, 1994). R1 is the only system for which plasmid pairing has been demonstrated *in vitro* (Jensen *et al.*, 1998). The plasmids pair via the ParR-*parC* partition complex (Jensen *et al.*, 1998). ParM has ATPase activity and interacts directly with the ParR-*parC* complex (Jensen and Gerdes, 1997), stimulating R1 plasmid pairing (Jensen *et al.*, 1998). The stimulatory effect of ParM on pairing requires ATP hydrolysis (Jensen *et al.*, 1998).

I-5 Partition models

The mechanism of plasmid partition is not understood, but it is essentially a positioning reaction. Sister plasmids must be properly positioned within the cell to allow septum formation and cell division to occur between them. Any model to explain plasmid partition must also explain the phenomenon of incompatibility, i.e. the inability of two different plasmids to be stably maintained in the same cell. Two types of incompatibility exist, the first mediated by the plasmid replication system and the second by the plasmid partition system. Replication-mediated incompatibility occurs because templates for replication are randomly selected from a pool of replicons. If two different plasmids have the same replicon, random replication from the mixed pool can lead to a discrepancy in the relative copy number of the two plasmids, eventually leading to loss of one or the other from a cell line (Austin and Nordstrom, 1990). In partition-mediated incompatibility, two different plasmids with the same partition region cannot be maintained in the same cell. In P1, the partition incompatibility region is *parS* (Abeles *et al.*, 1985; Martin *et al.*, 1987).

Two general partition models can account for partition-mediated incompatibility (Figure 1-6). In the first model, replicated plasmids bind a pair of unique, limiting host receptors, with one receptor on either side of the cell. Once a plasmid has bound one receptor, the other has to

bind the second receptor. Therefore different plasmids with the same partition site have to compete for a limited number of receptors, leading to incompatibility and the eventual loss of one plasmid type. Plasmids with different incompatibility determinants (centromere-like sites) would bind different receptors and would both be maintained (Fig. 1-4A). This model requires unique receptors for every possible plasmid (Austin and Nordstrom, 1990; Williams and Thomas, 1992), which has made it less intuitively appealing. It had been suggested that the bacterial chromosome might act as the receptor, with different plasmids binding different chromosomal regions. However both P1 and F plasmids are able to segregate into anucleate cells generated by *mukB* null mutations (Ezaki *et al.*, 1991; Funnell and Gagnier, 1995). MukB is an *E. coli* protein that is important in chromosome structure and segregation (see section III-4.1). The fact that F and P1 are faithfully partitioned into anucleate *mukB* cells indicates that they need neither the chromosome nor the MukB protein for maintenance.

The second model postulates that plasmids with the same partition site pair via these sites (Figure 1-4B). The paired plasmids then position themselves in the cell, by attachment to some cellular component, such that the septum forms between the plasmids at cell division. Different plasmids with the same partition sites would be mis-paired, leading to random distribution and plasmid loss. In this model host factors are invoked but need not be specific to a particular plasmid (Austin and Abeles, 1983b; Nordstrom and Austin, 1989; Austin and Nordstrom, 1990; Williams and Thomas, 1992).

Recently, a number of different groups have directly visualized plasmids and/or partition proteins in living and fixed bacterial cells (see section I-6) (Gordon *et al.*, 1997; Niki and Hiraga, 1997; Kim and Wang, 1998; Erdmann *et al.*, 1999; Jensen and Gerdes, 1999). In general, these studies support a partition model in which the newly replicated plasmids are initially paired. The sister plasmids are then rapidly separated and specifically positioned within the cell.

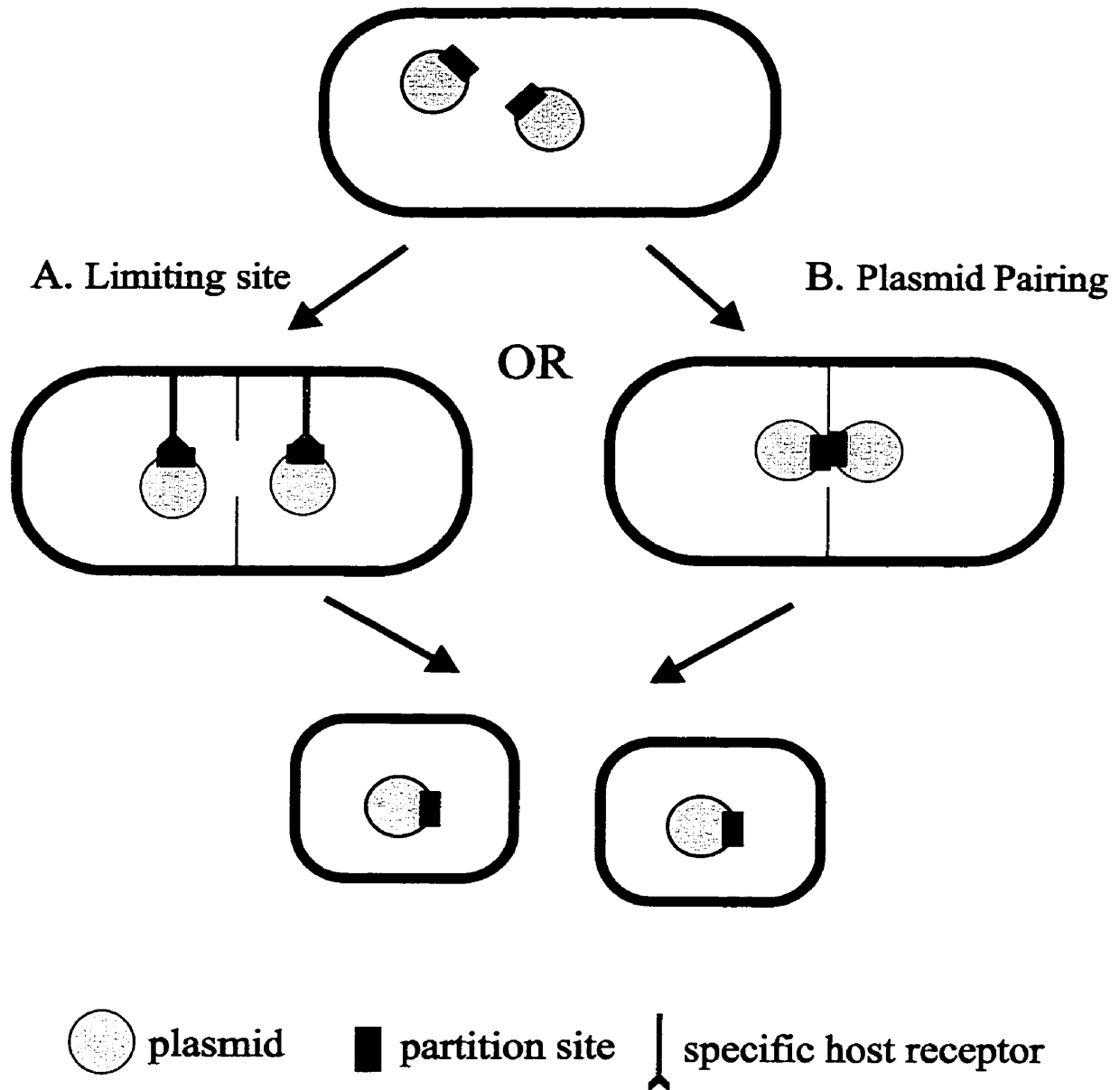


Figure 1-6. Models for P1 plasmid partition. Two alternative models to explain partition-mediated incompatibility. **A. Limiting sites.** Plasmids bind specific, unique host receptors in opposite sides of the cell via the partition complexes. **B. Plasmid pairing.** Plasmids pair via the partition complexes. The sister plasmids are then separated and positioned on opposite sites of the cell. The pink circles represent the plasmid, the blue boxes represent partition complexes and the red lines indicate unique host receptors.

I-6 Plasmid localization

Recent advances in cell biology have made it possible to visualize molecules within bacterial cells (e.g. (Gordon *et al.*, 1997; Niki and Hiraga, 1997; Kim and Wang, 1998). Different techniques have been used to track both plasmid and protein molecules (see also section III-1.1). To position DNA within the cell, the *lacO*/LacI-GFP system has been used by several groups (e.g. (Gordon *et al.*, 1997). Tandem repeats of the *lac* operator (*lacO*) are inserted into the DNA molecule of interest. Then a LacI-GFP protein fusion is expressed in cells carrying the *lacO* insertion. LacI-GFP binds the operator sequences so that the position of the DNA corresponds to the position of the GFP moiety. Fluorescent *in situ* hybridization (FISH) has also been used to localize DNA molecules. Fluorescently-labeled probes corresponding to different DNA sites are hybridized to the plasmid and visualized in fixed cells (e.g. (Niki and Hiraga, 1997). Finally, immunofluorescence microscopy has been used to position proteins within a cell. Fluorescent secondary antibodies mark the location of specific proteins within fixed cells (e.g. (Erdmann *et al.*, 1999).

I-6.1 P1: The intracellular localization of P1 was determined using the *lacO*/LacI-GFP system (Gordon *et al.*, 1997). In newborn cells, P1 localizes to midcell. Following replication the plasmids rapidly migrate to the $\frac{1}{4}$ and $\frac{3}{4}$ positions, relative to cell length, where they remain tethered until the completion of cell division. Once the cell has divided, these positions become the midcell of the daughter cells. Even in small (i.e. young) cells, two separated foci were often observed, implying that the plasmids separated early in the cell cycle, well before cell division.

The localization of P1 ParA and ParB in *E. coli* has also been examined by immunofluorescence microscopy of the endogenous levels of the proteins (Erdmann *et al.*, 1999). ParB forms discrete foci, primarily located close to the $\frac{1}{4}$ and $\frac{3}{4}$ positions of the cell. This correlates well with the observed position of the plasmid (Gordon *et al.*, 1997). In the

absence of *parS*, discrete ParB foci are not observed. Instead, ParB is dispersed throughout the cell, indicating that *parS* recruits ParB to form foci. This also strongly suggests that ParB foci and P1 plasmids co-localize.

The formation of ParB foci is dependent on *parS*, but independent of ParA. However, the proper localization of the ParB-*parS* complexes (partition complexes) within the cell requires ParA. In the absence of ParA, ParB foci form, but are not properly positioned at the $\frac{1}{4}$ and $\frac{3}{4}$ sites. In all cells, the foci were found in the centre or ends of the cells, corresponding to regions not occupied by the nucleoid. Therefore at least one of ParA's functions is to direct the partition complexes to their proper cellular positions. ParA may be required to separate paired partition complexes (see above), and/or to tether the complexes, and therefore the plasmids, to some cellular component at the $\frac{1}{4}$ and $\frac{3}{4}$ positions. Preliminary experiments indicate that ParA ATP-binding and/or hydrolysis activity is required for correct localization of the ParB-*parS* complexes (N. Erdmann, E. Fung and B.E. Funnell, unpublished data).

ParA was dispersed throughout the cell in the presence of *parS* and/or ParB, as determined by immunofluorescence microscopy (Erdmann *et al.*, 1999).

I-6.2 F: The intracellular localization of the F plasmid has also been established using the *lacO/LacI-GFP* system (Gordon *et al.*, 1997) and also by fluorescent *in situ* hybridization (FISH) (Niki and Hiraga, 1997). The position of F in *E. coli* is very similar to that of P1. F is localized at midcell in newborn cells and, following replication, is rapidly moved to the $\frac{1}{4}$ and $\frac{3}{4}$ positions of the cell. The plasmid foci remain at these positions until after cell division, when the cycle repeats itself.

Different groups have reported similar patterns of F plasmid localization (Gordon *et al.*, 1997; Niki and Hiraga, 1997). The localization of F SopB has been more contentious. In one study, SopA and SopB, each fused to the T7-Tag, were localized by immunofluorescence

microscopy (Hirano *et al.*, 1998). Both proteins formed foci in the presence of *sopC*. In the absence of *sopC*, but in the presence of both SopA and SopB, both proteins were dispersed throughout the cell. Differences were observed, however, when each protein was expressed alone. SopA localized exclusively to the nucleoid and SopB was distributed in the cytosolic spaces. Therefore the formation of SopA and SopB foci is dependent on the presence of the *cis*-acting DNA site and each protein affected the localization of the other. The dependence of SopB on *sopC* for foci formation is consistent with the results obtained using P1 ParB (Erdmann *et al.*, 1999) in which ParB foci did not form in the absence of *parS* (see section I-6.1). Perhaps as a consequence of overexpression (see below), several protein foci (4-10) were observed in cells and therefore the SopA-SopB-*sopC* foci were not exclusively at the cell $\frac{1}{4}$ and $\frac{3}{4}$ positions. Nonetheless, the protein foci were not localized to the cell poles, consistent with F plasmid localization.

In contrast, Kim and Wang (1998) found that SopB-GFP localized close to the cell poles, independent of both *sopC* and of SopA. Deletion analysis of SopB indicated that a region near the N-terminus of SopB was sufficient to effect this cellular localization. The authors suggested that SopB localized to these positions to keep the F plasmid pairs apart while the septum forms.

In both these studies (Hirano *et al.*, 1998; Kim and Wang, 1998) the proteins were overexpressed. Therefore, the physiologically relevant localization could have been masked in one or both of these studies. T7-tagged SopB was shown to be functional for partition (Hirano *et al.*, 1998) but while SopB-GFP was able to mediate gene silencing, it was not tested for function in partition (Kim and Wang, 1998). Therefore SopB-GFP may be deficient in some aspect of partition, and its localization may be aberrant. It is also possible that the fraction of SopB-GFP bound and localized to *sopC* is not visible over the background of overexpressed SopB-GFP in the cell.

I-6.3 R1: The intracellular localization of R1 was examined using the *lacO/LacI-GFP* system (Jensen and Gerdes, 1999). In cells containing one focus, it was found either at midcell or near one pole. In cells with two foci, they were most often found at opposite poles of the cell. In a few cases two foci were observed close to each other at midcell or in intermediate positions. In these cases, the locations of plasmids were symmetrical with respect to mid-cell, suggesting the plasmids were en route from midcell to the cell poles following replication. The fact that few such intermediates were observed suggests that the plasmids rapidly migrate away from each other and toward the poles.

The localization of ParM (the ATPase) was determined using immunofluorescence microscopy and a ParM-GFP fusion protein (Jensen and Gerdes, 1999). In both cases, newborn cells had two ParM foci, one at either pole. As the cells grew, an additional ParM focus formed at midcell and was then duplicated. As the cells continued to grow, the two new foci migrated apart and the septum formed between them resulting in newborn cells with two polar foci. This pattern of localization was independent of any other components of R1.

The ParM foci co-localized with the R1 plasmid (Jensen and Gerdes, 1999). ParM does not interact directly with the plasmid partition site, *parC*, but does interact with ParR that is bound to *parC* (Jensen *et al.*, 1998) and in this way might tether the plasmid to the polar region. In general, there were more ParM foci than plasmid foci, suggesting that the additional protein foci may prepare for plasmid segregation in the next cell cycle. The authors (Jensen and Gerdes, 1999) proposed the following model. Following replication, the plasmids pair via *sopC* (Jensen *et al.*, 1998) at midcell. They are then separated and are somehow actively moved to opposite poles, essentially being passed from a central ParM focus to a polar ParM focus.

Localization of R1 is different from that of either P1 or F. The two latter plasmids are both localized to the cell $\frac{1}{4}$ and $\frac{3}{4}$ positions (Gordon *et al.*, 1997; Niki and Hiraga, 1997),

whereas R1 is localized to the cell poles (Jensen and Gerdes, 1999). Localization of R1 and the ParM protein is more similar to that of chromosomal *oriC* regions (Gordon *et al.*, 1997; Webb *et al.*, 1997; Hiraga *et al.*, 1998; Niki and Hiraga, 1998; Niki *et al.*, 2000) and chromosomal partition proteins such as *B. subtilis* Spo0J and *C. crescentus* ParB (Glaser *et al.*, 1997; Lin *et al.*, 1997; Mohl and Gober, 1997) (see sections III-1.1 and III-2).

I-7 Importance of the cell $\frac{1}{4}$ and $\frac{3}{4}$ positions

Both P1 and F are localized to the $\frac{1}{4}$ and $\frac{3}{4}$ positions of the *E. coli* cell (Gordon *et al.*, 1997; Niki and Hiraga, 1997) (Figure 1-7). How are these plasmids tethered to these locations? What cellular component(s) are involved? Despite many investigations (e.g. (Ezaki *et al.*, 1991; Funnell and Gagnier, 1995; Xu, 1995; Surtees, 1996; Erdmann, 1998), no *E. coli* proteins other than IHF (Funnell, 1988b) have been found that directly affect plasmid partition. However, one possible mechanism for plasmid localization is interaction with the replication machinery.

PolC, the catalytic subunit of DNA polymerase in *B. subtilis*, has been visualized (Lemon and Grossman, 1998). PolC-GFP localized to discrete positions in the cell, primarily at or near midcell, rather than being randomly distributed throughout the cell as might be expected if the polymerase moved along the DNA strands. These observations indicate that PolC is anchored in the centre of the cell and the DNA template moves through a stationary replication factory. Recently, *E. coli* SeqA was localized to the $\frac{1}{4}$ and $\frac{3}{4}$ positions of *E. coli* (Hiraga *et al.*, 1998). SeqA regulates initiation of DNA replication by sequestering hemi-methylated, or newly replicated, DNA (Lu *et al.*, 1994; Slater *et al.*, 1995; Bahloul *et al.*, 1996; Boye *et al.*, 1996) and its position may indicate the location of a stationary replisome in *E. coli*. If the replisome is in a fixed position, it would be an attractive target for components of plasmid partition systems (Fig. 1-7).

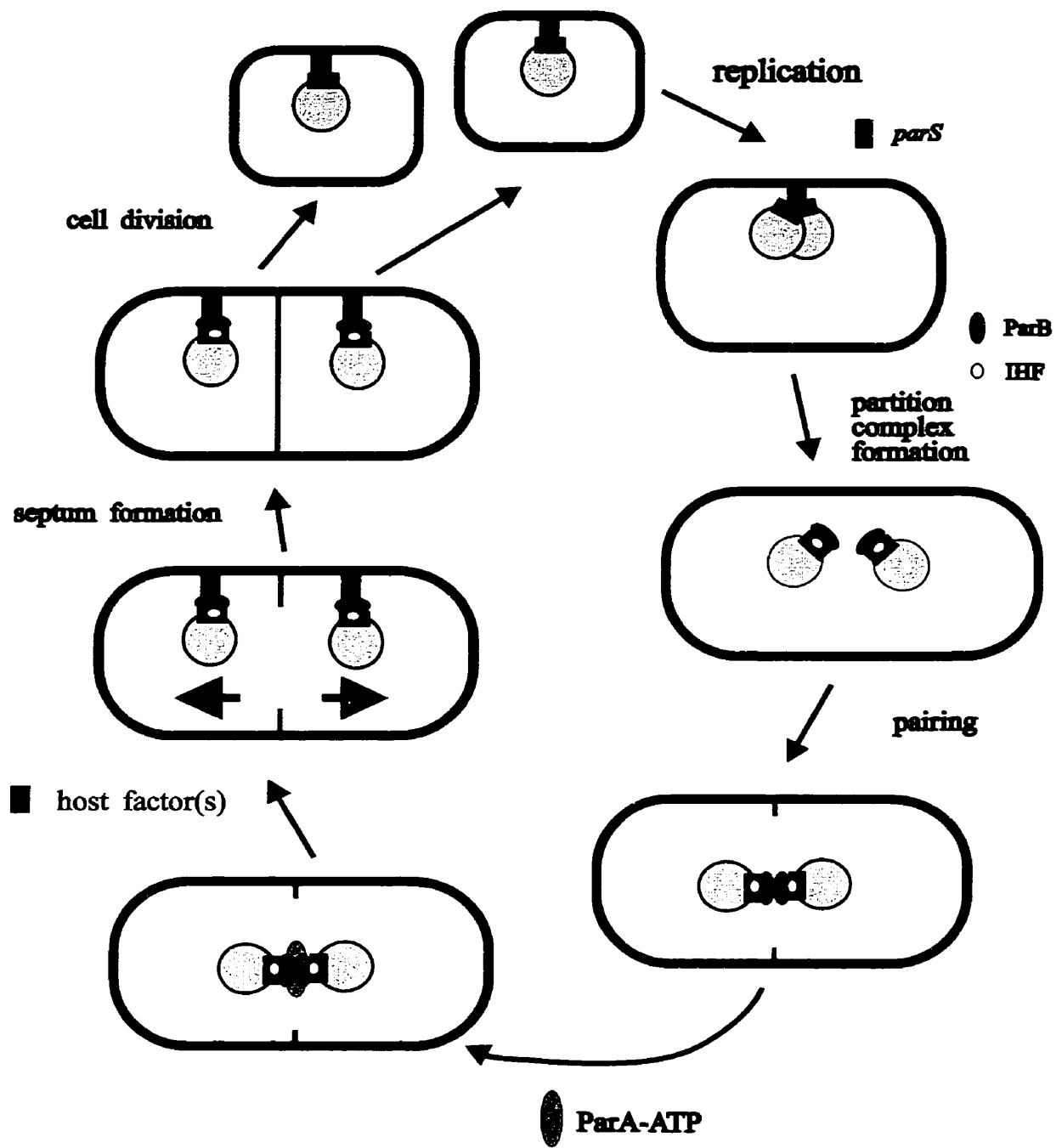


Figure 1-7. Model of the P1 partition cycle. In new-born cells, P1 is positioned at mid-cell, then replicated. ParB and IHF bind *parS* to form the partition complexes. The complexes pair, presumably at mid-cell, and set up directionality of separation. ParA-ATP interacts with the paired plasmids and somehow initiates separation and/or positioning. The separated plasmids are specifically positioned at the cell quarter positions prior to cell division. The pink circles represent plasmids, the blue boxes represent *parS*, the purple ovals and yellow circles represent ParB and IHF, respectively. The orange oval represents ParA-ATP dimers and the red box represents host factor(s). The model is described in more detail in the text.

II. Additional factors in plasmid stability

II-1 Plasmid copy number control

Plasmid maintenance within a bacterial population must be balanced with any selective disadvantage the plasmid may impose upon the cell. Small plasmids make few metabolic demands of the cell and therefore can be maintained at high copy number. These plasmids are randomly distributed at cell division. Consequently efficient control of the copy number of such plasmids is crucial in order to avoid a high frequency of plasmid loss.

The P1 prophage is very large, about 90 kb, and is maintained at a very low copy number, which would presumably minimize the metabolic burden on the cell (Prentki *et al.*, 1977). However, there must be two copies of the plasmid prior to cell division in order that both daughter cells receive one copy. Therefore tight regulation of P1 copy number is essential for both plasmid maintenance and optimal cell growth. Such regulation is established by two mechanisms: control of plasmid replication initiation and site-specific recombination to resolve plasmid multimers following replication.

II-1.1 Replication control: RepA is the replication initiator protein encoded by P1 (Abeles, 1986). The replication region of P1 contains a “copy-number control” locus, *incA*, which consists of nine repeats of a DNA sequence that is specifically recognized by RepA (Pal *et al.*, 1986). Five copies of these “iterons” are found within the plasmid origin, *oriR* (Chattoraj *et al.*, 1985; Abeles, 1986). RepA binding to both regions mediates interactions between *incA* and *oriR*, through RepA protein-protein interactions (Pal and Chattoraj, 1988). Such DNA looping has been observed by electron microscopy (Chattoraj *et al.*, 1988; Pal and Chattoraj, 1988). These interactions, called handcuffing, inhibit DNA replication, probably by steric hindrance (Pal and Chattoraj, 1988). As the copy number is increased by replication, the number of sites

available for RepA to bind also increases. This increases the number of possible “handcuffing” interactions, thereby inhibiting further replication.

II-1.2 Multimer resolution: Homologous recombination can occur between sister plasmids, resulting in oligomeric plasmids. Plasmid multimerization reduces the number of segregating plasmid units in a cell and leads to plasmid loss. This is a particular concern for plasmids such as P1, whose copy number is already very low. To alleviate this problem, several plasmids use site-specific recombination. In some cases, the plasmid encodes its own site-specific recombination systems. The Cre-*loxP* system, used extensively to promote site-specific recombination in eukaryotic molecular biology, is the P1 system whose primary function is to aid plasmid stability. P1 encodes the Cre recombinase that mediates site-specific recombination between two *loxP* sites, each 34 bp in length (Austin *et al.*, 1981). Other plasmids use host recombinases to effect resolution. One example of this is the ColE1 plasmid that directs the *E. coli* XerC and XerD proteins to its recombination site, *cer* (Colloms *et al.*, 1990; Clerget, 1991; Blakely *et al.*, 1993).

II-2 Post-segregational killing

One way used by a variety of plasmids to ensure their survival within a bacterial population is to eliminate any cells that have lost the plasmid. To do this, many plasmids encode post-segregational killing systems, also called plasmid-addiction systems. In these systems, the plasmid encodes a poison and an antidote to the poison. The poison is very stable, whereas the antidote is rapidly degraded. Therefore once a cell loses the plasmid, the poison remains but the antidote does not and the cell is killed. The killing system of P1 consists of two proteins: Doc (death on curing), the toxin, and Phd (prevent host death), the antidote (Lehnherr *et al.*, 1993). Doc is a stable protein that is resistant to proteolysis, while Phd is efficiently degraded by the ClpXP-protease system (Lehnherr and Yarmolinsky, 1995). Therefore continual expression of

Phd is required to prevent toxicity by Doc (Lehnherr and Yarmolinsky, 1995). The cellular target of Doc is unknown. Phd has been shown to interact directly with Doc to form a heterotrimeric complex (P₂D) that is thought to inhibit the toxic activity of Doc (Gazit and Sauer, 1999).

Killing systems have also been identified in other plasmids. The F plasmid encodes the *ccd* system in which CcdB is the toxic protein and CcdA is the antidote protein (Hiraga *et al.*, 1986). CcdB targets gyrase and causes double strand breaks in the chromosome (Bernard and Couturier, 1992). CcdA binds directly to CcdB to inactivate it (Maki *et al.*, 1992). The R1 plasmid encodes an RNA killing system. The toxin is the *hok* mRNA and the antidote (Sok) is a small antisense RNA that prevents translation of the *hok* mRNA (Gerdes *et al.*, 1986; Gerdes *et al.*, 1990). The *hok* mRNA encodes two reading frames, *hok* (host killing) and *mok* (modulation of killing) that are translationally coupled (Thisted and Gerdes, 1992). The Hok protein kills cells by damaging the cell membrane (Gerdes *et al.*, 1986). Sok-RNA represses *hok* translation indirectly through *mok* by binding the *mok* translational initiation region (Thisted *et al.*, 1994).

Chromosomal homologues of the killer, or addiction, modules have also been described (Masuda *et al.*, 1993). The *mazEF* operon of *E. coli* (Metzger *et al.*, 1988), also called *chpA* (Masuda *et al.*, 1993), is one such system. MazE is a labile protein that is degraded by the ClpPA serine protease and protects the cell from the effects of MazF, the stable toxin (Aizenman *et al.*, 1996). Expression of *mazE* and *mazF* is controlled by the cellular levels of ppGpp, which increase under conditions of nutritional stress. Increasing ppGpp inhibits *mazEF* gene expression (Aizenman *et al.*, 1996). The labile MazE is thus degraded and not replaced, leaving the stable MazF protein to kill the cell. It has been speculated that the *mazEF* operon mediates programmed bacterial cell death upon starvation (Aizenman *et al.*, 1996).

III. Bacterial Chromosome Segregation

The mechanism of chromosome segregation in bacteria is not well understood.

Interestingly, homologues of plasmid partition systems have been detected in a number of different bacterial chromosomes, although not in the chromosome of *E. coli*, and several are involved in chromosome segregation (see section III-2) (Ireton *et al.*, 1994; Mohl and Gober, 1997; Webb *et al.*, 1997; Gerdes *et al.*, 2000).

III-1 Chromosome positioning

Less than 0.03% of *E. coli* cells are anucleate (Hiraga *et al.*, 1989), but how is the stability of the chromosome maintained? Is there a bacterial mitotic apparatus? In early reports, stained chromosomes were visualized to track their movement. Rapid movement of the stained chromosomes from mid-cell to the $\frac{1}{4}$ and $\frac{3}{4}$ positions of the cell was initially interpreted as evidence for active segregation, presumably via a mitotic-like mechanism (Donachie and Begg, 1989; Hiraga *et al.*, 1990). However, this conclusion was based on measuring movement of the nucleoid centre. Later, similar experiments were performed and movement of the nucleoid was measured with respect to the nucleoid borders. The latter measurements implied that the chromosomes moved slowly and continuously toward the cell poles throughout the cell cycle (vanHelvoort and Woldringh, 1994) and therefore that chromosome segregation was a passive process dependent on cell growth.

III-1.1 Chromosome localization: Is chromosomal segregation active or passive? This question has been answered by recent advances in cell biology allowing visualization of bacterial chromosomes and proteins in fixed and/or live bacterial cells (Glaser *et al.*, 1997; Gordon *et al.*, 1997; Lin *et al.*, 1997; Mohl and Gober, 1997; Webb *et al.*, 1997; Hiraga *et al.*, 1998; Lin and Grossman, 1998; Niki and Hiraga, 1998; Webb *et al.*, 1998; Marston and Errington, 1999; Quisel *et al.*, 1999; Niki *et al.*, 2000). In these studies, chromosomes were specifically oriented and

rapidly segregated toward opposite cell poles, strongly supporting an active mechanism of chromosome segregation in bacteria.

Specific regions of the chromosome in *E. coli* and *B. subtilis* were visualized directly in one of three ways. First, tandem copies of the *lac* operator of *E. coli* were integrated into specific regions of the chromosome and GFP-LacI fusion proteins were expressed in these cells (Gordon *et al.*, 1997; Webb *et al.*, 1997; Webb *et al.*, 1998). Second, fluorescently labeled probes corresponding to different chromosomal loci were hybridized with the chromosome in fixed cells (FISH) (Niki and Hiraga, 1998). Finally, different regions of the *B. subtilis* chromosome were labeled with the nucleotide analogue BrdU (5-bromodeoxyuridine) and α -BrdU antibodies were visualized with fluorescent secondary antibodies (Lewis and Errington, 1997).

The chromosomes of *E. coli* and *B. subtilis* showed very similar localization patterns within the cell. In both bacteria, the replication origin region (*oriC*) was polarly localized (Gordon *et al.*, 1997; Webb *et al.*, 1997; Niki and Hiraga, 1998; Webb *et al.*, 1998; Niki *et al.*, 2000). After replication of the region, one *oriC* moved to the opposite cell pole. Time lapse microscopy of this movement in *B. subtilis* indicated that the *oriC* regions moved apart very rapidly, with a maximum velocity of $> 0.27 \mu\text{m}$ per minute in an 11 minute burst in cells with a doubling time of over 100 minutes and an average cell length of approximately $2 \mu\text{m}$. For the sake of comparison, the growth rate of the cells was approximately 0.011 - $0.025 \mu\text{m}$ per minute (Webb *et al.*, 1998). In contrast, the terminus region of the chromosome (*ter*) was generally localized at mid-cell (Gordon *et al.*, 1997; Webb *et al.*, 1997; Niki and Hiraga, 1998; Webb *et al.*, 1998; Niki *et al.*, 2000). Prior to cell division, the duplicated termini separated and the septum formed between them (Gordon *et al.*, 1997; Webb *et al.*, 1997; Niki and Hiraga, 1998; Webb *et al.*, 1998). Even very young (i.e. short) cells had duplicated *oriC* regions at opposite

poles of the cell (Gordon *et al.*, 1997; Webb *et al.*, 1997; Niki and Hiraga, 1998; Webb *et al.*, 1998; Niki *et al.*, 2000). In these cells, replication of the chromosome was not complete. Therefore bipolar migration of *oriC* regions occurred during ongoing replication.

III-2 Chromosome partition systems

The specific orientation of the chromosome throughout the cell cycle implies a mechanism that organizes the chromosome and ensures that it is localized, i.e. a partition system. Recently, homologues of P1 *parA* and *parB* have been identified in the chromosome of a number of different bacteria, including *Pseudomonas putida*, *B. subtilis*, *Caulobacter crescentus*, *Streptomyces coelicolor*, *Borrelia burgdorferi*, *Mycobacterium tuberculosis* and *Mycobacterium leprae* (Ogasawara and Yoshokawa, 1992; Fraser *et al.*, 1997; Mohl and Gober, 1997; Gal-Mor *et al.*, 1998; Kim *et al.*, 2000). The *par* regions are, in general, linked to the *oriC* region of the chromosome. The genetic organization of the *parAB* loci is, in many cases, similar to that of the plasmid partition systems (e.g. P1 and F), including inverted repeat sequences downstream of the *parB* component that may be centromere-like sites. No *par* region has been identified in the chromosome of *E. coli*.

III-2.1 *Streptomyces coelicolor*: Deletion analysis of the *parAB* locus of *S. coelicolor* showed that this region is involved in the proper segregation of its linear chromosome during sporulation (Kim *et al.*, 2000). When portions of *parB* or of *parA* and *parB* were removed, more than 13% of spore compartments did not inherit the full DNA complement. A potential *cis*-acting site, a 14 base pair inverted repeat to which the *parB* gene product might bind, was also identified (Kim *et al.*, 2000).

III-2.2 *Caulobacter crescentus*: In *C. crescentus*, the *parA* and *parB* genes are essential for cell viability (Mohl and Gober, 1997). The ParB protein binds specifically to an approximately 400 base pair DNA fragment immediately downstream of *parB*. The specific

binding site within this fragment has not yet been identified. Immunofluorescence microscopy revealed cell-cycle dependent localization of both ParA and ParB. Both proteins were dispersed throughout the cell until about 60% of the chromosome had been replicated. At this point, ParB was predominantly localized to the polar region. Upon completion of replication, both ParA and ParB exhibited bipolar localization. When DNA replication was inhibited, ParB tended to localize at midcell, suggesting that the polar localization is dependent on DNA replication and/or the subsequent movement of the chromosomes. This also suggests that the origin region of the chromosome is localized to the cell poles since the *parS* locus is near the origin. It is not clear whether ParA and ParB participate in chromosomal migration toward the poles or are simply carried to the poles when bound to the chromosomes. However, overexpression of either ParA or ParB, or both, resulted in mislocalization of ParB and a severe defect in chromosome partition, with at least 10% anucleate cells in the population. This suggests an active role for the Par proteins in properly orienting the chromosomes and promoting the segregation of sister chromosomes to opposite cell poles (Mohl and Gober, 1997).

III-2.3 *Bacillus subtilis*: The ParA and ParB homologues in *B. subtilis* are called Soj and Spo0J, respectively. The genes encoding these proteins were initially identified via their important roles in sporulation (Mysliwiec *et al.*, 1991) and they were later found to be involved in chromosome partition in both sporulating and vegetative cells (Ireton *et al.*, 1994; Sharpe and Errington, 1996).

Spo0J interacts with an origin-proximal region of the chromosome (Lewis and Errington, 1997; Lin *et al.*, 1997) and specifically recognizes a 16 base pair inverted repeat sequence (called *parS*) that occurs 10 times in the chromosome (Lin and Grossman, 1998). All copies are within the origin-proximal ~20% of the chromosome and eight are bound by Spo0J *in vivo*, as determined by chromatin immunoprecipitation experiments (Lin and Grossman, 1998). This

short DNA sequence is sufficient to stabilize a plasmid in *B. subtilis* in the presence of both Spo0J and Soj (Lin and Grossman, 1998). Thus Spo0J likely binds the *parS* sequences to form a large nucleoprotein structure that is involved in first pairing sister origins (analogous to the proposed plasmid pairing) and then in directing the chromosomes to their destinations within the cell. The cellular localization of Spo0J was determined by immunofluorescence microscopy in fixed cells and by following Spo0J-GFP fusions in living cells (Glaser *et al.*, 1997; Lewis and Errington, 1997; Lin *et al.*, 1997). Spo0J was positioned near the cell poles and was associated with the nucleoid. Following replication, two Spo0J foci separated, with one focus migrating to the opposite pole corresponding to the movement of the *oriC* region of the chromosome (see above). Both Spo0J and its binding site, *parS*, are conserved in a number of bacterial species, suggesting a common role for the pair in chromosome segregation.

The role of Soj, the ParA homologue, in chromosome segregation is not well understood. The protein is required to stabilize a plasmid containing the *B. subtilis parS* site (Lin and Grossman, 1998), but deletion of *soj* alone does not appear to cause a defect in partition of the bacterial chromosome (Ireton *et al.*, 1994). Soj negatively regulates the transcription of certain sporulation genes (Ireton *et al.*, 1994; Cervin *et al.*, 1998; Quisel and Grossman, 2000) by specifically interacting with their promoter regions (Cervin *et al.*, 1998; Quisel *et al.*, 1999; Quisel and Grossman, 2000). Spo0J is antagonistic to the repressor activity of Soj (Ireton *et al.*, 1994). In the absence of Spo0J, the interaction of Soj with the promoter regions increases, as determined by chromatin immunoprecipitation experiments (Quisel *et al.*, 1999; Quisel and Grossman, 2000).

Immunofluorescence microscopy did not reveal Soj localization. However, examination of Soj-GFP protein fusions in living, stationary phase cells revealed dynamic localization of the protein (Marston and Errington, 1999; Quisel *et al.*, 1999). Soj-GFP oscillates between large

nucleoid-associated patches and a polar localization on a time-scale of minutes. This may occur primarily in cells about to undergo sporulation, when establishing the appropriate regulatory pathway is important. In the absence of Spo0J, Soj remains associated with the nucleoid and does not dissociate. Furthermore, point mutations in the putative ATPase domain of Soj disrupted its localization and function, indicating that ATP binding and hydrolysis by Soj is required for its activity (Quisel *et al.*, 1999).

The nucleoid localization of Soj presumably occurs, at least in part, when the protein binds the promoters of sporulation genes. Given the importance of the putative ATP binding regions in Soj, it is possible that Soj activity is modulated by adenine nucleotides, analogous to P1 ParA (Bouet and Funnell, 1999). If so, one way that Spo0J could regulate Soj localization might be by affecting its ATPase activity, thereby regulating the proportions of Soj-ATP and Soj-ADP (Quisel *et al.*, 1999).

Interestingly, Soj also affects Spo0J localization (Marston and Errington, 1999). In a *soj* strain, the large, discrete Spo0J foci were replaced by smaller, scattered foci. These small Spo0J foci likely represent *parS*-binding, but in this case the *parS* sequences throughout the origin region of the chromosome have not converged. This suggests that Soj localization to the nucleoid also represents an involvement in organizing Spo0J foci, that is, in condensing the Spo0J-*parS* complexes from one chromosome into a single focus. Once the Spo0J nucleoprotein structures have been established, Soj leaves the nucleoid. This, in turn, would relieve repression of the sporulation initiation genes. Therefore Soj may act as a checkpoint protein, only allowing sporulation to initiate once the chromosome has been properly organized with Spo0J (Marston and Errington, 1999).

III-3 Model of chromosome segregation

The visual localization of chromosomal regions and of ParA- and ParB-like proteins in bacterial cells has provided strong evidence that chromosome segregation is an active process that requires some form of motive force to allow rapid separation of the origin regions. Several questions regarding the mechanism of separation remain. What energetic process drives the chromosomes apart? How is the ATPase activity of the ParA-like protein involved? How are the polar regions distinguished from other regions of the cell? While the answers to these questions are still unclear, a more coherent picture of chromosome positioning and segregation is emerging and the homologues of ParA and ParB play crucial roles in these processes. A model for chromosome partition is as follows. Spo0J/ParB binds its recognition sites within the origin-proximal region to form an important nucleoprotein structure. Soj/ParA promotes this organization. Once the origin is replicated, the Spo0J-DNA structure mediates sister chromosome pairing, thereby orienting the chromosomes. The origin regions are then actively separated, with one moving to the opposite end of the cell. Soj/ParA ATPase activity may aid in the migration of the sister chromosomes. The model is very similar to that for P1 plasmid partition (Fig. 1-7), except that the chromosomes, and particularly the *oriC* region, are targeted to a different region of the cell.

Lemon and Grossman (1998) proposed that extrusion of newly replicated DNA from a stationary replication factory located at midcell might be sufficient to separate sister chromosomes and direct them to opposite poles. However, time lapse microscopy experiments have shown that the *oriC* regions move apart quite suddenly and rapidly (Webb *et al.*, 1998) rather than gradually moving apart, as would be expected if replication was the only motive force for segregation. Therefore the replication machinery could initiate chromosome separation, but additional components may be required for rapid movement of the chromosomes. Alternatively,

the newly replicated *oriC* regions may be quickly separated, followed by slower movement of the rest of the chromosome.

III-4 Chromosome condensation

Recently, chromosome condensation has been found to play an important role in chromosome segregation. Decondensation causes segregation defects. The MukB protein of *E.coli* and the SMC proteins of other bacteria have a role in maintaining the structural organization of the chromosome.

III-4.1 *E. coli* Muk proteins: MukB is a 177 kDa protein with globular domains at both its amino- and carboxy-termini. The N-terminal globular domain has a Walker A-type NTP-binding domain and can bind and hydrolyze both ATP and GTP (Niki *et al.*, 1992; Lockhart and Kendrick-Jones, 1998). The C-terminal globular domain of MukB is essential for its DNA-binding activity, which appears to be non-specific (Saleh *et al.*, 1996), possibly mediated through putative zinc finger motifs (Niki *et al.*, 1991; Niki *et al.*, 1992). This domain also contains a putative Walker B nucleotide-binding motif (Melby *et al.*, 1998). MukB forms an anti-parallel homodimer via the central coiled-coil regions that form a flexible hinge region. This organization brings the N-terminal and C-terminal globular domains into close proximity at either end of the protein, bringing the putative Walker A and Walker B motifs close together (Melby *et al.*, 1998). Two proteins, MukE and MukF, interact directly with MukB (Yamanaka *et al.*, 1996; Yamazoe *et al.*, 1999). MukF is required in order for MukB and MukE to interact, indicating that MukF directly mediates MukBFE complex formation.

Initial reports emphasized the apparent structural similarities between MukB and eukaryotic motor proteins, such as myosin and kinesin heavy chains (Vale and Goldstein, 1990). More recently, however, structural similarities have also been noted between MukB and SMC (structural maintenance of chromosome) proteins. SMC proteins are structural proteins that were

initially identified in eukaryotic cells and are involved in chromosome condensation (see section III-4.2). Genetic experiments have also indicated that MukB has a role in establishing and/or maintaining the appropriate structure of the *E. coli* chromosome.

In *mukB* mutant cells, the *E. coli* nucleoid is unfolded and expands to fill the entire cell (Niki *et al.*, 1991). A similar phenotype was observed when *E. coli* cells were treated with camphor, a chemical that is lethal to *E. coli* (Hu *et al.*, 1996; Harrington and Trun, 1997). Overexpression of *crcA*, *cspE* and *crcB*, homologues of cold shock proteins, reversed the unfolding of the nucleoid, condensing it to occupy only about a third of the cell (Yamanaka *et al.*, 1994; Hu *et al.*, 1996) in the presence of either camphor or a mutation in *mukB*. These results suggested that MukB is involved in condensing the chromosome.

Further support for a structural role for MukB came when mutations in topoisomerase I were shown to suppress both point and null mutations of *mukB* (Sawitzke and Austin, 2000). These suppressor mutations led to excessive negative supercoiling of the chromosome by gyrase, thereby compacting the chromosome. Inhibition of gyrase by coumermycin reversed the suppressor effect of the topoisomerase I mutations. Furthermore, Muk mutants were hypersensitive to coumermycin in the absence of any other mutations. These observations led the authors to the conclusion that MukB is required to condense and organize the chromosome into a compact structure and that in the absence of MukB, excessive negative supercoiling can largely substitute for this condensation (Sawitzke and Austin, 2000). MukB is therefore thought to be functionally similar to the SMC (structural maintenance of chromosomes) proteins.

III-4.2 SMC proteins: SMC proteins are a family of proteins with homologues in bacteria, archaea and eukaryotes (Melby *et al.*, 1998). In eukaryotes, SMC proteins are involved in chromosome condensation and segregation (Koshland and Strunnikov, 1996; Hirano *et al.*, 1997), X chromosome dosage compensation (Lieb *et al.*, 1998), sister chromatid cohesion

(Guacci *et al.*, 1997; Michaelis *et al.*, 1997) DNA supercoiling (Kimura and Hirano, 1997) and DNA repair (Jessberger *et al.*, 1996).

SMC proteins have also been identified in many bacterial species, including *B. subtilis* (Britton *et al.*, 1998; Moriya *et al.*, 1998), *C. crescentus* (Jensen and Shapiro, 1999) and *M. tuberculosis* (Cole, 1998). The structural organization of SMC homodimers is very similar to that of MukB homodimers. The conserved Walker A and Walker B motifs are at opposite ends of each subunit and the two domains are separated by a long coiled-coil domain (Lockhart and Kendrick-Jones, 1998). Interestingly, neither *E. coli* nor *Haemophilus influenzae* has an *smc* gene, although both encode MukB.

Bacterial SMC proteins are involved in chromosome structure and segregation in *B. subtilis* (Britton *et al.*, 1998; Moriya *et al.*, 1998) and *C. crescentus* (Jensen and Shapiro, 1999). Subcellular localization of SMC in *B. subtilis* suggests that SMC acts at discrete loci on the chromosome and is loaded onto chromosomes from polar foci to facilitate chromosome condensation during or following DNA replication (Graumann *et al.*, 1998). Furthermore, *B. subtilis* SMC preferentially binds single-stranded DNA (ssDNA), leading to aggregation, likely through ATP-induced protein-protein interactions (Hirano and Hirano, 1998). *B. subtilis* SMC also has ssDNA-stimulated ATPase activity and it has been proposed that ATP regulates interactions between *B. subtilis* SMC molecules that are bound to different regions of ssDNA along the chromosome, leading to chromosomal compaction, or condensation (Hirano and Hirano, 1998).

Eukaryotic SMC proteins have been isolated as part of a multisubunit complex that is involved in both chromosome condensation and sister chromatid cohesion prior to separation at anaphase (Guacci *et al.*, 1997; Michaelis *et al.*, 1997). Prokaryotic SMC proteins may similarly provide a link between these two processes. Cells in which *smc* is disrupted have decondensed,

extended nuclei and Spo0J is mislocalized (Britton *et al.*, 1998; Moriya *et al.*, 1998). In *smc spo0J* double mutants, the partition defects are more severe than in either single mutant and many more cells have aberrant nucleoids (Britton *et al.*, 1998). SMC may facilitate the assembly of Spo0J-mediated paired complexes through its role in chromosome condensation (Britton *et al.*, 1998).

III-5 Chromosome separation

As with plasmids, newly relicated chromosomes must be single-copy units in order to be properly segregated prior to cell division. Chromosomes must be decatenated and monomerized and the processes that insure chromosome separation are similar to those that separate plasmids (see section II).

III-5.1 Chromosome decatenation: During chromosome replication, catenanes are formed, interfering with chromosome separation. *E. coli* encodes two type 2 topoisomerases, gyrase and topoisomerase IV. These enzymes make transient double strand breaks, through which another DNA piece can pass, then reseal the breaks. Both gyrase and topoisomerase IV consist of two subunits, encoded by *gyrA* and *gyrB* (gyrase) and *parC* and *parE* (topoisomerase IV). All of these genes are essential (Kato *et al.*, 1990; Luttinger *et al.*, 1991; Lynch and Wang, 1995). *In vivo* experiments have shown that topoisomerase IV is primarily responsible for chromosome decatenation (Adams *et al.*, 1992; Zechiedrich and Cozzarelli, 1995; Ullsperger and Cozzarelli, 1996). Gyrase, on the other hand, introduces negative supercoils in the DNA. Negative supercoiling provides superhelical tension that facilitates DNA melting for replication and transcription (Holmes and Cozzarelli, 2000). Negative supercoiling has also been implicated in chromosome condensation that is required for segregation (see section III-4) and that facilitates decatenation by topoisomerase IV (Holmes and Cozzarelli, 2000).

III-5.2 Multimer resolution: As with plasmids, sister chromosomes can be linked by homologous recombination, resulting in a circular dimer. In *E. coli* two site-specific recombinases, XerC and XerD, resolve these dimers. XerC and XerD bind co-operatively to a *dif* (deletion-induced filamentation) site in the terminus region of each chromosome (Blakely *et al.*, 1991; Kuempel *et al.*, 1991; Blakely *et al.*, 1993). XerC catalyzes the first strand exchange, producing a Holliday junction. XerD acts upon the Holliday junction, catalyzing a second strand exchange and generating recombinant products (Colloms *et al.*, 1996; Colloms *et al.*, 1997; Neilson *et al.*, 1999). FtsK is also required for XerC/XerD recombination at *dif* (Steiner *et al.*, 1999), probably to activate XerD strand exchange (Recchia *et al.*, 1999). Chromosomal dimers are thought to be the normal substrate for XerC/XerD recombination, so that site-specific recombination only occurs to generate monomeric chromosomes (Recchia *et al.*, 1999).

IV Thesis Rationale

ParB is a dimeric protein that binds *parS*, along with IHF, to form the partition complex. ParA interacts with the complex in an ATP-dependent manner. ParB also interacts with ParA in the absence of *parS* and stimulates ParA's biochemical activities. The work that I have done has focussed on determining the regions of ParB that are required for these different activities. I have defined the structural domains of ParB by limited proteolytic digestion. By deletion analysis of ParB I identified two regions of ParB that are involved in self-association, one at either end of the protein. Similarly, I localized the region of ParB required for ParA-ParB interactions to the extreme N-terminus of ParB. I have examined the stoichiometry of ParB binding to *parS* in partition complex formation. Finally, I identified the regions of ParB required for its DNA binding activity. I have found that 142-333 ParB contains all the information required to specifically bind *parS* in an IHF-stimulated manner. Within this fragment I have

tested the importance of the putative HTH and the C-terminal DRS and dimerization domains in *parS* binding activity. My results suggest a model of how a ParB dimer binds *parS* to form the minimal partition complex.

CHAPTER 2

The P1 ParB domain structure includes two independent multimerization domains

A version of this chapter has been published as:

Surtees, J.A. and B.E. Funnell (1999) *Journal of Bacteriology* **181**: 5898-5908.

I performed all of the experiments in this chapter.

Introduction

In this chapter I describe the use of limited proteolytic digestion of ParB to identify the resistant structural domains of the protein and begin to correlate these domains with function, specifically ParB's ability to dimerize.

The hydrodynamic and cross-linking properties of ParB indicate that it is an asymmetric dimer in solution (Funnell, 1991). However there are no canonical dimerization motifs, such as leucine zippers, in ParB and therefore the regions involved in dimerization are not obvious. Point mutations within the C-terminal region of ParB disrupt the protein's cross-linking activity, indicating that this region is important for dimerization (Lobocka and Yarmolinsky, 1996). In my Master's thesis, I began to define the boundaries of a C-terminal dimerization domain (Surtees, 1996). I produced a nested series of N-terminal fragments of ParB and tested them for an association with ParB missing the first 29 residues (30-333 ParB) in the yeast two-hybrid system. The C-terminal 59 residues of ParB were sufficient to interact with 30-333 ParB, but this C-terminal dimerization domain did not self-associate in this assay (Fig. 1-3).

Previous studies have indicated that ParB is involved in various types of self-association interactions. Excess ParB destabilizes plasmids containing *parS* (Funnell, 1988a). The data suggest that excess ParB self-associates and forms ParB-ParB-plasmid aggregates that cannot partition properly. Also, ParB can silence the expression of genes that are located near *parS* (Rodionov *et al.*, 1999), indicating that ParB binds *parS* and then polymerizes along the DNA, forming a nucleoprotein filament that extends beyond *par*. Finally, it has been proposed that plasmids pair during partition, mediated by ParB-ParB association (Nordstrom and Austin, 1989). A pairing interaction has been observed in an analogous plasmid partition system, that of the R1 plasmid. ParR, the ParB equivalent, binds DNA at *parC* and has an intrinsic pairing activity that is stimulated by ParM, the ParA analogue (Jensen *et al.*, 1998).

Limited proteolysis is a classical way to isolate and define functional domains within a protein (reviewed in (Konigsberg, 1995). Typically, at low protease concentrations, the more flexible linker regions of proteins are accessible to the protease and are cleaved, while the more stably structured regions are left intact. Recent examples of this approach include domain analysis of *Thermus thermophilus* UvrB protein (Nakagawa *et al.*, 1997), T4 intron-encoded I *TevI* endonuclease (Derbyshire *et al.*, 1997), the *Saccharomyces cerevisiae* transcription factor, Swi6 (Sedgewick *et al.*, 1998) and the human apurinic/apyrimidinic endonuclease (AP) (Strauss and Holt, 1998). SopB, a ParB homologue encoded by the F plasmid, has also been examined by limited proteolytic digestion (Hanai *et al.*, 1996) and the C-terminus of the protein was determined to be required for DNA binding activity *in vitro*. Here I show that the C-terminus of ParB forms a domain that is highly resistant to protease.

The yeast two-hybrid system, a genetic assay for protein-protein interactions performed in *S. cerevisiae* (Fields and Song, 1989), has been successful in identifying interacting partners in many eukaryotic systems (reviewed in (Fields and Sternglanz, 1994), and in several prokaryotic systems (Pichoff *et al.*, 1995; Huang *et al.*, 1996; Kiesau *et al.*, 1997; Wang *et al.*, 1997). A direct interaction between ParM and ParR of the R1 plasmid was initially demonstrated with the yeast two-hybrid system (Jensen and Gerdes, 1997). Self-association domains have also been identified by two-hybrid analysis (Creasy *et al.*, 1996; Zelicof *et al.*, 1996). I have previously demonstrated that ParB-ParB interactions can be detected in this manner (Surtees, 1996). In this study, I have used the yeast two-hybrid system as well as chemical cross-linking to further examine the self-association interactions of ParB.

Experimental Procedures

Bacterial and Yeast Strains. *Escherichia coli* DH5 [*F*⁻ *endA1 hsdR17* ($r_K^- m_K^+$) *supE44 thi-1 recA1 gyrA96 relA1*] was used for all plasmid constructions. *E. coli* BL21 [*F*⁻ *ompT hsdS_B* ($r_B^- m_B^-$) *dcm gal*] (λ DE3, pLysS) (Studier and Moffatt, 1986) and BB101 [*ara* Δ (*lac pro*) *halA argE* (Am) *rif thi-1* Δ *slyD* / *F*⁻ *lacI^f lacZ::Tn5 pro*⁺] (λ DE3) were used for fusion protein expression and purification.

Saccharomyces cerevisiae strain Y153 (*MATa gal4 gal80 his3 trp1-901 ade2-101 ura3-52 leu2-3,112 URA3::GALLacZ LYS2::GALHIS3*) (Durfee *et al.*, 1993) was used for the yeast two-hybrid analysis.

Media and Antibiotics. All bacterial cells were grown in LB medium or on LB plates (Sambrook *et al.*, 1989). The antibiotics and concentrations used were: ampicillin, 100 μ g/ml; chloramphenicol, 25 μ g/ml; and kanamycin, 25 μ g/ml. Yeast cells were grown in YPD medium (1% w/v yeast extract, 2% w/v Bactopeptone, 2% w/v glucose). Plasmid-containing yeast strains were grown in SD broth (0.67% w/v yeast nitrogen base, 2.5% w/v glucose) supplemented with the appropriate amino acids (tryptophan, 40 mg/L; leucine, 100mg/L; histidine, 20 mg/L; adenine, 40 mg/L; uracil, 20 mg/L). Agar was added to a concentration of 2% w/v for plates. To detect expression of the *HIS3* reporter gene, SD plates lacked histidine and contained 25 mM 3-amino 1,2,4-triazole (Durfee *et al.*, 1993).

Reagents and buffers. Sources for reagents were as follows: 3-amino 1,2,4-triazole, amino acids, dithiobis[succinimidyl propionate] (DSP), bovine serum albumin (BSA), guanidine hydrochloride (GuHCl), Sigma; trypsin and chymotrypsin, Worthington Biochemical; X-gal (5-bromo-4-chloro-3-indolyl β -D-galactopyranoside), Jersey Supply Lab; imidazole, Research Organics Inc.; yeast nitrogen base, Difco; Bradford reagent, Bio-Rad. Enzymes for cloning were purchased from New England Biolabs or Boehringer Mannheim. Resins used were Ni-NTA

resin (Qiagen) or Chelating Sepharose Fast-Flow (Pharmacia). The latter was pre-equilibrated with Ni²⁺ by washing twice with 4 volumes of sterile water, mixing with 2 volumes of 0.1 M NiSO₄ for at least 10 minutes and then washing with 5 volumes of water. The Ni²⁺-agarose resins were equilibrated with 10 volumes of the appropriate purification buffer before use. Sonication buffer was 50 mM Na-phosphate (pH 8.0), 300 mM NaCl, 7 mM β-mercaptoethanol. Wash buffer was sonication buffer with 10% (v/v) glycerol. Buffer A was 100 mM NaH₂PO₄, 10 mM Tris, 6 M guanidine-HCl, pH 8.0. Buffer F was 0.2 M acetic acid, 6 M guanidine-HCl.

Plasmid construction. The DNA encoding full-length ParA and ParB, and ParB fragments were cloned into one of four vectors for analysis in this work (Table 2-1). The vectors for the yeast two-hybrid system were pAS1 and pACTII (Durfee *et al.*, 1993) and for purification were either pET19b-HMK (Copeland *et al.*, 1996) or pJS124 (Table 2-1). To create pJS124, pET19b-HMK was digested with *Bam*HI and treated with Klenow DNA polymerase and dNTPs. Two complementary linkers, 5'GGATCCATGAGTGAGTGA and 5'TCACTCACTCATGGATCC, were then ligated into this site, creating a new *Bam*HI site and inserting stop codons in all three frames downstream of the *Bam*HI site. The stop codons provide translational stop signals for the 3' deletions of *parB*. The sequence of the linkers was designed to avoid hydrophobic residues at the C-terminus of the fusion proteins, to avoid targeting them for intracellular proteolysis (Bowie and Sauer, 1989; Parsell *et al.*, 1990).

Some of the plasmids used in this chapter, in particular plasmids used in the yeast two-hybrid analyses, were previously constructed as part of my M. Sc. work. These are indicated in Table 2-2. Parent *parB* plasmids were constructed for subsequent constructions. First, the *Dra*I site in P1 DNA downstream of *parB* was changed to a *Bam*HI site, and the resulting P1 *Bgl*II-*Bam*HI *parB* fragment was cloned into the *Bam*HI site of pBluescriptII SK+ (Stratagene), creating pJS9 and pJS10 (opposite orientations of the complete *parB* gene). Site-directed

TABLE 2-1. Vectors and P1 plasmids

<u>Vector</u>	<u>Description</u>	<u>Marker(s)^a</u>	<u>Reference</u>
pAS1	GAL4 DNA-binding domain vector	<i>TRP1</i> , Ap ^R	Durfee <i>et al.</i> , 1993
pACTII	GAL4 activation domain vector	<i>LEU2</i> , Ap ^R	Durfee <i>et al.</i> , 1993
pET19b-HMK	protein expression vector; N-terminal 10x histidine tag; heart muscle kinase (HMK) phosphorylation site	Ap ^R	Copeland <i>et al.</i> , 1996
pJS124	pET19b-HMK derivative; STOP codons inserted in all 3 frames at <i>Bam</i> HI site	Ap ^R	this study
pJS9	<i>parB</i> in pBluescript SK+	Ap ^R	Surtees, 1996
pJS10	<i>parB</i> in pBluescript SK+; opposite orientation of pJS9	Ap ^R	this study
pJS49	pJS10 with <i>Bgl</i> III site immediately upstream of <i>parB</i>	Ap ^R	this study

a. Ap^R indicates ampicillin resistance in *E. coli*. *TRP1* and *LEU2* are nutritional markers in *S. cerevisiae*

mutagenesis (Kunkel *et al.*, 1991) of pJS10 introduced a new *Bgl*III site upstream of the *parB* ATG, creating pJS49. The sequence was changed from 5' ACT GAG TAA GAT CTC CCC ATG to 5' ACT GAG ATC TAT CTC CCC ATG. The new *Bgl*III site allowed in-frame fusion of the *parB* ATG to the reading frames of the two-hybrid vectors and of pJS124.

The *parB* deletion plasmids were created by exonuclease III digestion of *parB* using a modified protocol from the NEB Biolabs Exo-Size kit. For 5' deletions, pJS9 was digested with *Kpn*I and *Eco*RI and then treated with exonuclease III. Exonuclease products were treated with mung bean nuclease and then Klenow DNA polymerase and dNTPs to ensure blunt DNA ends. Following ligation to 12 bp *Bam*HI linkers, the DNA was recircularized and used to transform *E. coli* DH5. The 3' deletions of *parB* were constructed in a similar manner, except that the starting plasmid was pJS49 (see above). The endpoint of each *parB* deletion was determined by dideoxy DNA sequencing (Pharmacia T7 sequencing kit) (Table 2-2). This process produced *parB* gene fragments flanked by *Bam*HI and/or *Bgl*III sites. Fragments in which the deletion was in the proper reading frame for insertion into the *Bam*HI sites of pAS1 and pACTII were chosen for the yeast two-hybrid experiments.

ParB fragments covering a wide range of sizes were selected for *in vitro* analyses. In most cases, the corresponding *parB* gene fragments were cloned as *Bam*HI or *Bam*HI/*Bgl*III fragments into the *Bam*HI site of pJS124 for protein purification. This created fragments fused to histidine Tag A (Fig. 2-1A). Several of the 5' deletions of *parB* were instead cloned into pET19b-HMK (Table 2-1). In this case, the vector was digested with *Xho*I and then treated with Klenow DNA polymerase and dNTPs. The plasmids bearing the *parB* fragments were digested with *Bam*HI and then treated with Klenow DNA polymerase. The blunt-ended DNA fragment was then ligated into pET19b-HMK. This cloning strategy removed the HMK sequence from the polyhistidine tag, resulting in Tag B (see Fig. 2-1A).

TABLE 2-2. Plasmids used for yeast two-hybrid analysis

<u>Plasmid</u>	<u>Vector</u>	<u>ParB fragment</u>	<u>Source</u>
pJS50	pAS1	FL-ParB	this study
pJS51	pACTII	FL-ParB	this study
pMR2*	pAS1	30-333 ParB	Surtees, 1996
pMR4*	pACTII	30-333 ParB	Surtees, 1996
pJS37*	pACTII	47-333 ParB	Surtees, 1996
pJS38*	pACTII	67-333 ParB	Surtees, 1996
pJS39*	pACTII	87-333 ParB	Surtees, 1996
pJS40*	pACTII	93-333 ParB	Surtees, 1996
pJS41*	pACTII	187-333 ParB	Surtees, 1996
pJS44*	pACTII	275-333 ParB	Surtees, 1996
pJS45*	pAS1	275-333 ParB	Surtees, 1996
pJS141	pACTII	1-312 ParB	this study
pMBP1	pACTII	1-293 ParB	this study
pJS136	pACTII	1-277 ParB	this study
pJS139	pACTII	1-234 ParB	this study
pJS140	pACTII	1-189 ParB	this study
pJS138	pACTII	1-177 ParB	this study
pJS137	pACTII	1-128 ParB	this study
pJS182	pACTII	1-61 ParB	this study
pJS181	pAS1	1-61 ParB	this study
pBEF217*	pACTII	FL-ParA	Surtees, 1996

* plasmids constructed for my Master's thesis (Surtees, 1996)

TABLE 2-3. Plasmids constructed for protein expression (all constructed for this study)

<u>Plasmid</u>	<u>Vector</u>	<u>ParB fragment^b</u>
pJS12	pET19b-HMK	FL-ParB (Tag A1)
pJS117	pET19b-HMK	47-333 ParB (Tag B)
pJS118	pET19b-HMK	67-333 ParB (Tag B)
pJS119	pET19b-HMK	87-333 ParB (Tag B)
pJS120	pET19b-HMK	93-333 ParB (Tag B)
pMD11	pET19b-HMK	152-333 ParB (Tag A2)
pMD12	pET19b-HMK	175-333 ParB (Tag A2)
pJS121	pJS124	187-333 ParB (Tag A3)
pMD13	pET19b-HMK	267-333 ParB (Tag A2)
pJS123	pJS124	275-333 ParB (Tag A3)
pJS172	pJS124	1-312 ParB (Tag A4)
pJS151	pJS124	1-293 ParB (Tag A4)
pJS128	pJS124	1-277 ParB (Tag A4)
pJS189	pJS124	1-274 ParB (Tag A4)
pJS146	pJS124	1-245 ParB (Tag A4)
pJS164	pJS124	1-234 ParB (Tag A4)
pJS143	pJS124	1-189 ParB (Tag A4)
pJS144	pJS124	1-188 ParB (Tag A4)
pJS145	pJS124	1-182 ParB (Tag A4)
pJS129	pJS124	1-177 ParB (Tag A4)
pJS166	pJS124	1-128 ParB (Tag A4)
pJS149	pJS124	1-114 ParB (Tag A4)
pJS148	pJS124	1-61 ParB (Tag A4)
pJS198	pJS124	47-177 ParB (Tag A3)

b. The sequence of the N-terminal tags is shown in Figure 2-1A.

Figure 2-1. A. Sequences of the N-terminal tags of the purified fusion proteins used in this chapter. Tags A1 to A4 are encoded by pET19b-HMK and pJS124. Slightly different versions of the tag were generated as a result of cloning from different sources. In tag B, the HMK sequence has been eliminated in the cloning procedure (see Experimental Procedures). The HMK recognition sequence is a phosphorylation site for the catalytic subunit of bovine heart muscle kinase. **B.** Sequences of ParB. The arrows indicate the N-terminus of each proteolytic fragment identified in this chapter. Bands A to E were generated by trypsin digestion. Band F was produced by chymotrypsin digestion.

To create the 47-177 ParB fragment, pJS18 (*parB* deleted for the nucleotides encoding amino acids 1-46 cloned into pBluescript SK+) was used as a substrate for PCR and the region encoding up to amino acid 177 was amplified. The upstream primer was the M13 reverse primer. The downstream primer (5' GCGCAGATCTTACAGCCCTTCTTTGGCTGC) changed amino acid 178 to a stop codon and created a *Bgl*III site to facilitate cloning. The PCR product was purified from an agarose gel, digested with *Bam*HI and *Bgl*III, and cloned into the *Bam*HI site of pJS124.

pBEF217 encodes a protein fusion of full-length ParA fused to the N-terminus of the GAL4 activation domain (Surtees, 1996; Surtees and Funnell, 1999).

Yeast two-hybrid analysis. Y153 cells were transformed by two different plasmids using an adaptation of a high efficiency transformation protocol (Gietz *et al.*, 1992). To test for expression of the *lacZ* reporter gene in yeast, transformants were grown as 1-2 cm patches on minimal plates. Cell patches were replica plated onto new plates overlaid with a #50 Whatman filter circle and incubated overnight at 30°C. Next, a #3 Whatman filter circle was immersed in 2.5 ml X-gal solution (60 mM Na₂HPO₄, 40 mM NaH₂PO₄, 10 mM KCl, 1 mM MgSO₄, 0.38 mM β-mercaptoethanol and 0.8% w/v X-gal) in a sterile Petri plate. The #50 replica filter was frozen in liquid N₂, warmed to room temperature, then overlaid colony side up on the saturated #3 circle. The plate was closed, wrapped in parafilm and incubated at 30°C. The time required for colour development ranged from 1 hour to overnight.

Protein purification. For native protein purification, a 500 ml culture of BL21(λDE3) pLysS cells transformed by a plasmid encoding a histidine-tagged ParB fusion protein was grown at 37°C in LB medium containing ampicillin and chloramphenicol to an A₆₀₀ of approximately 0.5. IPTG was added to 1 mM and the culture was incubated for an additional 2 hours at 37°C. The cells were collected by centrifugation, washed and resuspended in sonication

buffer and frozen in liquid nitrogen. The cells were thawed on ice, lysed by sonication bursts and centrifuged at 25,000x g for 1 hour at 0°C. The remaining steps were performed at 4°C. The supernatant was collected and loaded onto a small (0.5 – 1 ml) Ni²⁺-agarose column. The column was washed with 10 column volumes of sonication buffer and then with 20 column volumes of wash buffer. The fusion protein was then eluted in steps of increasing imidazole concentration. Most of the fusions eluted at about 400 mM imidazole and the majority of the ParB fragments purified well with this method. However, some fragments, particularly the small N-terminal fragments (1-33, 1-61 and 1-114 ParB), were much cleaner when purified with a denaturing protocol. This method did not affect the cross-linking of the proteins, as determined by examination of several proteins (His-ParB, 47-333 ParB and 1-293 ParB) that were purified in parallel using both methods.

For denaturing purification, *E. coli* BB101 cells were used. The deletion of *slyD*, whose gene product is a histidine-rich protein that binds nickel affinity chromatography resin, results in cleaner purifications, particularly in denaturing protocols. A 25 ml culture of BB101 cells transformed by a plasmid encoding a ParB fusion protein was grown at 37°C in LB medium containing ampicillin and kanamycin to an A₆₀₀ of approximately 0.8. IPTG was added to 1 mM and the culture was incubated at 37°C for another 2 hours. The cells were collected by centrifugation, resuspended in 0.75 ml Buffer A and mixed gently by slow rotation at room temperature for at least one hour. The lysate was centrifuged at 14,000 rpm for 15 minutes in a microfuge. The supernatant was removed and mixed gently with 75 µl of Ni²⁺-agarose resin at room temperature for 15 minutes. The resin was collected by centrifugation and washed three times with 1 ml of Buffer A. To elute protein, the resin was mixed with 750 µl Buffer F, and re-centrifuged. The supernatant was collected and dialysed against decreasing concentrations of guanidine-HCl until the protein was in wash buffer.

ParB (with no His-tag) was purified as described previously (Funnell, 1991; Davey and Funnell, 1994). Protein concentrations were determined by Bradford protein assay (Bradford, 1976).

DSP cross-linking. Protein samples were diluted to between 5 µg/ml and 20 µg/ml in 50 mM HEPES-KOH, pH 7.5; 150 mM NaCl; 0.1 mM EDTA. DSP (20 mg/ml in dimethylformamide) was added to 0.1 mg/ml, and the mixtures were incubated at room temperature. To stop the cross-linking reaction and to precipitate the protein, 750 µl samples were removed, mixed with an equal volume of 30% (v/v) trichloroacetic acid and incubated on ice for 20 minutes. The precipitate was collected by centrifugation at 4°C, washed with acetone and resuspended in 30 µl of 62.5 mM Tris-HCL (pH 6.8), 2% (w/v) SDS, 10% (v/v) glycerol and 0.025% (w/v) bromophenol blue. The samples were incubated at 90°C for 3 minutes and then analysed by SDS-polyacrylamide gel electrophoresis.

Proteolysis. ParB or ParB fragments were incubated with trypsin or chymotrypsin in 50 mM Tris-HCl (pH 7.5); 100 mM NaCl; 0.1 mM EDTA and 20% (v/v) glycerol at room temperature. The protein:protease ratios used ranged from 100:1 to 5000:1 (w/w), and are indicated in the figure legends. Digestion was stopped by the addition of acetic acid to 1% (v/v). For sequencing of the N-termini, proteolytic digestions were flash frozen on dry ice and stored at -20°C.

Protein sequencing. The protein products were separated by electrophoresis in a 15% SDS-polyacrylamide gel and then were transferred to a PVDF membrane using a Multiphor II Electrophoresis system (Pharmacia). The filter was rinsed several times in distilled water and stained with 0.2% (w/v) Coomassie Blue in 50% (v/v) methanol for 5 minutes. The filter was destained with several washes of 50% methanol, air-dried, wrapped in plastic and stored at -20°C.

Sequencing was performed at the HSC Biotechnology Service Centre, Toronto, Ontario, Canada and at the Alberta Peptide Institute, Edmonton, Alberta, Canada.

Results

ParB is a multifunctional protein with several different biochemical activities. These include its ability to dimerize, its specific DNA binding to sequences within *parS* and its interaction with ParA. It may also be involved in interactions with host cell components required for partition. In this work, I took two different approaches to identify and map the structural and functional domains in ParB. One approach was to use proteolytic digestion to analyse the domain structure of the protein. I also assayed fragments of ParB for dimerization activity to define functional domains.

Proteolytic digestion of ParB. I first treated ParB with low concentrations of trypsin, a protease that cleaves on the carboxy side of lysine and arginine residues (Konigsberg, 1995), and examined the digestion patterns by gel electrophoresis (Fig. 2-2). I compared this pattern to that produced from a version of ParB that was tagged at its N-terminus with a polyhistidine sequence (Fig. 2-2). ParB and His-ParB contain 55 and 59 arginine + lysine residues, respectively. After tryptic digestion of ParB and His-ParB, a discrete pattern of proteolytic products was seen. The major proteolytic fragments were identified by sequencing their N-termini (Fig. 2-1 and Table 2-2). The first major fragment that appeared migrated at about 32 kDa (Fig. 2-2, Band A) and started at amino acid 83. At later time points, a smaller band with an apparent size of 30 kDa (Band B), starting at residue 124 was produced. With more extensive digestion, two fragments (Band C and Band D) were generated, with apparent sizes of 25 kDa and 18 kDa, respectively. The latter two fragments began at residues 142 and 185, respectively, and persisted, even after very long periods of digestion. A smaller fragment of about 10 kDa (starting at residue 263) would occasionally be seen, especially in digestions performed at 30°C (Fig. 2-3), but in general Bands C and D were particularly resistant to further proteolysis. Note that the sizes cited here are only estimates (apparent molecular mass) because ParB runs anomalously on SDS-PAGE.

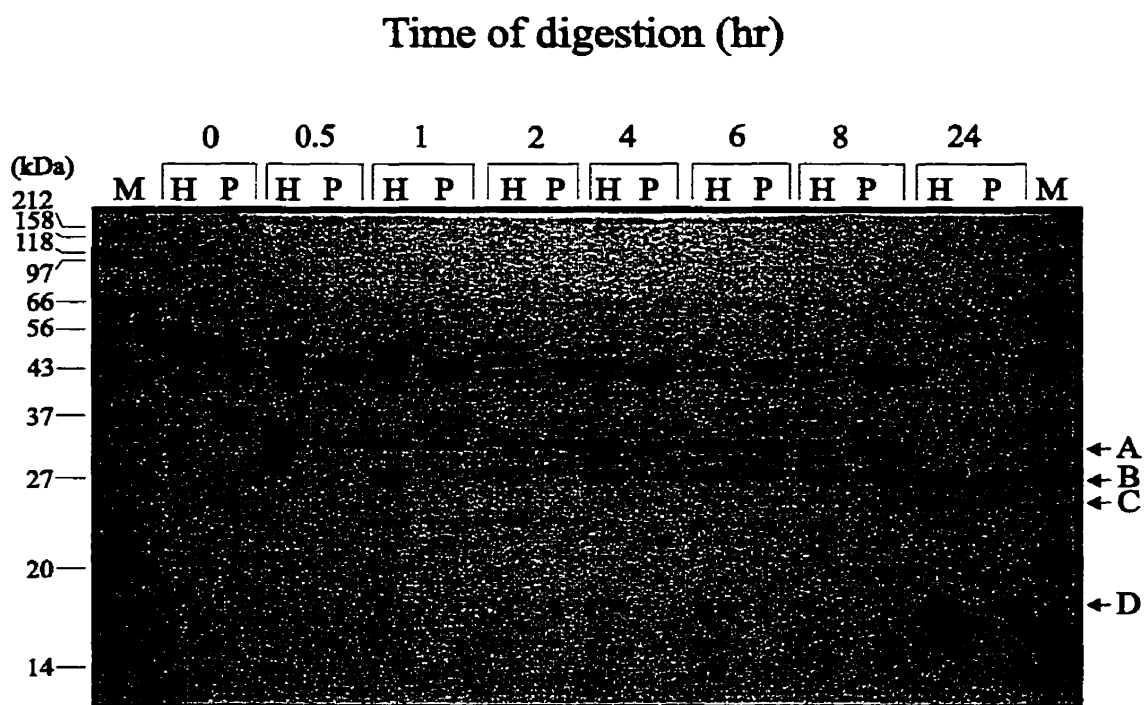


Figure 2-2. Tryptic digestion of ParB and His-ParB. ParB (P) and His-ParB (H) were treated with trypsin at a protein:protease ratio of 1000:1 (w/w) at 20 C for the indicated times. Digestion was stopped with 1% acetic acid. Proteolytic fragments were separated by electrophoresis in 15% SDS polyacrylamide gels and were visualized with Coomassie Blue. Undigested ParB and His-ParB migrate with 44 kDa and 50 kDa proteins, respectively. The arrows to the right of the figure indicate the major tryptic fragments identified in Table 2. M denotes size markers.

The calculated molecular masses of ParB and His-ParB are 38.5 kDa and 41.7 kDa, respectively, but they migrate at about 44 kDa and 50 kDa respectively.

The cleavage patterns of both proteins were very similar. The main difference was that His-ParB digestion generated a number of fragments that migrated slightly faster than the intact protein, which likely represent removal of the His-tag from His-ParB (these fragments no longer bound to Ni²⁺ affinity resin; data not shown). The similarity in rate and pattern of cleavage for both native and His-tagged ParB indicated that the N-terminal tag did not significantly alter the conformation of ParB. Consequently, to simplify purification of the truncated versions of ParB, I have used the His-tagged versions of ParB and ParB fragments for domain analysis.

Next I asked if chymotrypsin, which cleaves on the carboxy side of hydrophobic residues (Konigsberg, 1995) detects similar domains in His-ParB (Fig. 2-3). Several fragments with sizes similar to those produced by trypsin were observed. Specifically, Band F (Fig. 2-3) appeared only slightly larger than Band A, and was found to begin at amino acid 79, which was very close to the initial tryptic cleavage. The proteolytic data indicate that the N-terminal approximately 80 amino acids of ParB are relatively accessible to protease and are rapidly digested, suggesting that this region is less stably folded under these conditions.

Bands B, C, D and E represent increasingly C-terminal portions of ParB. Since these fragments, particularly Band D (starting at amino acid 185) and Band E (starting at amino acid 263), were observed only in the later time points, I concluded that they must be derived from the larger fragments that are subsequently reduced or disappear. All these proteolytic fragments migrated more slowly than predicted for fragments that extend to the C-terminus (Fig. 2-3) and Table 2-2), suggesting that the C-terminus is included in these fragments.

I compared the proteolytic patterns of digestion of full-length ParB with those of two C-terminal fragments and two N-terminal fragments of ParB (Fig. 2-4). The two C-terminal

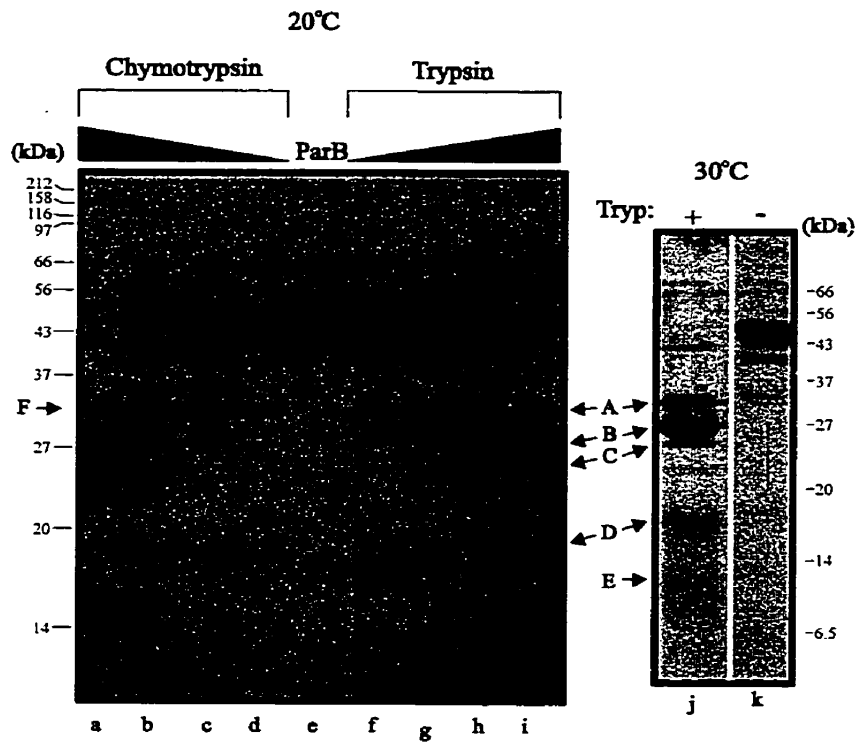


Figure 2-3. Chymotrypsin and trypsin digestion of His-ParB. In the left panel, five micrograms of protein were incubated with increasing amounts of protease for 2 hours at room temperature. Protein to protease ratios (w/w) were: lanes a and i) 100:1; lanes b and h) 500:1; lanes c and g) 1000:1; lanes d and f) 5000:1; and lane e) no protease. The arrows indicate the fragments whose N-termini were sequenced. The right panel shows a tryptic digest (protein:protease ratio of 1000:1) performed at 30 C for 7.5 hours and illustrates an additional band (E) that was also sequenced. The positions of size markers are indicated beside each gel.

TABLE 2-4. N-terminal sequences of proteolytic fragments generated by trypsin and chymotrypsin

<u>Band^a</u>	<u>N-terminal sequence^b</u>	<u>Starts at #</u>	<u>Molecular Mass (kDa)^c</u>	
			<u>Apparent (on gel)</u>	<u>Predicted (to C-terminus)</u>
A	?-Thr-Ile-Lys-His-Gln	83	32.2	28.4
B	Val-Leu-Val-Thr-Asp	124	27.9	23.9
C	Asp-Val-Gln-Thr-Ala	142	26.8	21.9
D	Ala-Leu-Gln-Ala-Ala	185	17.6	17.1
E	Glu/Gly-?-?-?-Leu	263	9.1	8.4
F	Lys-?-Ile-Arg-Ser-Thr	79	32.2	28.9

a. The bands refer to those indicated in Figures 2-2, 2-3 and 2-4.

b. The sequences were determined by Edman degradation and the first 5 or 6 residues are shown. Despite blanks in some sequences, each was consistent with only one position in ParB assuming that each N-terminal residue was preceded by either an arginine or a lysine for tryptic fragments and by a hydrophobic residue for chymotryptic fragments.

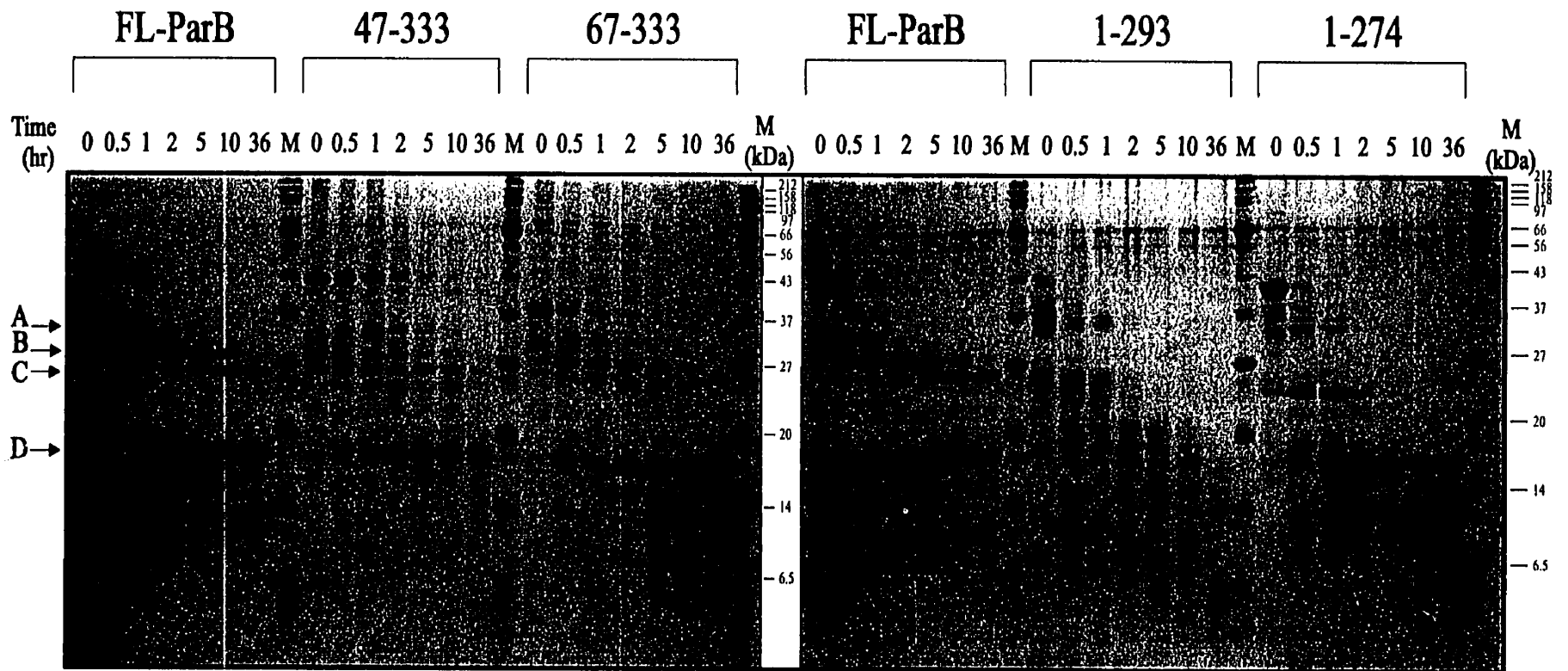
c. The apparent molecular weights were determined by linear regression analysis (Multi-Analyst software) of the protein gels and the predicted molecular weights were calculated assuming the fragments extend to the C-terminus of the protein.

fragments, His-47-333 ParB and His-67-333 ParB, both generated a cleavage pattern similar to that of full-length His-ParB, including the resistant domains (especially Band D) that remained at the later time points. The digestion of two N-terminal fragments, His-1-274 ParB and His-1-293 ParB, produced a series of fragments that were similar to each other, but were all smaller than those produced from full-length protein at comparable times. Therefore, removal of the C-terminus, but not of the N-terminus, of ParB altered the pattern of resistant regions. These results, along with the N-terminal sequences and the sizes (Table 2-2) of the proteolytic fragments, suggest the tryptic fragments of full-length ParB likely extend to, or very close to, the extreme C-terminus of ParB.

I attempted to confirm the identity of the tryptic fragments by matrix assisted laser desorption ionization time-of-flight (MALDI-TOF) mass spectroscopy. However, because His-ParB contains 59 arginine + lysine residues, there was a very large number of potential tryptic fragments. This complicated the analysis, particularly of fragments with a mass of less than 10 kDa. Also, the technique was unable to reproducibly detect fragments of His-ParB larger than about 21 kDa. Despite these problems, one peak of average mass of 17,106 +/- 30 Da was seen consistently by mass spectroscopy (data not shown). This mass corresponds only to a fragment consisting of amino acids 185-333, whose N-terminus is identical to that of Band D, and whose C-terminus corresponds to the C-terminus of ParB. Since it is likely that Band D is derived from the larger proteolytic fragments, I expect Bands A, B, C and F also extend to amino acid 333. Given the mobility and apparent molecular weight of Band E, it likely also extends to or close to the extreme C-terminus of ParB.

The data strongly suggest that the region from residues 185-333 forms a resistant core structure, within which lies a further resistant domain, from amino acid 263-333. Within this structural domain lies a region that has previously been implicated in ParB's dimerization

Figure 2-4. Tryptic digestion of His-ParB, two C-terminal fragments (His-47-333 ParB and His-67-333 ParB) and two N-terminal fragments (His-1-293 ParB and His-1-274 ParB). For each time course, the protein to protease ratio was 1000:1 (w/w) and the digestions were performed at room temperature. The arrows to the left of the figure indicate the major proteolytic fragments of His-ParB.








activity (Lobočka and Yarmolinsky, 1996). The proteolytic resistance of the C-terminal half of ParB may be the result of a core structure centred around a strong dimerization interface at the extreme C-terminus.

Definition of dimerization domains by yeast two-hybrid and *in vitro* cross-linking analysis. I used deletion analysis to define regions of ParB that are required for dimerization. The first approach was the yeast two-hybrid system, which provided the advantage that both homo- and hetero-interactions could be examined. In the system that I used, ParB or ParB fragments were fused to the DNA binding domain and/or to the activation domain of the *S. cerevisiae* GAL4 protein. The interaction of the DNA-binding fusion with an activation domain fusion activated a *lacZ* reporter gene, detected by filter tests with X-gal as a substrate, and a *HIS3* reporter gene, detected as growth on minimal plates lacking histidine and containing 3-aminotriazole. 3-AT inhibits imidazole glycerol phosphate (IGP) dehydratase, thus reducing basal histidine biosynthesis (Kishore and Shah, 1988). An interaction was considered positive only if both reporter genes were activated.

Examples of the activation of *lacZ*, as detected by X-gal filter tests, are shown in Fig. 2-5. When full-length ParB was tested for a self-association interaction (homodimerization) the yeast cells turned blue within a few hours on X-gal filter tests (Fig. 2-5A). These transformants also grew well in the absence of histidine. I concluded that ParB dimerization activity was detectable in yeast. Seven different C-terminal fragments of ParB, when fused to the GAL4 activation domain, interacted with FL-ParB (Fig. 2-6). Two of these fragments, 87-333 ParB and 187-333 ParB, correspond closely to tryptic fragments A and D, respectively. The shortest fragment consisted of only the last 59 amino acids of ParB, indicating that this region of ParB is sufficient to mediate a dimerization interaction with longer ParB fragments. All of the deletions, including 275-333 ParB, were also able to interact with 30-333 ParB when this ParB fragment was fused

A

		30-333 ParB + 30-333 ParB	30-333 ParB + GAL4 ACT
		FL ParB + FL ParB	FL ParB + 47-333 ParB
		FL ParB + 275-333 ParB	30-333 ParB + 275-333 ParB

B


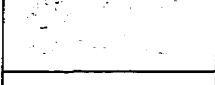


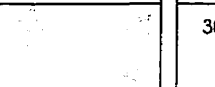
		FL ParB + 1-293 ParB	30-333 ParB + 1-293 ParB
		FL ParB + FL ParB	30-333 ParB + GAL4 ACT
		FL ParB + 1-177 ParB	FL ParB + 1-61 ParB
		30-333 ParB + FL ParA	FL ParB + FL ParA

Figure 2-5. Examples of filter tests to determine β -galactosidase activity in the yeast two-hybrid system. The light patches were scored as negative and the blue patches indicated a positive interaction. Each panel (A and B) is a separate filter, but the patches within each panel are from the same filter. The particular interactions tested are indicated in the key on the right of each filter. Various ParB and ParB fragment interactions (A and B) and ParA-ParB interactions (B) are shown. GAL4-ACT is the GAL4 activation domain alone encoded by pACTII, and represents one of the negative controls for these assays. FL ParB + GAL4 patches look like 30-333 ParB + GAL4 patches (A and B).

with the GAL4 DNA-binding domain (Figs. 1-2 and 2-6; Surtees, 1996). Western blotting of cell lysates indicated that in each instance the recombinant proteins were expressed in yeast (data not shown).

The 275-333 ParB fragment was then fused to the GAL4 DNA-binding domain in order to test it against itself and all other C-terminal fragments (Figs. 2-1 and 2-6) (Surtees, 1996). While it interacted with all larger fragments, 275-333 ParB did not interact with itself in yeast (Surtees, 1996). This suggested that a more N-terminal region, between amino acids 187 and 274, was required in at least one monomer for dimerization to be detectable in yeast. To measure dimerization independently of the yeast system, I turned to an *in vitro* cross-linking assay.

Full-length and truncated versions of ParB, fused to a polyhistidine sequence, were purified and then treated with DSP, a thiol-cleavable cross-linker that interacts with lysines. As has been shown previously (Funnell, 1991), full-length ParB cross-linked efficiently to a dimer-sized smear following this treatment (Fig. 2-7). Because ParB contains 29 lysines, both inter- and intramolecular cross-links occur, resulting in smeary rather than discrete bands on SDS-polyacrylamide gels. All of the C-terminal fragments, including His-275-333 ParB, cross-linked to dimer in this assay, although cross-linking was not always complete. I concluded that the most C-terminal 59 amino acids of ParB define a region that is sufficient for dimerization.

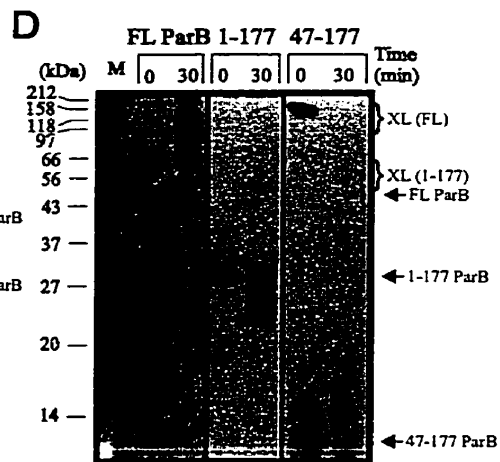
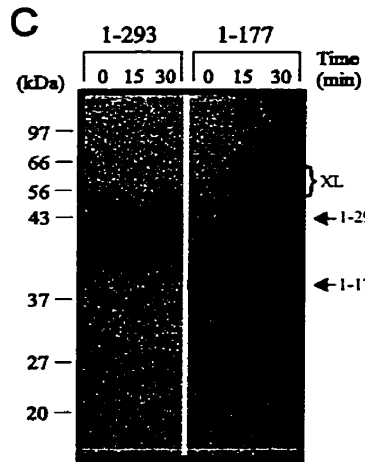
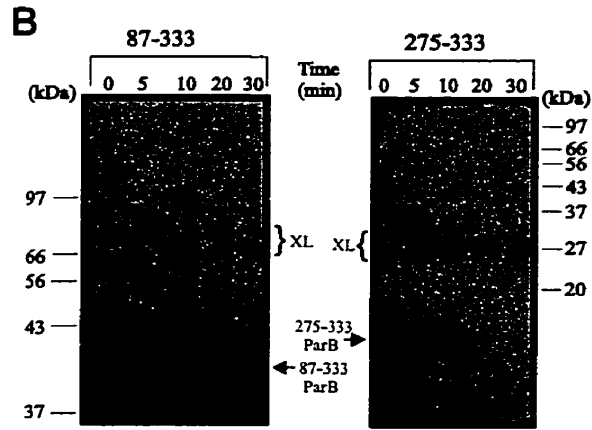
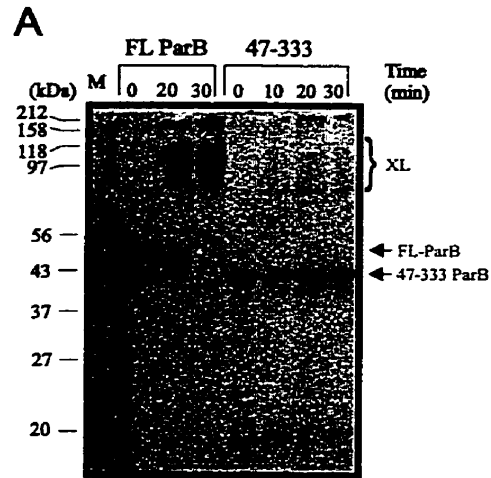
A second self-association domain of ParB. I next tested various N-terminal fragments (i.e. C-terminal truncations) for their ability to cross-link *in vitro*. Fragments lacking the extreme C-terminus (e.g. His 1-274 ParB) did not cross-link, which was expected since the C-terminal dimerization domain defined above was removed. Surprisingly, as more of the C-terminus of ParB was removed, the protein fragments recovered the ability to cross-link with DSP (e.g. His 1-177 ParB). This indicated a second multimerization domain within the N-terminal half of

ParB		Yeast two-hybrid			DSP cross-linking
NEH2	COOH	FL-ParB	30-333	275-333	
1	333 aa	++	++	++	++
30		++	++*	++	ND
47		++	++*	+	+
67		++	++*	+	+
87		++	++*	+	+
93		++	++*	+	+
152		ND	ND	ND	+
175		ND	ND	ND	+
187		+	+*	+	++
267		ND	ND	ND	++
275		+	+*	-*	++

(ND = not determined)

Figure 2-6. Summary of dimerization assays with C-terminal fragments of ParB. In yeast two-hybrid analysis, the ParB fragments shown in the diagram were fused to the GAL4 activation domain and were tested against FL-ParB, 30-333 ParB and 275-333 ParB (in the columns) that were fused to the GAL4 DNA-binding domain. For the cross-linking experiments, ParB fragments fused to a polyhistidine tag (Table 2-3) were purified and examined *in vitro* (Experimental Procedures). The results from the yeast two-hybrid experiments were categorized as follows: (-), no colour development on filter tests or no growth on plates without histidine; (+), moderate colour development and moderate growth in the absence of histidine; (++) , dark blue colour and good growth in the absence of histidine. ND, not determined. The DSP cross-linking results were similarly categorized: (-), no cross-linking; (+) some cross-linking activity; (++) strong cross-linking, often to completion. Neither set of categories is intended to imply relative strength of the interactions, which are presumably dependent on the assay. The N-termini of the tryptic proteolytic fragments are indicated above the schematic of ParB. *; these experiments were performed for my Master's thesis (Surtees, 1996).

Figure 2-7. Cross-linking of His-ParB and His-ParB fragments with DSP. Ten micrograms of protein were incubated with DSP at room temperature for the indicated times, and analysed by electrophoresis as described in Experimental Procedures. The arrows indicate the positions of monomers and the brackets indicate the positions of cross-linked products (XL). **A)** Cross-linking of His-ParB is compared with that of His-47-333 ParB on a 10% SDS-gel. His-ParB cross-links efficiently to a dimer- and possibly a tetramer-size smear. **B)** Two smaller C-terminal fragments cross-link in the presence of DSP. His-87-333 ParB and His-275-333 were treated with DSP and analysed on a 10% polyacrylamide gel (left) and a 12% polyacrylamide gel (right), respectively. **C)** Cross-linking reactions of two N-terminal fragments of ParB, His-1-293 ParB and His 1-177 ParB were analysed in a 12% polyacrylamide gel. **D)** Cross-linking reactions of His-ParB, His-1-177 ParB and His-47-177 ParB were analysed in a 12% polyacrylamide gel.



ParB. The data also suggested the presence of an inhibitory region within the C-terminal half of ParB. Fusions consisting of only the first 114 amino acids or less no longer cross-linked with DSP (Fig. 2-8), but this may be explained by the fact that only a few lysines remain in these fragments.

A possible trivial explanation for cross-linking of 1-177 ParB and 1-189 ParB is that the deletion created “sticky ends”, leading to non-specific hydrophobic interactions. Two experiments suggested that this was not the case. When an equal concentration of BSA was included in the assay, no interaction between 1-177 ParB and BSA was observed (data not shown). I also removed the N-terminal 46 amino acids from the His-1-177 construct. His-47-177 did not cross-link under the conditions in which His-1-177 did cross-link (Fig. 2-7). Both experiments imply that the interaction of His-1-177 with itself is specific. This was further supported by yeast two-hybrid analysis (see below). It also appears that deletion of the N-terminal 46 amino acids of ParB is sufficient to disrupt the N-terminal self-association domain.

A series of these N-terminal ParB fragments were tested for interactions with full-length ParB and ParB lacking the first 29 amino acids (30-333 ParB) in yeast (Fig. 2-8). All interacted with full-length ParB, including those that did not cross-link *in vitro*, indicating that only the first 61 amino acids of ParB are required for this interaction. However, none of the C-terminally truncated proteins interacted with 30-333 ParB-DB. Finally, as with cross-linking of 47-177 ParB, the removal of both the C-terminus and the N-terminus eliminated self-association of ParB. The inhibition that the C-terminus exerted on cross-linking of the N-terminal self-association domain was, however, not seen in yeast. All N-terminal fragments could interact with full-length ParB (Fig. 2-8). Unfortunately, it was not possible to test for homodimerization of these proteins in yeast because the DNA-binding fusions of 1-312, 1-293, 1-277 and 1-234 ParB activated both reporter genes in the absence of an interacting partner. Nevertheless, these

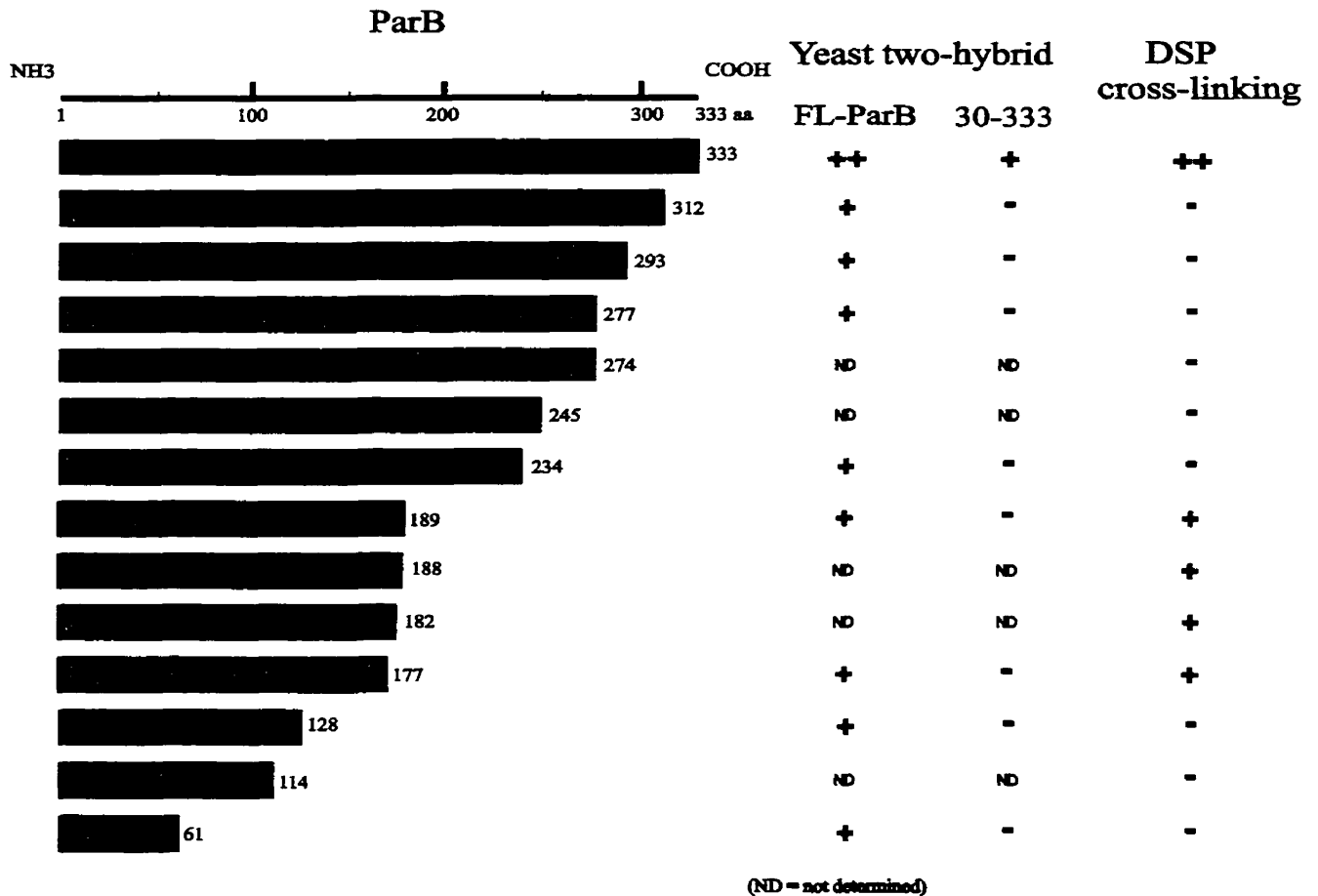


Figure 2-8. Summary of dimerization assays with N-terminal fragments of ParB. In yeast two-hybrid analysis, the ParB fragments shown in the diagram were fused to the GAL4 activation domain and were tested against FL-ParB and 30-333 ParB (in the columns) fused to the GAL4 DNA-binding domain. For cross-linking experiments, polyhistidine-tagged protein fusions were purified and tested *in vitro*. The categories are described in the legend to Figure 2-6.

results support the presence of a second multimerization domain within the N-terminal region of ParB.

ParA-ParB interactions. ParA fused to the GAL4 activation domain was able to interact with FL-ParB in the yeast two-hybrid system (Fig. 2-5B) (Surtees, 1996). However, when only the first 29 amino acids were removed from ParB, the interaction was eliminated (Fig. 2-5B). These data indicate that the extreme N-terminus of ParB is required for an interaction with ParA. They are consistent with recent results from experiments using P1-P7 hybrid partition proteins to probe the specificity of ParA-ParB interactions (Radnedge *et al.*, 1998). The latter showed that the first 28 amino acids of ParB are necessary for P1 ParB to recognize P1 ParA.

Discussion

I have probed the domain structure of ParB by partial proteolysis and by analysis of ParB fragments for self-association interactions. My model of ParB from these experiments is shown in Fig. 2-9. The major proteolytic fragments were identified and shown to be C-terminal, extending to or very close to the extreme C-terminus of ParB (Table 2-4). My proteolysis results suggest that an approximately 80 amino acid region at the N-terminus of ParB forms an unstable domain (or domains), that is/are easily accessible and rapidly digested by protease (Region I, Fig. 2-9). The remaining approximately 250 amino acid region is more structured (Region II, Fig. 2-9). In particular, the 185-333 fragment (Band D in Figs. 2-2 to 2-4) is very resistant to protease, although further digestion to the 263-333 fragment was also observed. Therefore, the last approximately 140 residues of ParB form an inaccessible, folded structure (Region IIa, Fig. 2-9), within which is a smaller resistant core of 70 amino acid residues. This core structure contains the C-terminal dimerization domain that is defined by chemical cross-linking and yeast two-hybrid analyses. The dimerization interface may contribute to the protection of these C-terminal residues from proteolytic digestion.

ParB's dimerization domains. *In vitro* cross-linking and the yeast two-hybrid system have provided complementary information regarding the dimerization activities of ParB. The last 59 amino acids of ParB were sufficient to interact with full-length ParB and with the other C-terminal fragments in the yeast two-hybrid system (Figs. 2-5A and 2-6). This fragment was also cross-linked by DSP *in vitro*. These data indicate that the C-terminal 59 amino acids contain a dimerization domain. I also discovered that a fragment consisting of the first 177 amino acids of ParB was cross-linked by DSP in the absence of the C-terminal dimerization domain, providing evidence of an additional multimerization determinant within the N-terminal

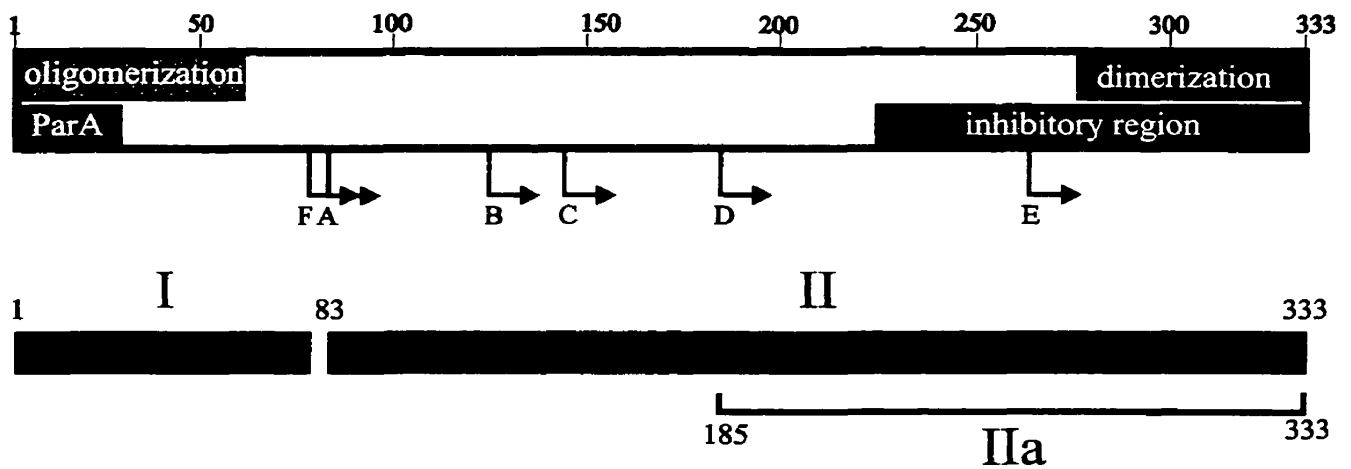


Figure 2-9. Model of ParB's functional and structural domains. The coloured boxes represent regions of the protein involved in ParB-ParB and ParA-ParB interactions. The arrows indicate the N-termini of the proteolytic fragments (A to F) identified in this chapter. I propose that the C-terminal self-association domain is required for ParB dimerization and the N-terminal self-association domain mediates oligomerization. The “inhibitory region” affects the self-association of ParB that is mediated by the N-terminal oligomerization domain, as measured by cross-linking assays. The “ParA” box indicates a region of ParB that is necessary for interactions with ParA. The lower black boxes predict the general structural domains of ParB, from proteolytic assays. Region I represents the protease-accessible N-terminal region, which may mean that it is less structured in solution. Region II is more stable and more protease-resistant. Region IIa represents the smallest highly protease resistant region of ParB.

half of ParB. Deletion of the first 46 amino acids from 1-177 ParB disrupted this determinant. Similarly, while all the N-terminal fragments interacted with FL-ParB in the yeast two-hybrid system, none interacted with 30-333 ParB (Fig. 2-8). These results strongly suggest that an intact N-terminus in both partners is crucial for an interaction in the absence of the C-terminus in even one partner. Finally, the data also indicate that removal of only 21 amino acids from the C-terminus disrupts the C-terminal dimerization domain.

A C-terminal region of ParB inhibits cross-linking in the absence of the C-terminus.

ParB fragments missing only a portion of the C-terminus (21-100 residues) did not cross-link in the presence of DSP, but removal of an additional 54 residues (from residue 190) restored cross-linking activity. Therefore a region at the C-terminus (Fig. 2-8) is inhibitory to dimerization via the N-terminus in a cross-linking assay. This result may explain why point mutations in the C-terminus of ParB destroyed its cross-linking ability (Lobocka and Yarmolinsky, 1996) and failed to reveal the N-terminal self-association domain. On the other hand, this inhibition was not apparent in the yeast two-hybrid experiments. ParB fragments lacking the C-terminus, when fused to the GAL4 activation domain, could interact with full-length ParB that was fused to the GAL4 DNA-binding domain (Fig. 2-8). If an inhibition occurred, it was not sufficient to completely destroy the interaction. Alternatively, the yeast two-hybrid system may provide a distinct context that allows these interactions to occur. For example, the full-length partner may prevent the “free” C-terminus of its partner from occluding its N-terminal domain, binding of ParB to DNA in yeast (presumably non-specifically) may alter the conformation of one or both partners, or the addition of a large GAL4 fusion at the N-terminus of the C-terminal deletions may expose the N-terminal self-association domain.

Whether the C-terminus of full-length ParB normally prevents self-association of the N-terminal domain is unknown, but this has interesting implications for partition. The C-terminus in the intact protein may physically block oligomerization through the N-terminus until a specific point in partition, for example, until ParB binds to *parS* or until ParB binds to ParA. A similar situation exists with the *E. coli* regulatory protein NtrC (Fiedler and Weiss, 1995), which contains two multimerization domains. The first mediates constitutive dimerization and is located at the C-terminus of the protein. The second is near the N-terminus and the central domain of the protein sterically inhibits its oligomerization activity, until it is phosphorylated by NtrB. That no resistant region corresponding to the N-terminus of ParB was detected following proteolytic digestion may also indicate that the N-terminus is not oligomerized in solution.

Possible roles for dimerization in ParB activity in partition. In this work, I have shown that ParB contains a distinct domain structure, within which exist two self-association determinants that can function independently. Do these two regions have distinct roles in partition? Experiments with hybrid P1-P7 ParB proteins indicate that the C-terminus of ParB likely contains more than one function (Hayes and Austin, 1993; Radnedge *et al.*, 1996). Bacteriophage P7 encodes a partition system that is very similar to that of P1, with homologous ParA and ParB proteins and a similar *cis*-acting *parS* site. Species specificity appears to be mediated through recognition of the *parS* box B sequences, since the *parS* box A sequence in both P1 and P7 are interchangeable. The C-terminus of a hybrid ParB protein is responsible for recognizing its cognate box B sequence. The dimerized C-terminus may bind directly to the box B sites, and dimerization at the C-terminus may be required for box B binding.

It has been proposed that a putative helix-turn-helix motif in the centre of ParB (amino acids 166-189) (Dodd and Egan, 1990) is responsible for box A binding (Radnedge *et al.*, 1996).

Classically, helix-turn-helix (HTH) DNA-binding proteins, such as the Trp repressor, λ Cro and E. coli CAP protein, must be dimeric in order to efficiently bind the DNA, with each partner contributing a DNA binding half site (Pabo and Sauer, 1992). ParB dimerization may bring two HTH motifs together to form a stable DNA binding domain and one or both multimerization domains may be required to ensure the HTH domain is intact (Fig. 2-9).

In vitro studies have shown that ParB is a dimer under all conditions tested (Funnell, 1991). I have shown that ParB fragments missing the extreme C-terminus do not dimerize *in vitro*. Similarly, point mutations within the C-terminus disrupt dimerization (Lobočka and Yarmolinsky, 1996). I therefore propose that the C-terminal domain promotes ParB dimerization. Since ParB exists as a dimer, this is likely a strong interaction (Fig. 2-9). I suggest that the N-terminal self-association domain mediates dimer-dimer interactions. This interaction occurs only under certain conditions, such as when ParB is bound to *parS*. It leads to the formation of tetramers and higher-order oligomers that are inferred from the observation of plasmid pairing of R1 ParR (Jensen *et al.*, 1998) and gene silencing by P1 ParB (Rodionov *et al.*, 1999). The *lac* repressor similarly has two multimerization domains, one that allows dimerization and a second at its extreme C-terminus that promotes tetramerization through dimer-dimer interactions (Chen and Matthews, 1994a; Chen *et al.*, 1994b).

The 29 amino acids at the extreme N-terminus of ParB are required for a ParA-ParB interaction (Radnedge *et al.*, 1998) (Fig. 2-5B). Therefore the N-terminal domain of ParB contains both a ParA and a ParB (self) association function. ParA-ParB interactions occur in at least two aspects of partition. ParB acts as a co-repressor to stimulate the repressor activity of ParA (Friedman and Austin, 1988), and ParA assembles on the ParB-IHF partition complex at *parS* in an ATP dependent reaction (Bouet and Funnell, 1999). In the latter case, it is interesting

to note that at high ParA to ParB ratios, ParA prevents or inhibits ParB binding to *parS*. Perhaps the ParA-ParB interaction (when in excess) interferes with the N-terminal ParB-ParB association. It is not known whether such ParA-ParB and ParB-ParB interactions both occur in the context of the partition complex or whether they are mutually exclusive. The next step is to establish how the self-association domains contribute to ParB's activities in partition.

CHAPTER 3

Stoichiometry of P1 ParB in plasmid partition complexes

The data in this chapter formed part of the publication:

Bouet, J.-Y., J.A. Surtees and B.E. Funnell (2000) *Journal of Biological Chemistry*
275: 8213-8219.

J.-Y. Bouet did the experiment in Fig. 3-2. I performed the experiments in Figs. 3-3 and 3-4.

Introduction

ParB and IHF bind *parS* to form a nucleoprotein structure called the partition complex (Davis and Austin, 1988; Funnell, 1988a; Funnell, 1988b; Davis *et al.*, 1990). The current picture of the P1 partition complex is derived from a variety of protein-DNA binding experiments *in vitro*, and examination of mutant *parS* sites *in vivo* (Davis *et al.*, 1990; Funnell, 1991; Funnell and Gagnier, 1993; Funnell and Gagnier, 1994; Hayes and Austin, 1994). ParB recognizes two distinct repeats, called box A and box B repeats, that flank an IHF binding site in *parS* (Fig. 3-1) (Funnell, 1988b; Funnell, 1991). Binding of IHF to *parS* creates a large bend in the DNA, which greatly increases ParB's affinity for *parS*, i.e. high affinity ParB binding (Funnell, 1991; Funnell and Gagnier, 1993). Proper phasing of the box A and box B sequences across the bend is functionally important for formation of the partition complex (Funnell and Gagnier, 1993; Hayes and Austin, 1994). ParB affinity for *parS* is also greatly increased by superhelicity in the DNA substrate. All these data suggest a partition complex structure in which the DNA is wrapped around a protein core of ParB and IHF. IHF binds its specific site as a heterodimer (IHF α /IHF β) (Yang and Nash, 1989; Rice *et al.*, 1996). ParB is a dimer in solution (Funnell, 1991), but the stoichiometry of ParB in the partition complex is not known.

In this chapter, and in collaboration with Jean-Yves Bouet, I have examined the nature and stoichiometry of ParB binding to *parS* by gel electrophoresis. One dimer is sufficient to interact with ParB binding sequences that span the IHF-directed bend, resulting in the high affinity binding to *parS* that is observed for ParB and IHF. At higher concentrations of ParB, more dimers of ParB join this complex to create even higher order protein-DNA complexes.

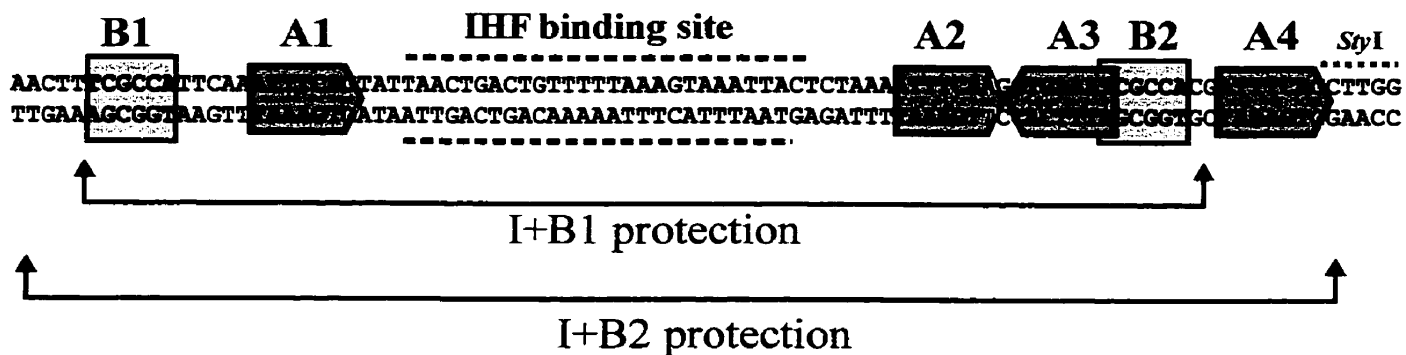


Figure 3-1. The P1 *parS* site. Blue and pink boxes indicating the ParB box A and box B recognition motifs, respectively, are drawn behind the DNA sequence. The left end is 25 bp from the *TaqI* restriction site in P1 (see Figure 1-1). The IHF binding site, determined by DNaseI footprinting (Funnell, 1991), is indicated with dashed lines. The brackets below indicate the sequence that was protected in OP-CU chemical footprinting experiments (Bouet, et al., 2000) in the I+B1 and I+B2 ParB-IHF-*parS* complexes (see Results).

Experimental Procedures

Reagents and enzymes. Sources for reagents were as follows: bovine serum albumin (BSA, Fr V), Sigma; ³²P-dATP, NEN life Science Products. Restriction enzymes and DNA polymerases were purchased from New England Biolabs or Roche Molecular Biochemicals.

DNA and Proteins. The plasmids pBEF165 and pBEF166 contain the P1 *parS* sequence between the P1 *TaqI* and *StyI* restriction sites, cloned in opposite orientations into a modified pBlueScript vector (Funnell, 1991). For gel mobility shift assays, the DNA substrates were total restriction digests of pBEF166 and thus included both *parS* and vector sequence. Digestion with different restriction enzymes yielded DNA fragments of different size. Digestion with *XbaI* or *BamHI* produced *parS*-132 or *parS*-252, respectively (the numbers correspond to the length of the DNA in bp). DNA fragments were labeled with ³²P-dATP and DNA polymerase I large fragment, and purified by phenol-chloroform extraction and ethanol precipitation steps (Sambrook *et al.*, 1989).

His-ParB has 36 amino acids, including a 10x polyhistidine tag, fused to the N terminus of ParB (Surtees and Funnell, 1999). ParB (Fr V), His-ParB and IHF were purified as previously described (Chapter 2)(Bouet and Funnell, 1999; Surtees and Funnell, 1999).

Gel mobility shift assays. The standard reaction mixture (10 ul) contained 0.5 nM ³²P-labeled *parS* DNA in a buffer containing 50 mM Hepes KOH (pH 7.5), 50 mM NaCl, 10 mM MgCl₂, 10% (v/v) glycerol, 100 ug BSA/ml, 100 ug sonicated salmon sperm DNA/ml, and 3.5 mM β-mercaptoethanol. The mixtures were assembled on ice, incubated for 20 minutes at 30°C and analyzed by electrophoresis in 5% polyacrylamide gels in TBE buffer (90 mM Tris-borate, 1 mM EDTA). Electrophoresis was performed at 150 V for 5 hours at 4°C. The gels were dried

onto Whatman DE81 paper and exposed to a phosphor screen for imaging by a PhosphorImager (Molecular Dynamics).

Results

Characterization of two forms of the partition complex. ParB and IHF cooperate to form the partition complex at *parS*. *In vitro*, IHF greatly increases the affinity of ParB binding to *parS* (Funnell, 1991). The structure of the partition complex is of considerable interest because its assembly represents an early step in partition. Jean-Yves Bouet (a former post-doctoral fellow in our lab) and I have examined the nature and number of complexes of ParB and IHF that assemble at *parS* by gel mobility shift assays (Fig. 3-2A). We were specifically interested in ParB-*parS* complexes with IHF. Even though IHF is not required for partition, *in vivo* competition (or “incompatibility”) assays indicate that IHF is always a component of wild-type P1 partition complexes (Funnell, 1988b; Funnell, 1991). In gel mobility shift assays, two distinct ParB-IHF-*parS* complexes (“I+B1” and “I+B2”) were observed in addition to IHF complexes alone (“I” complex) (Fig. 3-2; Bouet *et al.*, 2000). This is consistent with previous studies of these complexes by gel electrophoresis that revealed a single ParB-IHF-*parS* complex at low concentration, and a second, more slowly migrating, complex at higher concentrations (Davis and Austin, 1988; Lobočka and Yarmolinsky, 1996). When ParB concentration was increased, I+B3 (Figure 3-2) and higher complexes formed (data not shown).

Relative stoichiometry between the two partition complexes. The difference between I+B1 and I+B2 could represent (i) a difference in the shape of these complexes; (ii) a difference in the amount of ParB bound in each complex; or (iii) a pairing event between two *parS* DNA molecules. To discriminate among these possibilities, Jean-Yves Bouet performed shift western blotting (Demczuk *et al.*, 1993) to measure the relative stoichiometry of ParB on *parS* in the two complexes (Bouet *et al.*, 2000). ParB-IHF DNA complexes were transferred to membranes. The relative amounts of DNA and ParB present in the different complexes were detected successively

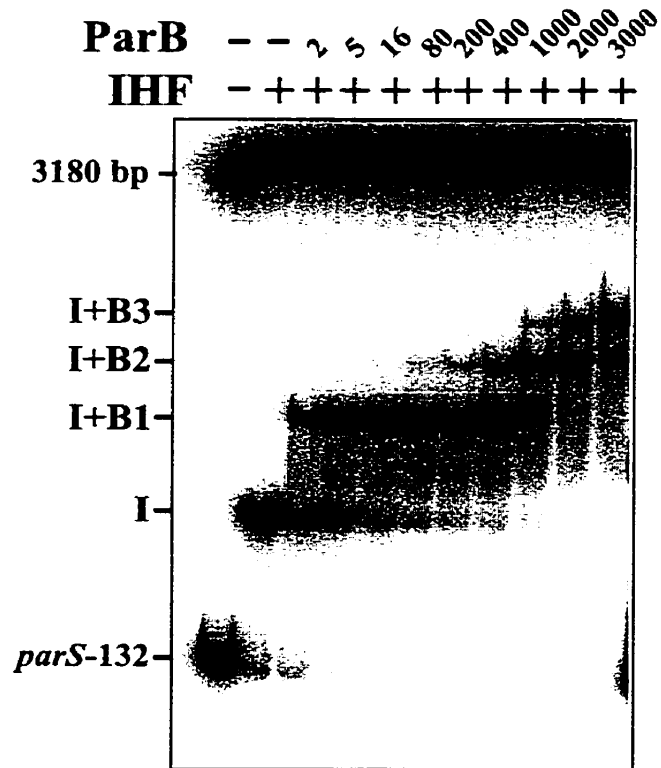


Figure 3-2. Multiple partition complexes form at *parS* with increasing ParB concentration. ³²P-labeled DNA fragments, resulting from an *Xba*I digest of pBEF166 were the substrates for ParB and IHF binding. This restriction digestion produced a 132 bp *parS* fragment and a 3280 bp vector DNA fragment. Following incubation with ParB and IHF, the reaction mixtures were analyzed by electrophoresis in a 5% polyacrylamide gel. ParB concentrations (in nM dimer) are indicated above each lane. IHF, when present (+), was at 400 nM. The positions of free DNA fragments and protein-DNA complexes are indicated on the left. Note that the large vector fragment also contains an IHF binding site. This experiment was performed by Jean-Yves Bouet (Bouet, et al, 2000).

on the same membrane by PhosphorImager scanning and quantitative Western blot analyses, respectively. His results revealed that I+B2 contains, on average, twice as much ParB as I+B1 per molecule of *parS* (Bouet *et al.*, 2000).

This result makes it unlikely that I+B2 corresponds to a pairing event between two I+B1 complexes. If this were true, then the protein:DNA ratio for both complexes would be the same; complex I+B2 would have twice as much ParB and twice as much DNA as I+B1. Similarly, if complexes I+B2 represented an I+B1 complex that had captured and paired with a naked (or IHF-bound) *parS* DNA molecule, the ParB:DNA ratio would decrease by half in complex I+B2 ($I+B2/I+B1 = 0.5$). Nevertheless, I checked for pairing by including an unlabeled *parS* DNA fragment of different size in the binding mixture (Fig. 3-3). The expectation was that “paired” complexes would form between fragments of different size, producing two distinct I+B2 complexes when only one of the fragments was radioactively labeled. Conversely, ParB bound to only one *parS* DNA fragment would simply be competed by the unlabeled *parS* DNA fragment. The latter result was observed (Fig. 3-3), indicating that the I+B2 complex does not represent a pairing event.

The I+B1 complex contains one ParB dimer. ParB is a dimer in solution (Funnell, 1991), but its stoichiometry at *parS* is unknown. Since ParB recognizes 4 box A and 2 box B sequences (Davis *et al.*, 1990; Funnell and Gagnier, 1993), it seemed reasonable to predict that a tetramer would be required to occupy all sites. On the other hand, both genetic and chemical interference studies suggest that only two box A sequences are essential for *parS* activity (A2 and A3 in Fig. 3-1) (Davis *et al.*, 1990; Funnell and Gagnier, 1993; Funnell and Gagnier, 1994). To examine the stoichiometry of ParB in I+B1 and I+B2 complexes, I designed a mixing experiment using ParB and a larger polyhistidine version of the protein, His-ParB (Surtees and

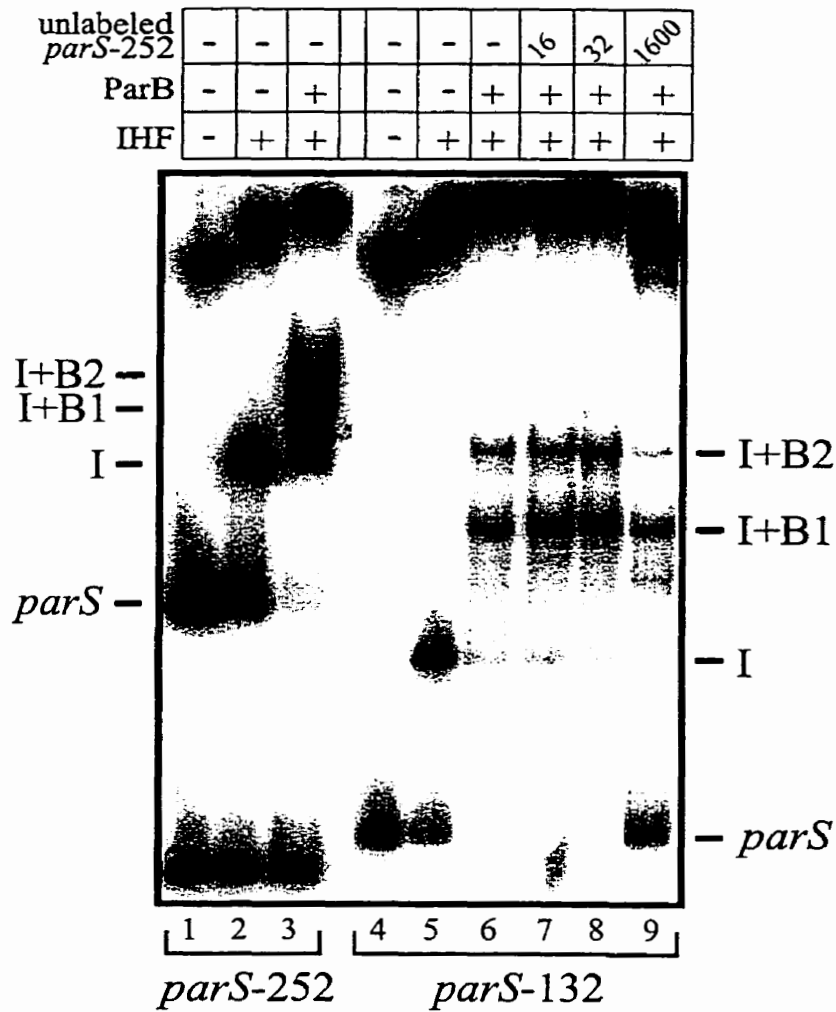
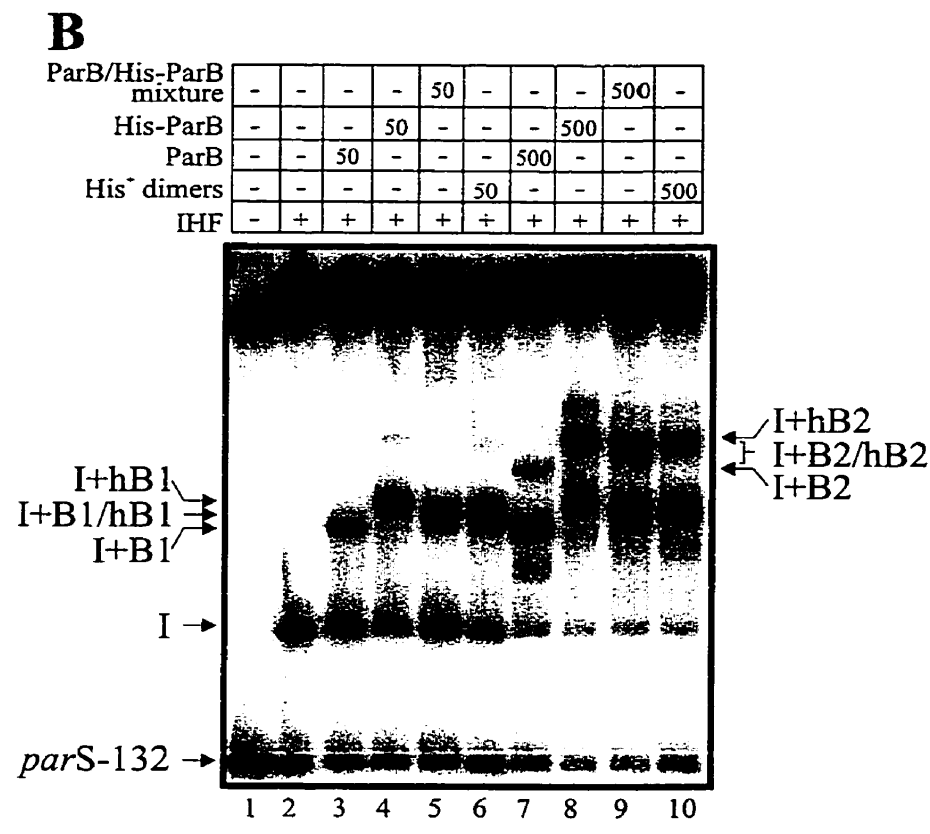
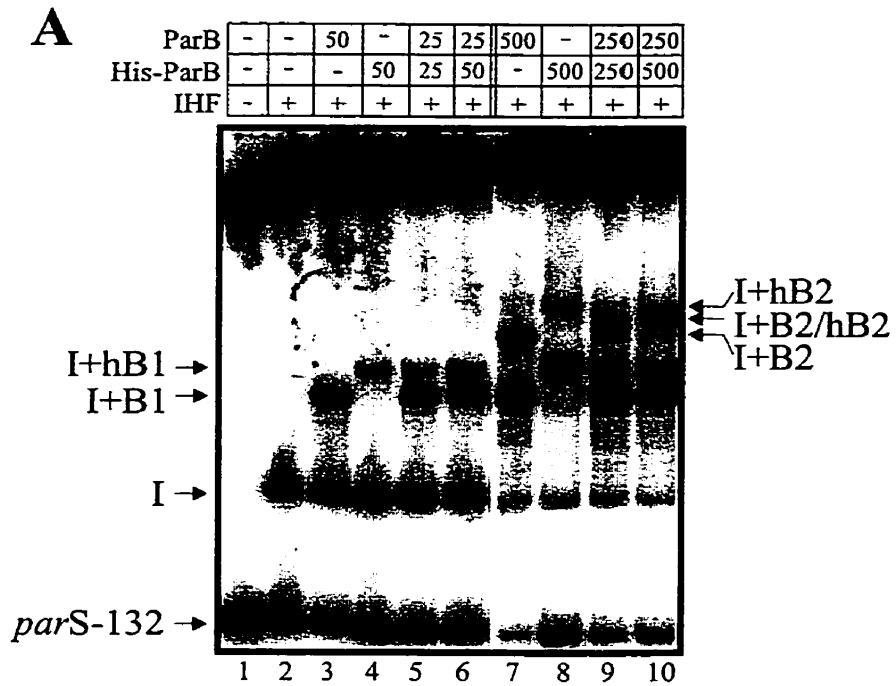


Figure 3-3. Competition analysis of ParB binding to *parS*. Gel mobility shift assays were performed with *parS*-252 (lanes 1-3) or *parS*-132 (lanes 4-6) DNA fragments as the ³²P-labeled substrates. The reaction mixtures contained 16 fmol of ³²P-labeled DNA fragments. When present (+), IHF and ParB concentrations were 400 nM and 250 nM (dimer), respectively. In lanes 7 to 9, increasing amounts of unlabeled *parS*-252 (indicated above the lanes in fmol) were added to the reaction mixtures prior to the addition of ParB.

Funnell, 1999). His-ParB binds to *parS*, but produces a larger, more slowly migrating complex (complex I+hB1; Fig. 3-4A, lane 4). When ParB and His-ParB were both added to a binding reaction mixture, I expected that complexes containing more than one dimer would produce hybrid bands in a gel mobility shift assay. At low concentration of both ParB proteins, only ParB (I+B1) and His-ParB (I+hB1) were observed (Fig. 3-4A, lanes 5 and 6). At high concentrations, an intermediate complex was observed (I+B2/hB2) that migrated between the ParB I+B2 and the His-ParB I+hB2 complexes (Fig. 3-4A, lanes 9 and 10). The simplest explanation for these results is that the I+B1 complexes contain only one dimer of ParB and that the I+B2 complexes contain two dimers of ParB.

Formally, the lack of an intermediate I+B1 complex could be interpreted as indicating that this complex contains only one monomer of ParB, since heterodimers of ParB/His-ParB would also be expected to produce hybrid complexes. However, I favoured the idea that the ParB dimerization interaction is too strong to completely reassort during this experiment. Furthermore, it seemed unlikely that a single monomer could interact with two box B sequences across the IHF band or to protect all of the sites within *parS* that were detected by chemical footprinting (see below) (Bouet *et al.*, 2000). Nonetheless, to test whether the I+B1 complex contains one dimer or one monomer of ParB, I forced the molecules to form heterodimers by denaturing and renaturing a mixture of both ParB proteins. ParB and His-ParB, alone or mixed together, were denatured by treatment with 6M guanidine, and then renatured by successive dialysis steps to remove the guanidine. When used in a DNA binding experiment at low ParB concentrations, the ParB-His-ParB mixture now produced an intermediate I+B1/hB1 complex (Fig. 3-4B, lane 5). This result is consistent with the formation of a complex containing a heterodimer of ParB/His-ParB. Therefore the I+B1 partition complex contains one ParB dimer

Figure 3-4. Mobility of ParB and His-ParB homodimers and heterodimers bound to *parS* DNA. **A**, DNA binding by native ParB and His-ParB. ParB or His-ParB were incubated with *parS*-132 DNA fragments (as an *Xba*I restriction digest of pBEF166) in the presence of IHF (400 nM), and the reaction mixtures were analyzed by electrophoresis in a 5% polyacrylamide gel. The concentrations of ParB and His-ParB (in nM) are indicated above each lane. **B**, DNA binding by denatured/renatured ParB, His-ParB and ParB/His-ParB heterodimers. To form heterodimers, 25 µg each of ParB and His-ParB were mixed, diluted in 150 µl of buffer A (6 M guanidine HCl, 100 mM NaH₂PO₄, 10 mM Tris, pH 8.0) and then dialyzed against 300 ml buffer a for 4 hours to denature both proteins. They were renatured by successive dialysis steps against decreasing concentrations of guanidine HCl (3, 1 and 0.5 M) followed by a final dialysis against 50 mM sodium phosphate (pH 8.0), 300 mM NaCl, 10% (v/v) glycerol, 7 mM β-mercaptoethanol. Dialysis was performed at 4°C. The resulting mixture of homo- and heterodimers (ParB/His-ParB mixture, lanes 5 and 9) was used in DNA binding assays. As controls, 25 µg each of ParB and of His-ParB were independently denatured and renatured (in separate dialysis bags) as above and used in DNA binding assays (ParB, lanes 3 and 7; His-ParB, lanes 4 and 8). To isolate “His⁺ dimers” (dimers in which at least one monomer contains a polyhistidine tag), 15 µg of the denatured/renatured mixture of ParB and His-ParB were purified over a 20 µl nickel-agarose chromatography column as described in Chapter 2 (Surtees and Funnell, 1999). Bound protein was eluted with 500 mM imidazole, and used in DNA binding assays (His⁺ dimers, lanes 6 and 10). ParB protein concentrations (in nM dimers) are indicated above each lane.



and the I+B2 complex contains two ParB dimers. As controls, ParB and His-ParB were individually denatured and renatured, and both proteins were able to bind *parS* (Fig. 3-4B, lanes 3 and 4).

To further demonstrate that the intermediate complex I+B1/hB1 (Fig. 3-4B, lane 5) was formed by heterodimers, the ParB/His-ParB denatured/renatured mixture was repurified by nickel affinity chromatography. ParB protein that bound to the nickel resin, which must contain at least one polyhistidine tag per dimer (His⁺ dimers), was used in a DNA binding assay (Fig 3-4B, lane 6). This protein mix produced primarily the intermediate I+B1/hB1 and upper I+hB1 complexes. Since the latter are identical to those produced by His-ParB homodimers, I conclude that the intermediate complex contains His-ParB/ParB heterodimers. Therefore, the I+B1 complex contains one ParB dimer, and the I+B2 complex contains two ParB dimers.

Jean-Yves Bouet performed 1.10-phenanthroline-copper (OP-Cu) footprinting experiments to determine the regions within *parS* that were protected in the I+B1 and I+B2 complexes (Bouet *et al.*, 2000). In I+B1 complex, protection due to ParB binding was observed in boxes A1 and B1 (left side) and boxes A2, A3 and B2 (right side) on both DNA strands. The protection of *parS* by ParB was very similar in complex I+B2, but extended outward to include box A4 as well as sequence to the left of box B1 (see Fig. 3-1). The DNA sequence left of box B1 is outside the minimal *parS* region required for partition (Davis *et al.*, 1990). Therefore, the additional contacts made by ParB in complex I+B2 probably represent both specific and non-specific interactions.

Discussion

The formation of the P1 partition complex is an essential step in the segregation of the unit-copy number plasmid P1 at cell division. In this chapter, I have shown that the initial ParB+IHF complex visualized by gel mobility shift assays (I+B1) contains a single dimer of ParB, while the next complex formed (I+B2) contains two dimers of ParB. At higher concentrations of ParB, complexes with increasingly slower migration are observed (I+B3, I+B4, etc.), which presumably is a result of additional ParB dimers loading onto the nucleoprotein complex.

The stoichiometry of ParB binding has interesting implications for the architecture of the partition complex. In particular, the observation that a single ParB dimer is responsible for the I+B1 complex is intriguing given the number of specific sequences in *parS* that are recognized by ParB. *parS* contains two copies of the box B repeat and four copies of the box A repeat (Fig. 3-1). I favour a model in which one dimer of ParB is precisely docked to occupy both box B repeats and the box A2 and A3 repeat. First, since both box A2 and A3 repeats are required for high affinity ParB binding, both must be filled to form the I+B1 complex. Second, although the OP-Cu footprints indicate an additional protection in the region of box A1, previous deletion and mutational analyses and DMS interference experiments have shown that boxes A1 and A4 in *parS* are not essential for partition or for high affinity binding by ParB (Davis *et al.*, 1990; Funnell and Gagnier, 1993; Funnell and Gagnier, 1994). Previous DNaseI footprinting experiments showed that ParB and IHF protected the region that contains box A1 from DNaseI cleavage even when box A1 was mutated (changed by a 4 bp substitution mutation; Davis *et al.*, 1990). This implies that ParB is in the same position in the complex with or without the box A1 sequence. Therefore, the box A1 region is likely protected from OP-Cu and DNaseI cleavage by

alterations in the geometry of the DNA, such as compression of the minor groove caused by tightening of the bend, for example. The alternative possibility is that I+B1 complex represents a mixture of ParB orientations on *parS*, in which case the domain of ParB that is responsible for recognition of box A must be quite flexible with respect to the domain responsible for recognizing box B. Given that box A1 cannot substitute for either box A2 or A3 (Davis *et al.*, 1990; Funnell and Gagnier, 1993), this scenario seems unlikely.

Previous data indicate that the IHF bend in *parS* allows ParB to simultaneously contact its DNA recognition sequences that flank the bend (Funnell and Gagnier, 1993). The results in this chapter show that it is one dimer of ParB that interacts across this bend. Dimerization of ParB is mediated through a domain located at the C-terminus of the protein (Lobocka and Yarmolinsky, 1996; Surtees and Funnell, 1999; Chapter 2). This region has also been shown to be involved in box B binding (Radnedge *et al.*, 1996). These observations lead to a model in which the dimerized C termini of one ParB dimer interact with both box B sequences simultaneously, perhaps threading the DNA between the monomers. In other words, the extreme ends of the *parS* site are brought together near or at the dimerization interface. This model is consistent with the biochemical data that indicate that the DNA is wrapped around a core of protein (Funnell, 1991; Funnell and Gagnier, 1993). It has been suggested that a putative helix-turn-helix motif in the centre of ParB binds the box A motif (Dodd and Egan, 1990; Radnedge *et al.*, 1996). In this case, these regions of each monomer would be directed toward the box A2 and A3 inverted repeat, but would be positioned on one side of the IHF bend rather than flanking it. The way in which ParB binds the box A and box B sequences within *parS* will be addressed and extended in Chapter 4.

An important question is whether the I+B1 complex is sufficient for partition *in vivo*. The affinity of ParB for the I+B2 complex is about 100-fold lower than its affinity for the I+B1 complex (Bouet *et al.*, 2000). ParB exists at relatively high concentrations in the cell (micromolar amounts) (Funnell, 1991; Funnell and Gagnier, 1994), and therefore progressive loading of ParB onto the DNA to form higher complexes probably also occurs *in vivo*. This is supported by the observation that ParB binding can spread a great distance along the DNA on both sides of *parS* under conditions where ParB can silence genes that are located close to *parS* (Lobocka and Yarmolinsky, 1996; Rodionov *et al.*, 1999). In addition, immunofluorescence analysis shows that ParB forms bright, discrete foci at the intracellular locations occupied by P1 plasmids, suggesting that much of the ParB in the cell converges on P1 at the *parS* site (Erdmann *et al.*, 1999). However, the minimal amount of ParB that is necessary for partition *in vivo* has not been measured. Larger complexes (I+B2, I+B3, etc.) may be necessary to interact with ParA or with host factors. Alternatively, the I+B1 complex may be sufficient for partition, but not for competition (incompatibility). Weaker *par* sites (weakened by mutation for *parS*, for example (Funnell and Gagnier, 1993) are competent for partition but unable to compete with wild-type sites.

Presumably binding of ParB to complex I+B1 to form complex I+B2 is mediated chiefly by protein-protein (dimer-dimer) interactions, which are weaker than the protein-DNA interactions that mediate complex I+B1, since much higher ParB concentrations are required for complex I+B2 formation. Such dimer-dimer interactions may occur via a self-association domain identified near the N-terminus (Surtees and Funnell, 1999; Chapter 2). It seems likely that both specific and non-specific DNA contacts also contribute to the formation of complex I+B2.

The architecture of ParB binding to *parS* is intriguing, given the organization of box A and box B motifs (Fig. 3-1) and the current result that one dimer interacts with these motifs to form the initial partition complex. These results define the minimal protein requirements for *parS* binding. The high affinity core (complex I+B1) then recruits more ParB molecules by both protein-DNA and protein-protein interactions.

CHAPTER 4

The DNA binding domains of P1 ParB and the architecture of the P1 plasmid partition complex

A version of this chapter has been accepted for publication in *The Journal of Biological Chemistry*. I performed all of the experiments in this chapter.

Introduction

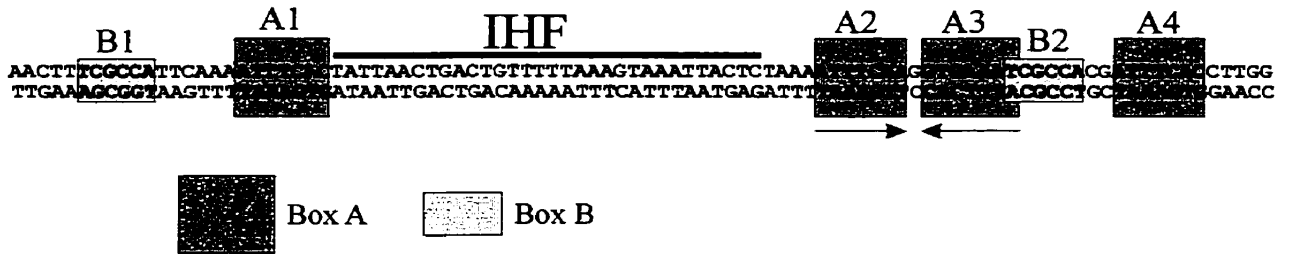
ParB is a site-specific DNA binding protein. Its target is the plasmid centromere-like site, *parS*. In this chapter I have examined the interaction of ParB with *parS* by asking how different regions of the protein contribute to its DNA binding activities.

parS is a multipartite DNA site. An IHF binding site is flanked by two types of distinct sequences, called box A and box B, which are specifically recognized by ParB (Davis *et al.*, 1990; Funnell and Gagnier, 1993) (Fig. 4-1A). Previous mutational and deletion analyses have shown that the presence and relative spacing of boxes A2, A3, B1 and B2 are essential for *parS* function *in vivo*, while boxes A1 and A4 are dispensable (Davis *et al.*, 1990; Funnell and Gagnier, 1993; Funnell and Gagnier, 1994). ParB and IHF enhance each other's affinity for *parS* (Funnell, 1991; Funnell and Gagnier, 1994). IHF binding creates a large bend in *parS* (Funnell, 1991) and a single dimer of ParB binds across the IHF-directed bend in *parS* (Chapter 3; (Bouet *et al.*, 2000), forming a structure in which the DNA is wrapped around the protein core (Funnell, 1988b; Funnell, 1991; Bouet *et al.*, 2000). Subsequent dimers load onto the partition complex with increasing ParB concentrations via a series of protein-protein interactions and specific and non-specific protein-DNA interactions that tether increasing amounts of ParB to the partition complex.

Two independent self-association domains have been identified within ParB (Fig. 4-2A) (Surtees and Funnell, 1999) (Chapter 2). One domain is located within the last 59 amino acids of ParB and is likely the domain that mediates dimerization in solution. Limited proteolytic digestion indicated that the C-terminal dimerization domain forms the core of a very stably folded C-terminal half of ParB (Chapter 2; (Surtees and Funnell, 1999). The second

A

P1 parS



B

Box A inverted repeat

```

    CTCAAATTCGCCATTCAAAATAAATTGACTGACAAAAATTCATTAAATGAGATTCTTGG
    GAGTTTATAATTGACTGACAAAAATTCATTAAATGAGATTCTTGG
  
```

non-specific

```

    TGTCACGAGAAAGTCAACAAGTGAC
    ACAGTGCTCTTTCAGTTGTTCACTG
  
```

Box B

```

    CCTTAAACTTTCGCCATTCAAAATAAATTGACTGACAAAAATTCATTAAATGAGATTCTTGG
    GGAATTTGAATGCGGTAAAGTTTATAATTGACTGACAAAAATTCATTAAATGAGATTCTTGG
  
```

Box B - scrambled

```

    CCTTAAACTTTCAGCTCTTCAAAATAAATTGACTGACAAAAATTCATTAAATGAGATTCTTGG
    GGAATTTGAATGTCGAGTAAAGTTTATAATTGACTGACAAAAATTCATTAAATGAGATTCTTGG
  
```

Box A/B

```

    GCGTAAATTCGCCATTCAAAATAAATTGACTGACAAAAATTCATTAAATGAGATTCTTGG
    CGCATAATTGACTGACAAAAATTCATTAAATGAGATTCTTGG
  
```

Figure 4-1. The *P1 parS* site. A. Blue and pink boxes outline the box A and box B sequences, respectively. The black line shows the IHF binding site (Funnell, 1991). B. Synthetic 25 base pair oligomers used as substrates in gel mobility shift assays (see Figure 4-7).

domain is located near the N-terminus of the protein. In Chapter 2, I suggested that this domain is involved in oligomerization (that is, dimer-dimer interactions) but that some type of conformational change in ParB is required for oligomers to form (Surtees and Funnell, 1999). This suggestion arose from two observations. First, the N-terminus of ParB is relatively susceptible to proteolysis (Fig. 2-2), suggesting it is not very stably folded in solution. Second, self-association, measured by chemical cross-linking experiments *in vitro*, of the N-terminus was observed only when the C-terminal half of ParB was removed (Figs. 2-7 and 2-8). One possibility is that DNA binding elicits a conformational change that removes the inhibitory effect of the C-terminus on N-terminal self-association, promoting oligomerization. The N-terminal oligomerization domain either overlaps or is adjacent to a region of ParB that is required for an interaction with ParA (Fig. 4-2A) (Radnedge *et al.*, 1998; Surtees and Funnell, 1999) (Chapter 2).

Two different regions of ParB appear to have a role in its specific DNA binding activity, one near the C-terminus of ParB and the second in the middle of the protein (Fig. 4-2A). Point mutations near the C-terminus disrupt DNA binding activity (Lobocka and Yarmolinsky, 1996). Proteins with these mutations also fail to dimerize and it has been suggested that lack of dimerization prevents DNA binding. These mutations all fall within the last 59 amino acids of ParB, a region that encompasses the C-terminal dimerization domain (Surtees and Funnell, 1999). This region also includes the “discriminator recognition sequence”, or DRS, defined by domain-swapping experiments (Radnedge *et al.*, 1996). When residues 281-302 of P1 ParB were swapped with the equivalent region of the ParB protein of P7, the resulting hybrid protein recognized P7 *parS* in an *in vivo* partition assay (Radnedge *et al.*, 1996). The P7 *parS* site is very similar to P1 *parS*. The P1 and P7 box A sequences are interchangeable (Hayes and Austin,

1993) but the box B sequences are not (Hayes and Austin, 1993). Thus the swapping experiment defined the DRS as a region that contacts box B sequences directly or promotes a fold that allows box B- binding. Analysis of the ParB sequence identified a putative helix-turn-helix (HTH) motif, from residues 166 to 189, that has also been implicated in ParB's DNA-binding activities (Dodd and Egan, 1990). Point mutations located on either side of the putative HTH domain disrupt DNA binding activity (Lobocka and Yarmolinsky, 1996). It has been proposed that this region of the protein binds the *parS* box A sequences (Radnedge *et al.*, 1996).

In this study, I have examined the interaction of ParB with its specific sequences in *parS* by asking how different regions of the protein contribute to its DNA binding activities. My results suggest a model of how protein-DNA (ParB-box A and ParB-box B) and protein-protein (dimerization) interactions contribute to the architecture of the partition complex.

Experimental Procedures

Bacterial strains, growth media, reagents and buffers are as described in Chapters 2 and 3.

Plasmid construction. The new constructs created for this work were generated by PCR and cloned into pET15b (Novagen), which encodes a hexa-histidine tag. pJS10 (Table 2-1) (Surtees and Funnell, 1999) was used as the substrate for PCR amplification. To create the 142-333 ParB fragment, the region of *parB* encoding this portion was amplified by PCR. The upstream primer (5'GCGCCATATGGACGTTTCAGACAGCATTG) added a single Met residue upstream of residue 142. M13 forward primer was the downstream primer. This PCR fragment was gel purified (QIAEX II), digested with *NdeI* and *BamHI* and ligated into pET15b, creating pJS208. For 1-330 ParB, 1-325 and 1-317 ParB, the upstream primer (5'GCGCATATGTCAAAGAAAAACAGACCAAC) incorporated an *NdeI* site at the start site. The downstream primers, 5'CGCGGGATCCTTACTTTTTATCGAGGCTC, 5'CGCGGGATCCTTACTTTCTAAGGATATGCCC and 5'CGCGGGATCCTTACCTGTCGAGTTCTTCCTG, created stop codons in place of residues 331, 326 and 318, respectively and created a *BamHI* site downstream of the stop codons. The *NdeI-BamHI* fragments were then cloned into pET15b, generating pJS207, pJS212 and pJS213.

To create the internal deletions of ParB, the region of *parB* encoding residues 185 to 333 was amplified using an upstream primer (5'CGCGCTCGAGTGCTCTCCAGGCAGCGAGTG) that placed a *XhoI* site just upstream of codon 185 and the M13 forward primer. The resulting *XhoI-BamHI* fragment was cloned into pET15b to create pJS206. The regions encoding residues 1-142 and residues 1-165 were amplified with an upstream primer, 5'GCGCATATGTCAAAGAAAAACAGACCAAC (placing an *NdeI* site at the start site), and a

downstream primer, either 5'CGCGCTCGAGTCTTTCGCTAAATTTTGCGC (creating a *XhoI* site just downstream of codon 142) or 5'CGCGCTCGAGCCATCATTTCATTCGCAT (creating a *XhoI* site just downstream of codon 165). The *NdeI-XhoI* fragments were cloned into pJS206 to generate pJS210, encoding Δ 142-185 ParB, and pJS211, encoding Δ 166-185 ParB. This cloning strategy replaced the region between residues 143 and 185 or between residue 165 and 185 of ParB with two serine residues.

DNA substrates. For gel mobility shift assays with the intact *parS* site, pBEF165 was digested and end-labeled as described in Chapter 3. For DNase I footprinting reactions, DNA substrates were generated by digesting either pBEF165 or pBEF166 with *Bam*HI and *Sma*I or *Bam*HI and *Bgl*II, generating a 211 bp or a 240 bp *parS* fragment, respectively. They were ³²P-labeled at the 3' end of the *Bam*HI site. The fragments labeled on the upper strand (as drawn in Fig. 4-1A) were generated from pBEF165 and fragments labeled on the lower strand were generated from pBEF166.

Competitor fragments for the gel mobility shift assays were 270 bp in length and were generated by PCR from pALA207 (Abeles *et al.*, 1985). The *parS*-containing fragment was amplified using the primers 5'CACTTGTGTGAATCCCTTTTC and 5'CAGGAAGAACTCGACAGGATG. The non-specific fragment was amplified with the primers 5'GCCTCTTGCGGGATATCGTC and 5'CTGTCGCAGCAGAGATGATG. The fragments were then purified from agarose gels.

The single site oligonucleotide substrates used for gel mobility shift assays are illustrated in Figure 4-1B. The lower strand of each pair was labeled at the 5' end with [γ ³²P]ATP and T4 polynucleotide kinase. The specific activity of each oligomer was determined by precipitating with trichloroacetic acid followed by liquid scintillation counting. The unincorporated

nucleotide was removed by gel filtration or by ethanol precipitation. The labeled oligomers were then mixed with an equal amount of the appropriate upper strand oligomer in 100 mM NaCl, 10 mM MgCl₂, 0.1 mM EDTA. The mixture was heated to 70°C and was then allowed to cool slowly to room temperature, to allow the two strands to anneal.

Electrophoretic mobility shift assays. These experiments were performed as described in Chapter 3. When the single site oligomers were used as substrates, 10 fmol of labeled substrates were used per assay.

DNase I protection assays. Standard 20 µl reaction mixtures contained 10 to 50 fmol of ³²P-labeled substrate, 50 mM HEPES-KOH (pH 7.5), 100 mM NaCl, 10% (v/v) glycerol, 100 µg of sonicated salmon sperm DNA/ml, 100 µg BSA/ml, 10 mM MgCl₂, 2 mM CaCl₂ and 7 mM β-mercaptoethanol. The mixtures were assembled on ice and incubated at 30°C for 15 min. Bovine pancreatic DNase I was then added (1 µl of a 1 µg/µl solution). After 2 min at 30°C, the reaction was stopped by addition of 80 µl of 1.6 M ammonium acetate, 400 µg sonicated salmon sperm DNA/ml and 0.1 M EDTA. After phenol:chloroform extractions of the mixtures, the DNA was precipitated with ethanol and resuspended in 4 µl formamide dye (Sambrook *et al.*, 1989).

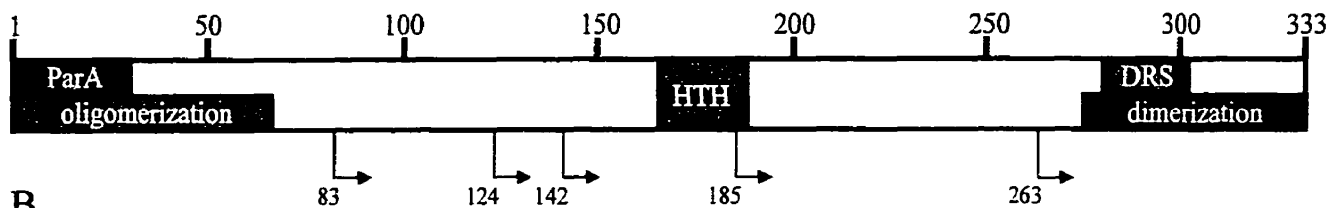
Results

In this work, I have examined the architecture of the partition complex by determining the DNA binding properties of various regions of ParB. ParB is 333 amino acids in length and I previously examined its domain structure by partial proteolysis mapping and by the self-association activity of various ParB protein fragments (Chapter 2) (Surtees, 1996; Surtees and Funnell, 1999). Here I have used several of those fragments to examine their interaction with the P1 *parS* site. All fragments contain a poly-histidine tag to facilitate purification. In addition, I have constructed six new derivatives of ParB (Fig. 4-2B). My previous partial proteolysis experiments identified two tryptic fragments that were relatively resistant to further digestion. His-142-333 ParB (constructed here) and His-187-333 ParB (Chapter 2; (Surtees and Funnell, 1999) correspond to these two tryptic fragments (Fig. 4-2A, (Surtees and Funnell, 1999). To examine the function of the extreme C-terminus of ParB, I removed 3, 8, and 16 residues from its C-terminus, generating His-1-330 ParB, His-1-325 ParB and His-1-317 ParB. Finally, I made two internal deletions of ParB that removed the putative helix-turn-helix motif. The first removed only this predicted motif (residues 166-184) and the second removed residues 143-184, the region between the start sites of the two stable tryptic fragments mentioned above (Fig. 4-2B).

I first tested the dimerization activity of the new protein fragments in a cross-linking assay (Fig. 4-3). His-142-333 ParB and both proteins with internal deletions (His- Δ 166-184 ParB and His- Δ 143-184 ParB) were cross-linked to dimer-sized smears in the presence of DSP, a cross-linking reagent that reacts primarily with lysines. His-1-330 ParB and His-1-325 ParB were also able to dimerize, as determined by this assay (Fig. 4-3). His-1-317 ParB, however, was not cross-linked, indicating that it is predominantly monomeric in solution. It behaves as

Figure 4-2. The structural and functional domains of ParB. **A.** Schematic of ParB domains. The coloured regions represent the regions of ParB involved in protein-protein and protein-DNA interactions. The HTH indicates a predicted HTH motif and the DRS represents a second region implicated in DNA binding (see text). The dimerization and oligomerization domains are at the C- and N-termini, respectively. The N-terminus also contains a region required for interactions with ParA. The arrows indicate the N-terminus of fragments generated by tryptic cleavage of ParB (Chapter 2). **B.** Diagram of ParB fragments used in this chapter. The coloured regions of ParB are as in **A**. Dimerization activity, as determined by DSP cross-linking, is indicated in the first column. The second column summarizes the ability of ParB fragments to bind *parS* and the third column indicates whether binding was stimulated by IHF. N/A, not applicable.

A



B

Residue Range	DSP cross-linking	<i>parS</i> -binding	IHF sensitivity
1-333	+*	+	+
1-47	+*	+	+
1-67	+*	+	+
1-142	+	+	+
1-187	+*	-	N/A
1-275	+*	-	N/A
1-330	+	+	+
1-325	+	+	+
1-317	-	+	-
1-312	-*	+	-
1-293	-*	+	-
1-274	-*	+	-
1-234	-*	-	N/A
1-165	+	-	N/A
142-185	+	-	N/A

* shown in Chapter 2 and (Surtees and Funnell, 1999)

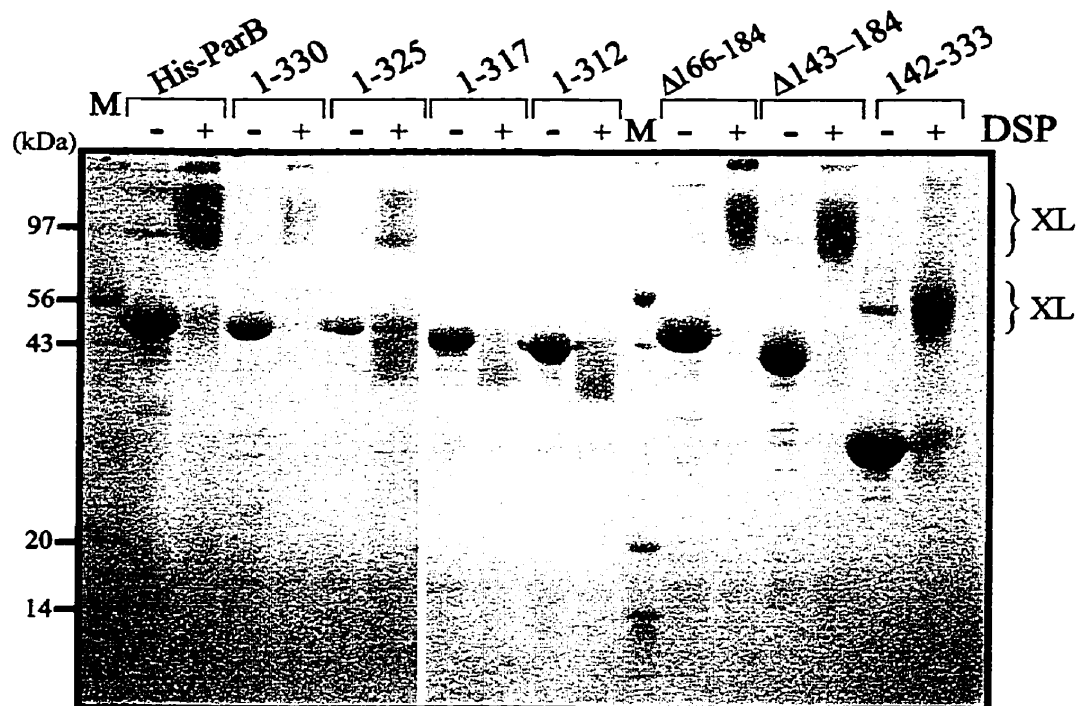


Figure 4-3. Cross-linking of His-ParB and of ParB fragments. His-tagged proteins were incubated with DSP at room temperature for 20 minutes and analyzed by electrophoresis through a 12% SDS polyacrylamide gel. These experiments were performed as described in Chapter 2. Lane M, size markers; XL, cross-linked products.

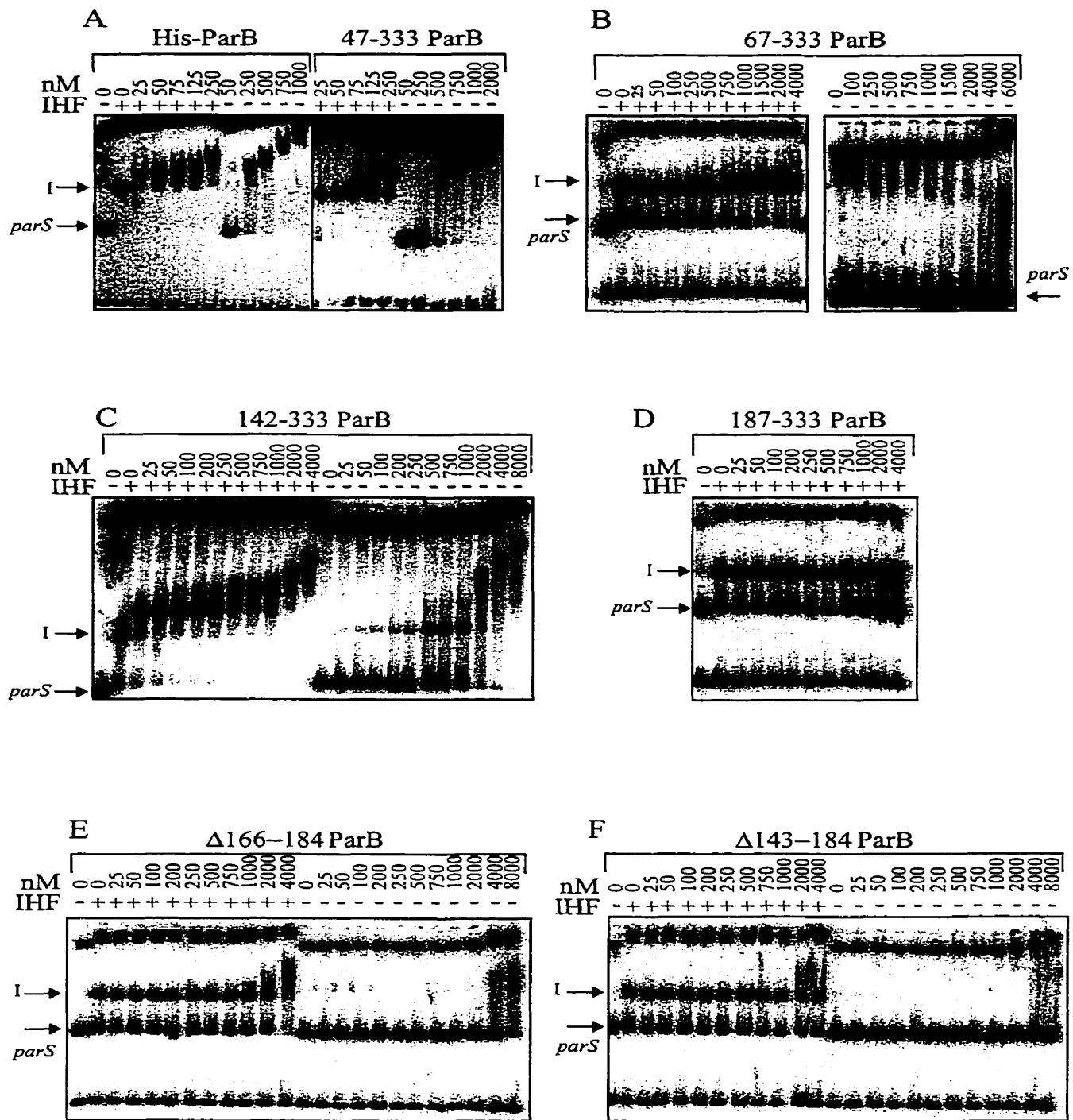
His-1-312 ParB (Fig. 4-3), which I previously reported to not be cross-linked by DSP (Chapter 2; Surtees and Funnell, 1999). Therefore, the region between residues 317 and 325 of ParB defines the C-terminal boundary of its dimerization domain. The abilities of previously isolated ParB fragments to dimerize are summarized in Fig. 4-2B (Surtees and Funnell, 1999).

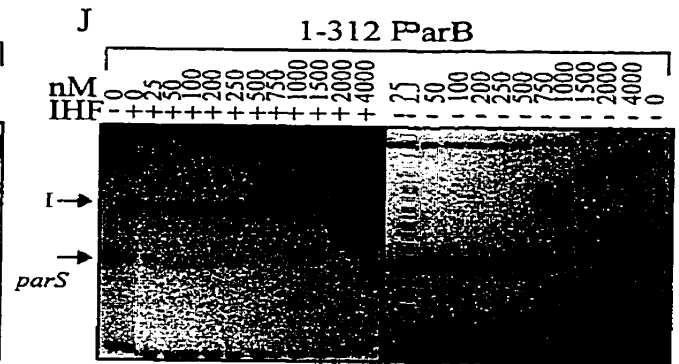
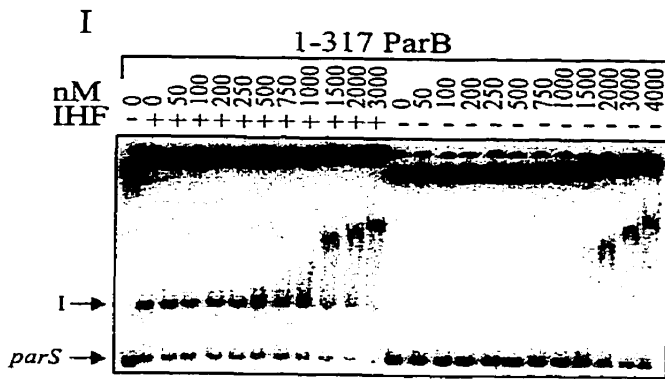
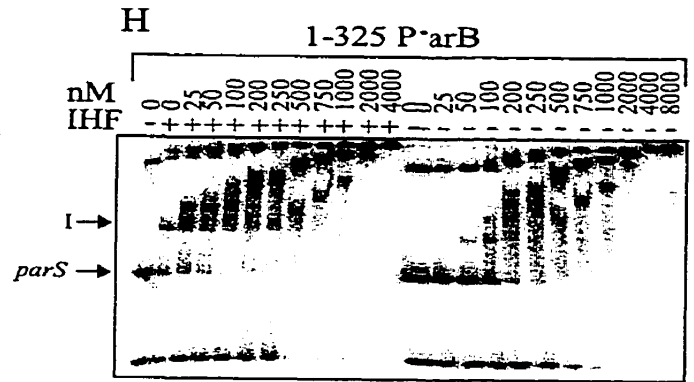
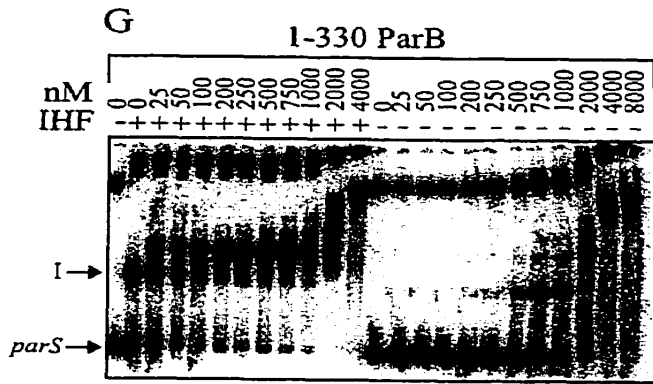
The region between residues 142 and 325 contains all information required for binding to the full *parS* site. In the presence of IHF, one dimer of ParB binds to *parS* in a very high-affinity protein-DNA complex (Chapter 3) (Funnell, 1991; Bouet *et al.*, 2000). This interaction requires that ParB contact its specific recognition sequences on either side of the IHF-directed bend simultaneously (Funnell and Gagnier, 1993). In the absence of IHF, ParB affinity for *parS* is much lower and binding is primarily dependent on the box A and box B sequences on the right side of the IHF site (Fig. 4-1A). Therefore one can distinguish two types of ParB binding: the latter (low-affinity), requiring specific contacts but not IHF, and IHF-stimulated DNA-binding (high-affinity), requiring both specific contacts and the IHF-directed bend in the DNA. In this work, I address the question of what regions of ParB contribute to the different aspects of ParB's DNA binding activities.

I first examined several C-terminal fragments of ParB (i.e. truncated from the N-terminus) for their *parS*-binding activity. Full-length ParB (or His-ParB in my assays), and three fragments, His-47-333 ParB, His-67-333 ParB and His-142-333 ParB, bound to *parS* and this binding was stimulated by IHF (Fig. 4-4A,B,C). The affinity of the fragments for *parS* differed, but the relative affinity of each ParB fragment for *parS* was much higher with IHF than without IHF. Therefore the first 141 residues of ParB are not required for IHF-stimulated *parS* binding.

Next, I assessed the importance of the central portion of ParB in DNA binding. His-187-333 ParB and His-275-333 ParB contain both the C-terminal dimerization domains and the

Figure 4-4. DNA binding activity of several ParB fragments in the presence and absence of IHF, measured in gel mobility shift assays. ³²P-labeled *parS* fragments were incubated with the ParB proteins and/or IHF, and the mixtures were analyzed by electrophoresis through a 5% polyacrylamide gel. The *parS* fragments were generated from *Bam*HI (panels **A,B,D,E,F,G,H,J**) or *Xba*I (panels **C** and **I**) digests of plasmid pBEF165, yielding 252-base pair and 132-base pairs substrates, respectively. The *Bam*HI digest also generated a 120 base pair and a 3040 base pair vector fragment. The *Xba*I digest created only one 3280 base pair vector fragment. IHF, when present, was 400 nM. The positions of free DNA (*parS*) and the IHF-*parS* (I) complexes are indicated. The concentrations of His-ParB and of all ParB truncations are nM monomers. Note that the large vector fragment contains an IHF binding site. **A**, His-ParB and His-47-333 ParB in the presence and absence of IHF. **B**, His-67-333 ParB in the presence or absence of IHF. The same substrate was used in both panels, but the gel in the right panel was run further and the small non-specific (non-*parS*) fragment ran off the bottom of the gel. **C**, His-142-333 ParB in the presence and absence of IHF. **D**, His-187-333 ParB in the presence of IHF. **E**, His-Δ166-184 ParB in the presence and absence of IHF. **F**, His-Δ143-184 ParB in the presence and absence of IHF. **G**, His-1-330 ParB in the presence and absence of IHF. **H**, His-1-325 ParB in the presence and absence of IHF. **I**, His-1-317 ParB in the presence and absence of IHF. **J**, His-1-312 ParB in the presence and absence of IHF.





discriminator recognition sequence (DRS), but are missing the putative helix-turn-helix domain located near the centre of ParB (Fig. 4-2). Neither fragment had any *parS*-binding activity, with or without IHF (Figs. 4-4D and 4-8 and data not shown). Therefore, a region N-terminal to residue 187 is required for stable *parS* binding in this assay. Since the first 141 residues were not required for binding (Fig. 4-4C), the region between amino acids 142 and 187, which includes the putative HTH motif, contains information required for DNA binding. I next examined the activity of ParB fragments lacking only this region, His- Δ 166-184 ParB and His- Δ 143-184. Neither protein bound *parS* with or without IHF (Fig. 4-4 E,F) although some apparently non-specific or unstable binding activity was observed at the highest protein concentrations. These results indicated that the central region of ParB is required for *parS* binding and the C-terminal DRS is not sufficient for stable *parS* binding.

Finally, I was interested in the role of the C-terminus of ParB in DNA-binding. I deleted 3 and 8 residues from the C-terminus of ParB, and tested the resulting fragments of ParB for their ability to bind *parS* in the gel mobility shift assay. His-1-330 ParB and His-1-325 ParB both exhibited IHF-stimulated DNA-binding (Fig. 4-4G,H), and both were able to dimerize as judged by cross-linking assays (Fig. 4-3).

DNase I footprinting experiments showed that His-ParB, His-47-333 ParB, His-67-333 ParB and His-142-333 ParB exhibited very similar patterns of protection of the *parS* sequence (Fig. 4-5A and data not shown). As predicted from the gel mobility shift experiments, these results indicate that the first 141 amino acids of ParB are not required for minimal partition complex formation. Neither His-187-333 ParB nor His-275-333 ParB provided any protection of *parS* from DNase I cleavage, also consistent with the results from the gel mobility shift assays (Fig. 4-5 E, F). Similarly, His- Δ 143-184 ParB and His- Δ 166-184 afforded no protection from

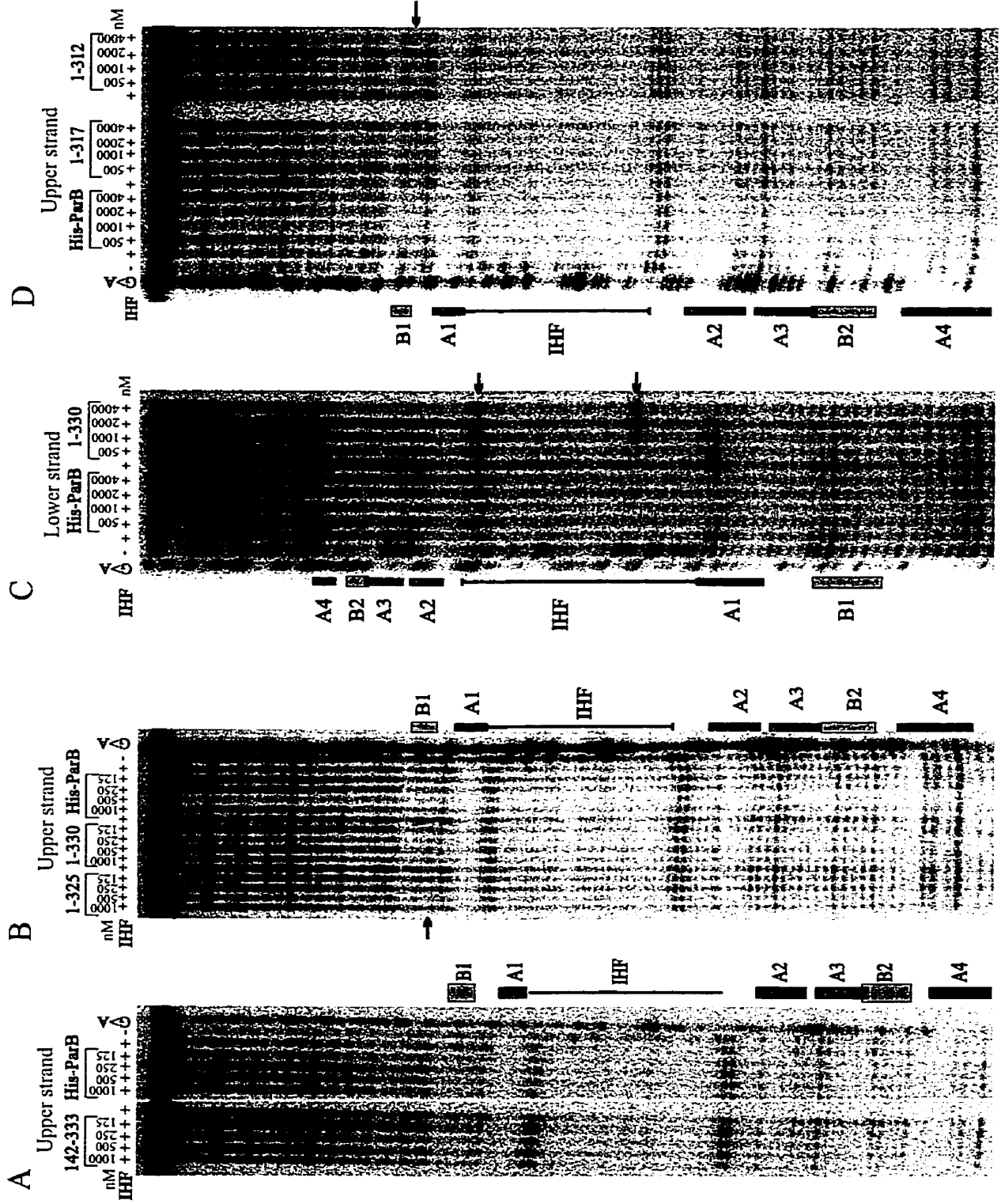
DNase I cleavage (data not shown).

Footprinting experiments with His-1-330 ParB produced a pattern of protection similar to that of His-ParB, but with additional enhancements (Fig. 4-5B,C). First, on the upper strand of *parS*, one band in box B1 is strongly enhanced (Fig. 4-5B). On the lower strand, one band near the centre and one near the right boundary of the IHF binding site are strongly enhanced (Fig. 4-5C). These differences indicate changes in the geometry of the complex that make the minor groove more accessible to DNase I in these regions. These enhancements were not observed in the presence of His-1-325 ParB, whose protection pattern was very similar to that of His-ParB.

C-terminal dimerization is required for high-affinity *parS* binding. In contrast to the fragments with small C-terminal deletions, His-1-317 ParB, His-1-312 ParB, His-1-293 ParB and His-1-274 ParB bound *parS*, but a high protein concentration was required in order to observe binding (500-1000 nM) and little or no stimulatory effect by IHF was observed (Fig. 4-4 I,J and data not shown). The IHF-insensitive binding is relatively weak (i.e. low affinity), as is full-length ParB binding to *parS* in the absence of IHF, (Funnell, 1991). Therefore removal of only 16 amino acids from the C-terminus removed the ability of IHF to stimulate ParB's specific DNA binding activity. The appearance of IHF-insensitive binding also correlated with the loss of dimerization activity (Surtees and Funnell, 1999, Figs. 4-2 and 3). Note that the N-terminal fragments with IHF-insensitive binding activity retain the putative helix-turn-helix domain. His-1-317 ParB and His-1-312 ParB also retain the DRS.

ParB fragments that exhibited IHF-insensitive DNA binding activity in a gel mobility shift assay showed no detectable protection patterns in *parS* in DNaseI footprinting experiments (Fig. 4-5D and data not shown). This was surprising because I had expected to observe binding to at least the box A motifs because these fragments retained the putative HTH motif. I

Figure 4-5. DNase I footprinting of His-ParB and ParB fragments at *parS*. The upper and lower strands correspond to the upper and lower strands drawn in Figure 4-1A. The DNA substrates were 211 bp (panels **A**, **B** and **D**) or 240 bp (panel **C**) DNA fragments that were ³²P-labeled at the 3'-end of either the upper or lower strand. Protein-DNA complexes were treated briefly with DNase I (see Experimental Procedures) and analyzed on 6% sequencing gels. IHF, when present, was at 400 nM. ParB concentrations are reported for monomers. On each gel, Maxam-Gilbert G>A sequencing reactions were included as markers. The box A, box B and IHF sites are drawn alongside each gel. **A**, Protection of the upper strand of *parS* from DNase I digestion by His-142-333 ParB or His-ParB. **B**, Protection of the upper strand of *parS* from DNase I by His-1-325 ParB, His-1-330 ParB or His-ParB. **C**, Protection of the lower strand of *parS* from DNase I by His-ParB or His-1-330 ParB. Arrows indicate enhancements created by His-1-330 ParB. **D**, Protection of the upper strand of *parS* from DNase I digestion by His-ParB, His-1-317 ParB or His-1-312 ParB. The arrow indicates the enhancement generated by His-1-317 ParB. **E**, Protection of the lower strand of *parS* from DNaseI digestion by His-275-333 ParB and ParB. **F**, Protection of the upper strand of *parS* from DnaseI digestion by His-ParB and His-187-33 ParB.

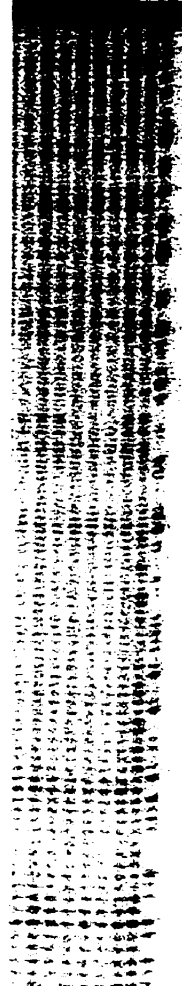


E

Lower strand

275-333 *ParB*

nM	[2500]		[1000]			
IHF	+	+	+	+	+	G>A
	+	+	+	+	+	
	+	+	+	+	+	

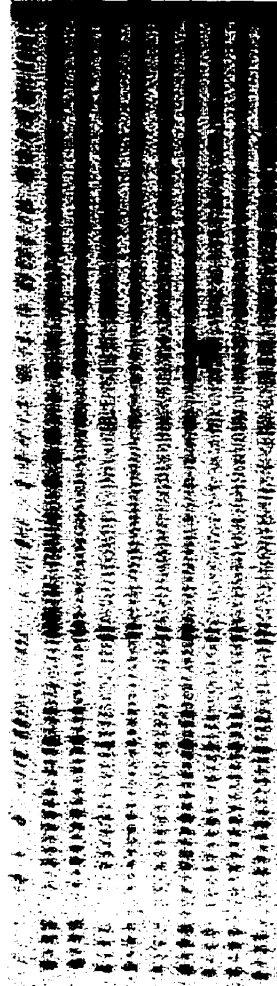


F

Upper strand

His-ParB 187-333

G>A	-	[+500]		[+1000]		[+2000]		nM
IHF	-	+	+	+	+	+	+	
		+	+	+	+	+	+	
		+	+	+	+	+	+	



concluded that the *parS*-binding activity of these IHF-insensitive ParB fragments was too weak to be detectable in a DNase I footprinting assay. For instance, the fragments may bind *parS* for too little time to protect the DNA from cleavage. However, His-1-317 ParB did show evidence of a specific interaction with *parS*. The same enhancements observed in the presence of His-1-330 ParB were also observed with His-1-317 ParB (Fig. 4-5C,D).

I tested whether the IHF-insensitive binding activity was still specific for *parS*, using competition assays (Fig. 4-6). The ability of an N-terminal fragment of ParB to bind to a labeled *parS* substrate was challenged by a 270 bp, unlabeled DNA fragment containing either the *parS* sequence or a non-specific sequence. With both His-1-317 ParB and His-1-312 ParB, the *parS* DNA was a better competitor than the non-specific DNA, indicating that binding is specific (Fig. 4-6 and data not shown). All ParB fragments that bound *parS* also contained some non-specific DNA binding activity, a property of the full-length protein (Funnell, 1991).

N-terminal fragments smaller than His-1-274 ParB had no DNA binding activity (data not shown). His-1-234 ParB is not cross-linked by DSP and His-1-189 ParB has some self-association activity through the N-terminal oligomerization domain (Chapter 2) (Surtees and Funnell, 1999). Neither fragment interacted with *parS*. Therefore a region C-terminal to residue 234 is required for binding and N-terminal self-association is not sufficient for DNA binding.

Binding to isolated box A or box B sequences. While the different DNA-binding activities of the ParB fragments used in this study supported the hypothesis that the putative HTH and the DRS regions interact with box A and box B sequences, respectively, I wanted to demonstrate direct interactions. I designed synthetic oligomer (25 bp) substrates that contained only the box A inverted repeat (i.e. box A2-box A3), only a single box B sequence (box B2) or the box A inverted repeat overlapping a box B sequence (box A2-A3/box B2) (Fig. 4-1B). As

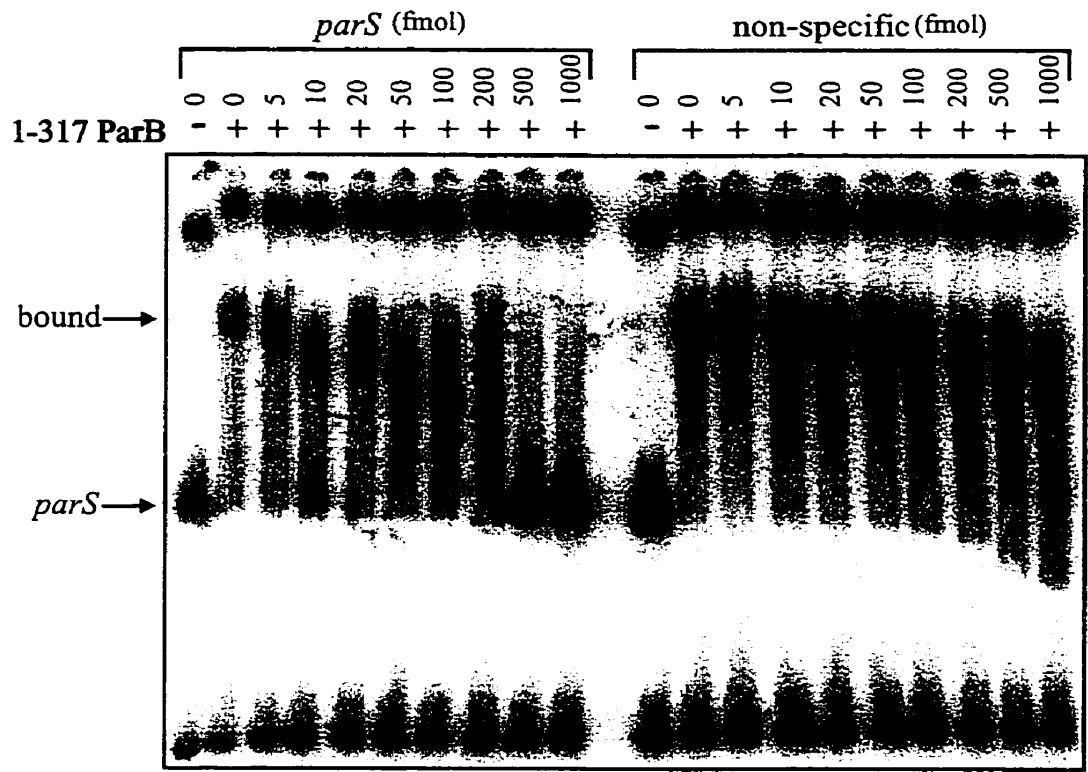


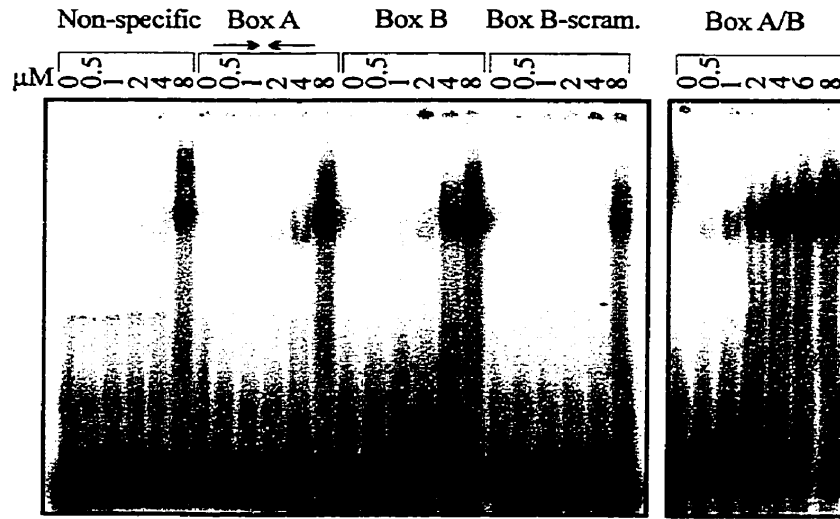
Figure 4-6. Competition analysis of His-1-317 ParB binding to *parS*. The ³²P-labeled DNA substrate was a *Bam*HI restriction digest of pBEF165. The fragment containing *parS* was 252 bp (arrow). Increasing amounts of unlabeled 270 bp DNA fragments containing *parS* or non-specific sequence (indicated above lanes in fmol) were added to the reaction mixtures prior to the addition of His-1-317 ParB (at 1 μM monomer). No IHF was added and the mixtures were analyzed by electrophoresis in a 5% polyacrylamide gel (Experimental Procedures).

controls, I designed two non-specific oligomer substrates. One contained the same sequence as the box B oligomer, except that the box B sequence itself was scrambled, and the second contained an unrelated 25 bp sequence (Fig. 4-1B). Since the synthetic substrates were small, I expected, and found, that the affinity of the various versions of ParB for the sequences would be significantly reduced. Much higher protein concentrations were required for binding compared to reactions with intact *parS*, indicating weaker binding to the sites. Further, in most cases, smeary rather than discrete complexes were observed, indicating less stable binding. Nonetheless, I did observe specific binding with several protein-substrate combinations that provided additional insight into ParB binding. To control for differences in the specific activity of different substrates, I quantified the amount of binding as the loss of substrate band migrating at the “free” position (Table 4-1). I observed similar binding activity when I performed these experiments so that the substrates were adjusted to approximately equal specific activity with unlabeled substrate (data not shown).

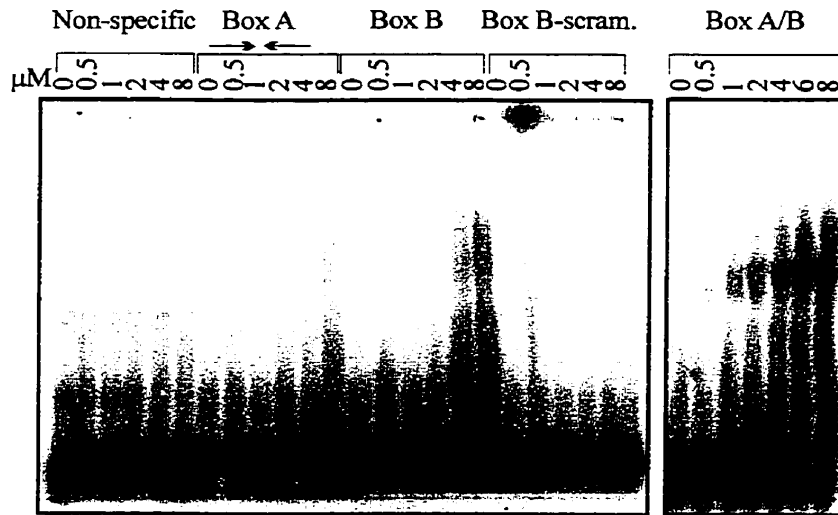
His-ParB bound all of the synthetic substrates, including the negative controls. However, His-ParB formed complexes with the box A and the box B substrates at lower protein concentrations than with the control substrates, indicating site specificity. Furthermore, His-ParB bound the box A/B substrate at even lower protein concentrations than it bound to the other substrates, indicating that the presence of both sites has at least an additive effect on binding. While I believe that these experiments represent specific binding to the box A and box B sequences, there remains a significant amount of non-specific binding. This is consistent with previous work that showed wild-type ParB has high non-specific DNA binding activity, particularly in the absence of IHF (Funnell, 1991). This property appears to be unique to the full-length protein (Fig. 7A-F).

Figure 4-7. DNA binding activity of ParB fragments to oligomeric DNA substrates. The oligomeric DNA substrates are described in Figure 4-1B. Increasing amounts of His-ParB and ParB fragments were incubated with each of the oligomeric substrates and analyzed by electrophoresis in a 5% polyacrylamide gel. Protein concentrations at μM monomer.

(A) His-ParB



(B) His-142-333 ParB



(C) His- Δ 166-184 ParB

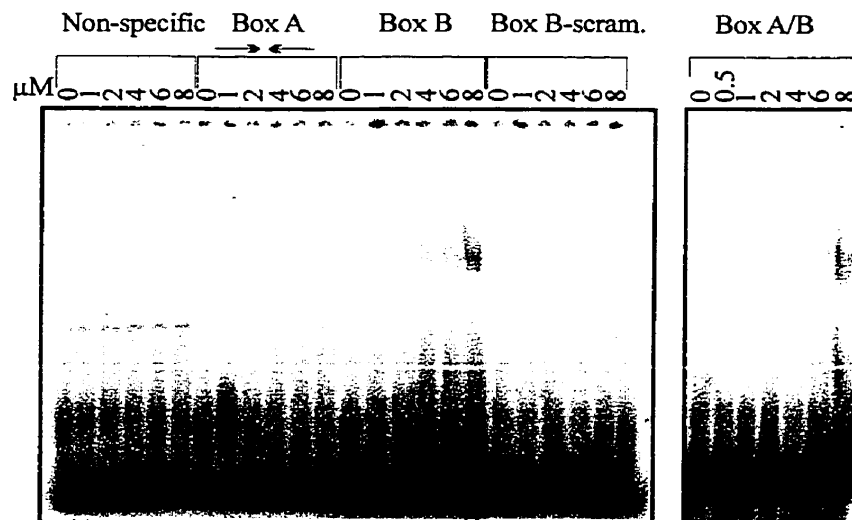


TABLE 4-1. Quantification of synthetic substrate binding activity

Protein	Substrate	% Free Substrate (at 8 μM)
His-ParB	Non-specific	52 +/- 19
	Box A	21 +/- 7
	Box B	17 +/- 9
	Box B-scrambled	73 +/- 15
	Box A/B	20 +/- 9
His-142-333 ParB	Non-specific	99 +/- 12
	Box A	67 +/- 8
	Box B	48 +/- 21
	Box B-scrambled	105 +/- 11
	Box A/B	33 +/- 5
His- Δ 166-184 ParB	Non-specific	105 +/- 10
	Box A	97 +/- 5
	Box B	75 +/- 11
	Box B-scrambled	99 +/- 18
	Box A/B	69 +/- 11
His-1-330 ParB	Non-specific	87 +/- 14
	Box A	48 +/- 11
	Box B	48 +/- 5
	Box B-scrambled	92 +/- 4
His-1-317 ParB	Non-specific	93 +/- 5
	Box A	60 +/- 9
	Box B	79 +/- 13
	Box B-scrambled	98 +/- 11
His-1-312 ParB	Non-specific	96 +/- 9
	Box A	58 +/- 13
	Box B	97 +/- 3
	Box B-scrambled	98 +/- 6

For these experiments, binding was defined as the disappearance of the substrate band. In quantifying the data, I determined the ratio of substrate to total signal in each lane. The ratios were then normalized to the “no protein” lane for each substrate. Each value is the average of at least 3 separate experiments.

His-142-333 ParB exhibited weak binding to the single site substrates (Fig. 7B), but showed a reproducible preference for these substrates over the control substrates (Table 4-1). As with the full-length protein, His-142-333 ParB bound to the box A/B substrate better than to either single-site substrate. The effect of the presence of both the box A and the box B sequences is more than additive, strongly supporting the idea that His-142-333 ParB interacts with both the box A and the box B sequences. This is in contrast to His- Δ 166-184 ParB and His- Δ 143-184 ParB (Fig. 7C and data not shown). Both showed detectable but weak binding to the box B sequence, whereas only background binding was observed with the box A sequence, as compared to non-specific DNA. Furthermore the binding activity of His- Δ 166-184 ParB is apparently unaffected by the presence of the box A inverted repeat in combination with the box B sequence. These results support an essential role for the putative HTH in box A recognition and indicate that this region is not required for box B binding, although the additional protein length did stabilize the contacts with box B.

His-1-330 ParB and His-1-325 ParB bound to both the box A and the box B substrates (Fig. 4-7D and data not shown). Non-specific DNA binding activity appeared to be reduced compared to His-ParB. I tested the ability of His-1-317 ParB and His-1-312 ParB, fragments which showed no dimerization activity but contain the DRS, to bind in the oligomer assay. Both bound box A (Fig. 4-7 E,F). Only His-1-317 ParB also bound the box B substrate, albeit weakly. These results suggest that residues more C-terminal than the DRS also form part of the box B binding domain of ParB.

The putative helix-turn-helix domain can function as a monomer. My experiments indicate that a dimerized C-terminus of ParB is necessary but not sufficient for IHF-stimulated DNA binding activity: ParB must contain both the C-terminus (including the DRS) as well as the

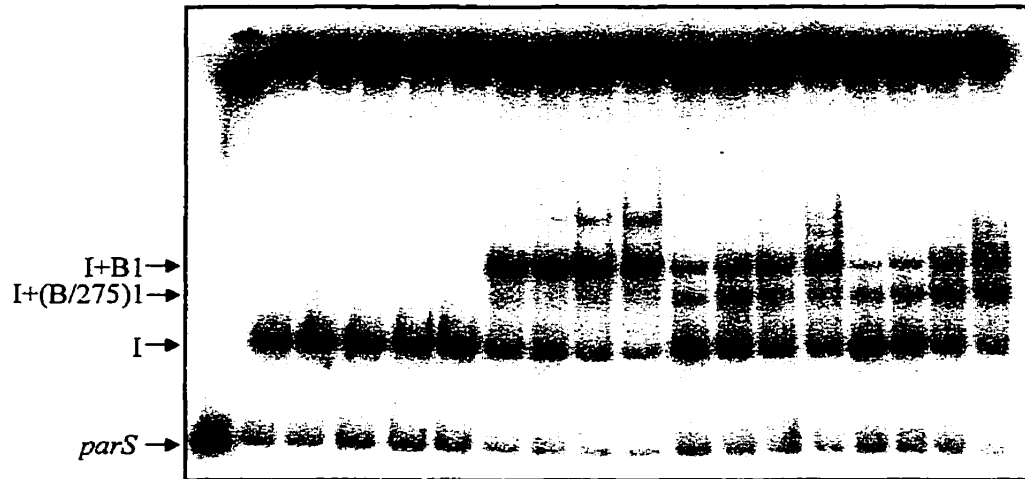
HTH for this activity. Since helix-turn-helix domains often function as dimers (Pabo and Sauer, 1992), I asked whether this region in ParB must be dimerized via the C-terminal domain in order for ParB to bind *parS*. I formed heterodimers between native ParB (no histidine tag) and His-275-333 ParB, at a 10:1 molar ratio, by denaturing and then slowly renaturing the protein mixture. This small C-terminal fragment of ParB is able to dimerize but has no DNA-binding activity (Figs. 2B and 8A). To confirm that heterodimers were formed, a portion of the ParB/His-275-333 ParB mixture was purified by nickel affinity chromatography. The majority of the mixture was retained on the column (data not shown). ParB dimers that bound the column must contain at least one histidine tag and therefore must be present in the form of heterodimers.

The renatured proteins were used in gel mobility shift assays (Fig. 4-8). In the presence of IHF (Fig. 4-8A), the ParB/His-275-333 ParB heterodimer mix formed a complex that migrated between the *parS*+IHF complex and the *parS*+IHF+ParB complex (Fig. 4-8A). This intermediate complex, I+(B/275)1, represents heterodimers binding to *parS*. Therefore a single putative helix-turn-helix domain, in the presence of a dimerized C-terminus is sufficient to allow IHF-stimulated *parS* binding. Native ParB dimer complexes were also produced from the mixture, even when the heterodimers had been repurified over nickel affinity column. This suggested that homodimerization of native ParB occurred over the course of the experiment. Finally, no intermediate complexes were observed in the absence of IHF (Fig. 4-8B); only complexes of the size expected from full-length ParB were seen.

Figure 4-8. ParB/His-275-333 ParB heterodimers bind to *parS*. **A**, DNA binding by His-275-333 ParB, ParB homodimers and ParB/His-275-333 ParB heterodimers in the presence of IHF. The proteins were incubated with 132 bp *parS* fragment and the reaction mixtures were analyzed by electrophoresis through a 5% polyacrylamide gel. The protein concentrations (as dimers) are indicated above each lane. The concentration of ParB/His-275-333 ParB heterodimers assumes that all ParB monomers are paired with a His-275-333 ParB fragment. When present, IHF was at 400 nM. To form ParB/His-275-333 ParB heterodimers, 25 µg of ParB and 65 µg of His-275-333 ParB (10-fold molar excess) were mixed, diluted in 100 µl of 6 M guanidine-HCl, 0.1 M NaH₂PO₄, 0.01 M Tris; pH 8.0 and then dialyzed against 300 ml of the same buffer for 4 hours at 4°C to denature both proteins. The proteins were renatured by successive dialysis steps against decreasing concentrations of guanidine HCl followed by a final dialysis against 50 mM Na-phosphate, pH 8.0, 300 mM NaCl, 7 mM β-mercaptoethanol, 10% (v/v) glycerol. Both His-275-333 ParB and ParB were denatured and renatured in separate dialysis bags as controls. To repurify the ParB/His-275-333 ParB mixture, half of the denatured/renatured mixture was purified over a 20 µl nickel-agarose affinity chromatography column (Surtees and Funnell, 1999). Bound protein was eluted with 500 mM imidazole. The arrows indicate the following complexes: I complex, IHF complex; I+B1 complex, IHF plus ParB complex 1; I+(B/275)1, IHF plus ParB/His-275-333 ParB complex 1. **B**, DNA binding by homo- and heterodimers in the absence of IHF. B1, ParB complex 1.

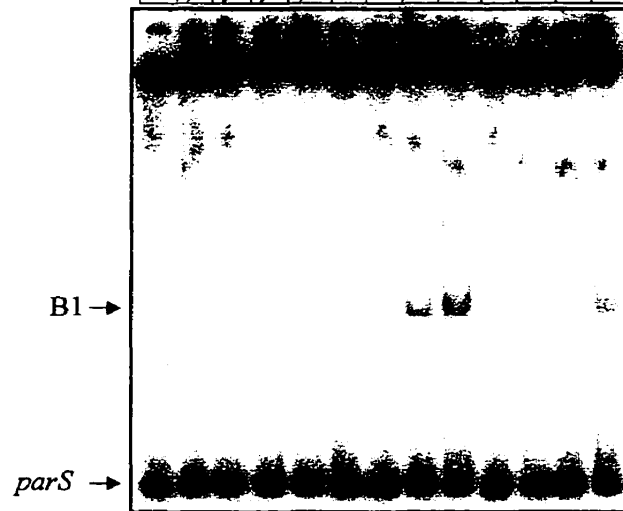
A

ParB/275-333 (re-purified)	-	-	-	-	-	-	-	-	-	-	-	-	-	-	125	250	500	1000
ParB/275-333	-	-	-	-	-	-	-	-	-	-	125	250	500	1000	-	-	-	-
ParB	-	-	-	-	-	125	250	500	1000	-	-	-	-	-	-	-	-	-
275-333	-	-	1250	2500	5000	10000	-	-	-	-	-	-	-	-	-	-	-	-
IHF	-	+	+	+	+	+	+	+	+	+	+	+	+	+	+	+	+	+



B

ParB/275-333	-	-	-	-	-	-	-	-	-	-	125	250	500	1000
ParB	-	-	-	-	-	125	250	500	1000	-	-	-	-	-
275-333	-	1250	2500	5000	10000	-	-	-	-	-	-	-	-	-



Discussion

Assembly of the P1 partition complex first requires the binding of one dimer of ParB and one α/β heterodimer of IHF to *parS*, forming a very high-affinity protein complex. Previous biochemical experiments have shown that ParB simultaneously contacts its recognition sequences on both sides of the IHF-induced bend in the DNA (Funnell and Gagnier, 1993). Here, I have used a series of ParB fragments to determine the role of different domains in *parS*-binding activity and to position the different regions of ParB within the nucleoprotein complex. My results show that dimerization is essential for the ability of IHF to stimulate ParB binding to *parS*. Therefore the ParB-ParB interaction across the IHF-directed bend is at the dimerization interface. In addition, my data support the prediction that the ParB HTH region recognizes the box A motifs, and that the DRS is part of the domain that recognizes the box B motifs. While ParB recognizes two distinct sequences with two distinct regions of the protein, both interactions are important in order to observe maximal *parS*-binding activity.

Figure 4-9 illustrates how I think one dimer of ParB interacts with and might be positioned on *parS* in the presence of IHF. His-142-333 ParB interacts with both the box A and box B sequences and this interaction is stimulated by IHF. Therefore His-142-333 ParB contains all the information required for assembly of the minimal partition complex that contains one dimer of ParB. The putative HTH motif of ParB is required for stable binding to the intact *parS* site (Fig. 4-4E,F), and is necessary for a detectable interaction with an oligonucleotide substrate containing a box A inverted repeat (Fig. 4-7C). In my model, the HTH region of each monomer interacts with a box A sequence in the A2-A3 inverted repeat, similar to a typical HTH protein such as the lambda repressor. My results also indicate that the C-terminus is directly involved in box B binding (Fig. 4-7C,E,F), and that the bend induced by IHF is unable to stimulate ParB

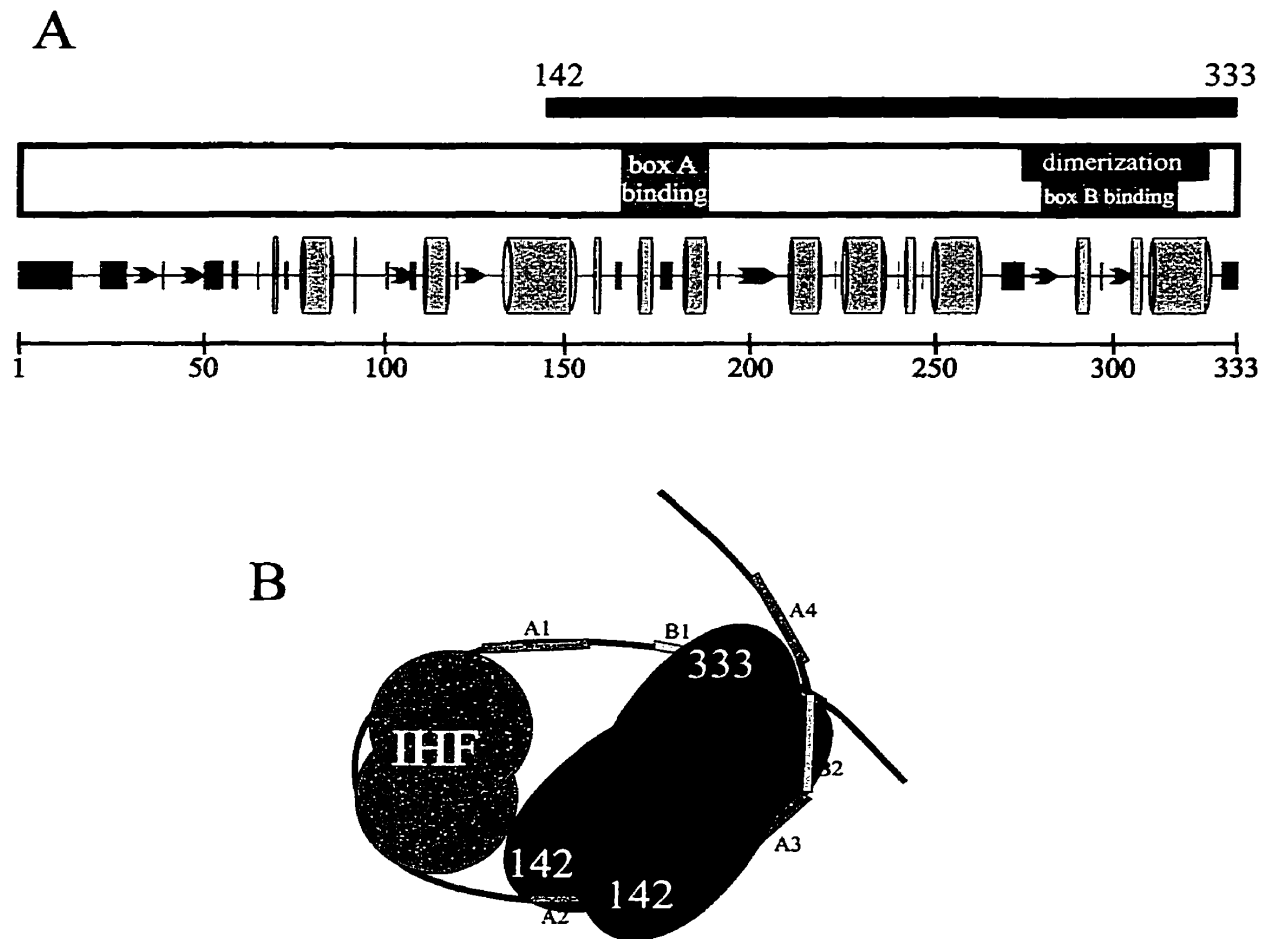


Figure 4-9. Model of the minimal partition complex. **A.** Schematic of the regions of ParB that are involved in binding the box A and box B sequences of *parS*. The black bar above represents the minimal region sufficient for *parS*-binding activity. Below the schematic is the predicted secondary structure of ParB (PHD) (Rost and Sander, 1993; Rost and Sander, 1994). The green boxes indicate predicted loops, the red arrows show predicted β -sheets and the orange cylinders denote predicted α -helices. Only structures predicted with greater than 82% probability are shown. **B.** Model of a single ParB dimer in the partition complex. 142-333 ParB contains all of the information required for DNA binding therefore the N-terminus is omitted from this diagram. The dimerized C-termini hold the two box B sites together, effectively wrapping the DNA around the ParB dimer. The two HTH motifs bind the box A2-A3 inverted repeat. The N-terminus of ParB (not shown) would be available for dimer-dimer and ParA-ParB interactions.

binding to *parS* in the absence of the C-terminal dimerization domain of ParB (Fig. 4-4I,J).

These observations support the previous prediction that the dimerized C-termini of a ParB dimer interact with both box B1 and B2 simultaneously at or near the dimerization interface (Chapter 3; Bouet *et al.*, 2000).

Two observations suggest that dimerization and box B binding are at least partially separable functions. First, His-1-317 ParB, a protein fragment that did not dimerize, was able to recognize the box B sequence, as evidenced by the enhancement observed in its DNase I footprint (Fig. 4-5C). Second, His-1-317 ParB bound the box B oligomer with higher affinity than it bound the scrambled box B oligomer (Fig. 4-7E), supporting the idea that dimerization and box B binding are separable functions. However I cannot exclude the possibility that a small amount of dimerization occurs in the presence of the DNA, particularly if this deletion has only partially destabilized the dimerization domain.

The putative helix-turn-helix domain. Based on sequence alignments, ParB has been predicted to contain a helix-turn-helix domain between residues 166 and 187 (Dodd and Egan, 1990). Secondary structure prediction of ParB by PHD (Rost and Sander, 1993; Rost and Sander, 1994), shown schematically in Fig. 4-9A, indicates a high probability that a helix is formed between residues 169 and 174 and between residues 180 and 188 of ParB. Between these two helices is a gap that includes a glycine residue, a residue that is highly conserved in the turn region of a classical HTH motif (Pabo and Sauer, 1992). While my biochemistry does not provide any structural evidence for such a domain, I have shown that the region spanning this putative motif is required for native DNA binding activity.

Typically, helix-turn-helix proteins, such as the lambda repressor, bind their recognition sites as dimers (Pabo and Sauer, 1992). The arrangement of a ParB dimer interacting with boxes

A2 and A3 resembles that of a typical HTH dimer interacting with an inverted repeat binding site. The formation of an IHF-stimulated complex by ParB/His275-333 ParB heterodimers (Fig. 4-8) shows that the HTH region need not act as a dimer. However, binding of ParB/His-275-333 ParB heterodimers to *parS* was completely dependent on IHF. Therefore in the absence of IHF, both HTH domains must be present. These results suggest that the relative importance of box A and box B sequences differs in complexes with and without IHF. Without IHF, both box A2 and A3 must be filled to promote binding, whereas with IHF, the box B sequences tethered at the dimerization interface can compensate for the loss of one HTH-box A interaction.

ParB-like proteins share only limited homology (Motallebi-Veshareh *et al.*, 1990; Hanai *et al.*, 1996; Mohl and Gober, 1997), but one thing that many have in common is a predicted helix-turn-helix motif (Dodd and Egan, 1990). Similarly, the sequences of the specific sites that have been identified to date are quite different, but all the known sites contain an inverted repeat (Davis and Austin, 1988; Ludtke *et al.*, 1989; Mori *et al.*, 1989; Lin and Grossman, 1998). It will therefore be interesting to see whether these other proteins bind their cognate site in a manner similar to that of P1 ParB.

Higher-order partition complexes. The minimal partition complex contains one dimer of ParB, but at higher protein concentrations additional dimers join the complex to form even higher-order complexes (Bouet *et al.*, 2000). I have suggested that additional ParB dimers are stabilized by interactions between the N-terminal self-association domains in ParB, as well as by protein-DNA interactions (Chapters 2 and 3; (Surtees and Funnell, 1999; Bouet *et al.*, 2000). DSP cross-linking experiments showed that this domain was in the N-terminal half of ParB, but yeast two-hybrid experiments suggested that it is within the N-terminal 61 residues (Surtees and Funnell, 1999). Both His-ParB and His-47-333 ParB formed higher order complexes in my

experiments, while His-67-333 ParB did not, consistent with my model. However, His-142-333 ParB also appeared to form higher-order complexes. I cannot tell whether there are additional self-association contacts that are more C-terminal to residue 142 of ParB, or whether these higher-order complexes are promoted only by protein-DNA interactions. Another possibility is that the N-terminal oligomerization domain is mainly involved in dimer-dimer interactions that mediate pairing of partition complexes. The role of this domain awaits further structural analyses of ParB in these higher-order complexes.

CHAPTER 5
Influence of deletions and DNA on ParB's structural domains

Future Directions

I performed all of the experiments in this chapter.

Introduction

A ParB dimer has a distinct domain structure with specific characteristics, defined by limited proteolytic digestion of the protein (Chapter 2; Surtees and Funnell, 1999). As proteolysis progressed, trypsin cleaved ParB at increasingly C-terminal sites, and generated fragments that extended to, or close to, the C-terminus of the protein (Fig. 5-1A) (Surtees and Funnell, 1999). The way in which the tryptic digestion of ParB occurs in time course experiments suggests that Band B is derived from Band A, Band C from Band B and Band D from Band C (Fig. 5-1B, Chapter 2; Surtees and Funnell, 1999). Therefore each subsequent cleavage may be dependent upon the previous cleavage.

This proteolytic pattern has particular implications about the domain structure of ParB. It shows that the N-terminal approximately 80 residues of ParB are quickly degraded by trypsin, indicating that this region is not stably folded and may be flexible in solution. In contrast, the C-terminal half of ParB folds into a very stable domain that is quite resistant to further proteolysis. One major tryptic cleavage site in ParB is on the C-terminal side of residue 184, near the C-terminal boundary of the predicted helix-turn-helix motif. The accessibility of this predicted DNA binding region is reminiscent of studies with other DNA-binding proteins that have shown that DNA recognition domains are sometimes hypersensitive to proteases (Tasayco and Carey, 1992), consistent with a surface location of the domain. Alternatively, a DNA binding domain may be somewhat disordered, or not stably folded, in the absence of DNA (Spolar and Record, 1994).

In this chapter, I examined the domain structure of ParB in the presence of DNA to determine whether binding of ParB to DNA protected regions of the protein from proteolysis or resulted in any conformational changes. I have also examined the domain structure of several

additional ParB fragments to determine whether they retain the same domain structure as intact ParB, again by limited proteolytic digestion.

Experimental Procedures

Proteins. All fragments of ParB used in this chapter contained a histidine tag. They were purified as described in Chapters 2 and 4. IHF was purified as described previously (Bouet and Funnell, 1999).

DNA fragments. The *parS* and non-specific DNA fragments were each 270 bp in length. They were generated by PCR and purified as described in Chapter 4.

Proteolysis. His-ParB or ParB fragments were incubated with trypsin in 50 mM Tris-HCl (pH 7.5); 100 mM NaCl; 0,1 mM EDTA and 20% (v/v) glycerol at room temperature. The protein:protease ratios used was 1000:1 (w/w). Digestion was stopped by the addition of acetic acid to 1% (v/v). For sequencing of the N-termini, proteolytic digestions were flash frozen on dry ice and stored at -20°C.

Protein sequencing. The protein products were separated and prepared as described in Chapter 2. Sequencing was performed at the Alberta Peptide Institute, Edmonton, Alberta, Canada.

Results and Discussion

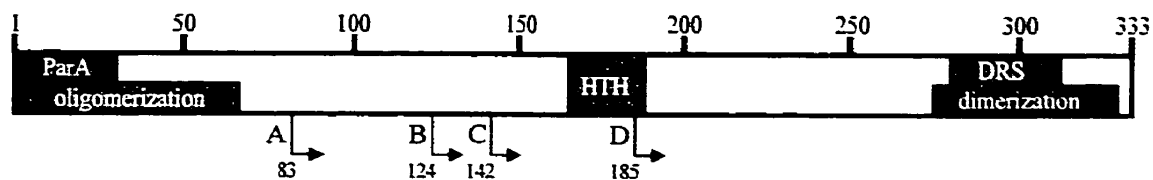
Disruption of the C-terminal dimerization domain destabilizes ParB's domain

structure. In this chapter I have treated several of the ParB fragments described in Chapter 4 with low levels of trypsin to determine the effect of the amino acid deletions on ParB's domain structure (Fig. 5-1B,C,D). All ParB fragments used here were His-tagged and were treated with a limiting amount of trypsin for a 24-hour time course. Samples were removed and proteolysis was stopped at the indicated times (Fig. 5-1). Initial tryptic fragments (especially of His-ParB) represent the clipping of the histidine tag from the N-terminus (Fig. 2-2). His-1-330 ParB produced a pattern of tryptic digestion similar to that of the full-length protein (Fig. 5-1), although each band had a slightly faster mobility than those generated by His-ParB, presumably as a result of the missing C-terminal residues. Therefore, removing the last three residues of ParB does not disrupt the overall folding of the protein. These data also support my previous suggestion that the extreme C-terminus of ParB is included in these proteolytic fragments (Chapter 2, (Surtees and Funnell, 1999). Treatment of His-1-317 ParB with trypsin gave a pattern that was very similar to His-1-293 ParB and His-1-312 ParB when treated with trypsin (Chapter 2, Figs. 2-4 and 5-1; Surtees and Funnell, 1999). These ParB fragments were relatively unstable in the presence of protease and produced a different pattern of proteolytic fragments when compared with His-ParB. In full-length ParB, the C-terminal half of the protein is very stably folded, presumably around the C-terminal dimerization domain. C-terminal deletions that disrupt C-terminal dimerization (e.g. His-1-317 ParB, His-1-312 ParB, His-1-293 ParB) likely destabilize the C-terminal core of ParB, leading to decreased stability in the presence of protease.

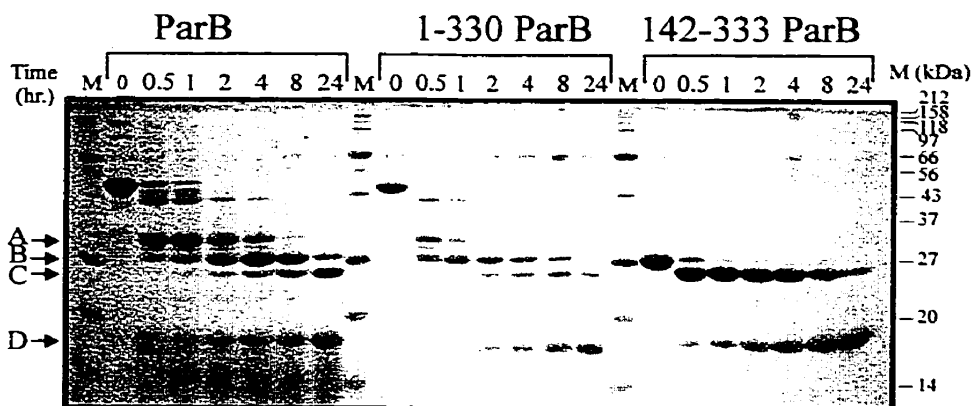
His-1-325 ParB produced a tryptic pattern that was intermediate between that of His-ParB (and His-1-330 ParB) and that of His-1-317 ParB (Fig. 5-1). Fragments that likely

Figure 5-1. Tryptic digestion of His-ParB and ParB fragments. Each protein was treated with trypsin at a 1000:1 (w/w) ratio of protein:protease at 20°C for the indicated times. Digestion at each time point was stopped with 1% (v/v) acetic acid. The resulting proteolytic fragments were separated by electrophoresis in SDS-15% polyacrylamide gels and visualized by Coomassie blue. **A.** Schematic of the structural and functional domains of ParB. The arrows (A-D) indicate the N-termini of the four major tryptic fragments identified in Chapter 2 and (Surtees and Funnell, 1999). **B.** Tryptic digestion of His-ParB, His-1-330 ParB and His-142-333 ParB. **C.** Tryptic digestion of his-ParB, His-1-325 ParB and His-1-317 ParB. Arrows (a) and (b) (red) indicate tryptic fragments of His-1-325 ParB that are similar to those produced by His-1-317 ParB. **D.** Tryptic digestion of His-ParB, His- Δ 143-185 ParB and His- Δ 166-184 ParB. Arrows 1 and 2 (red) indicate stable fragments generated by tryptic digestion of His- Δ 143-185 ParB and His- Δ 166-184 ParB that were subsequently sequenced (see Table 5-1). M, size markers.

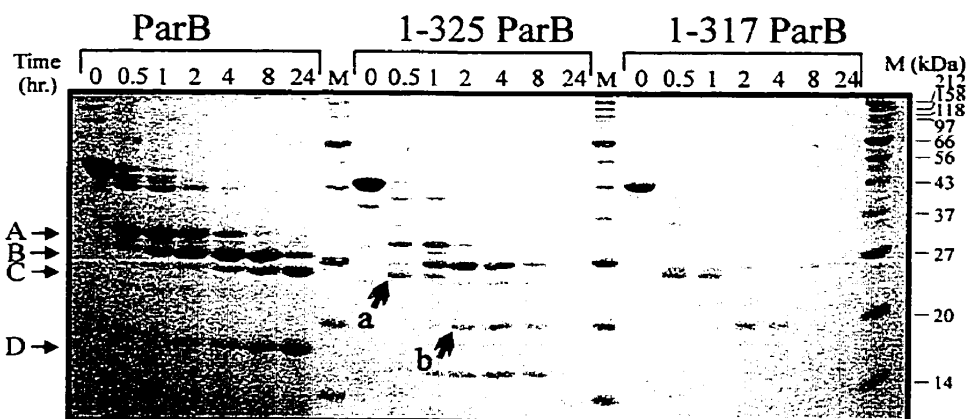
A



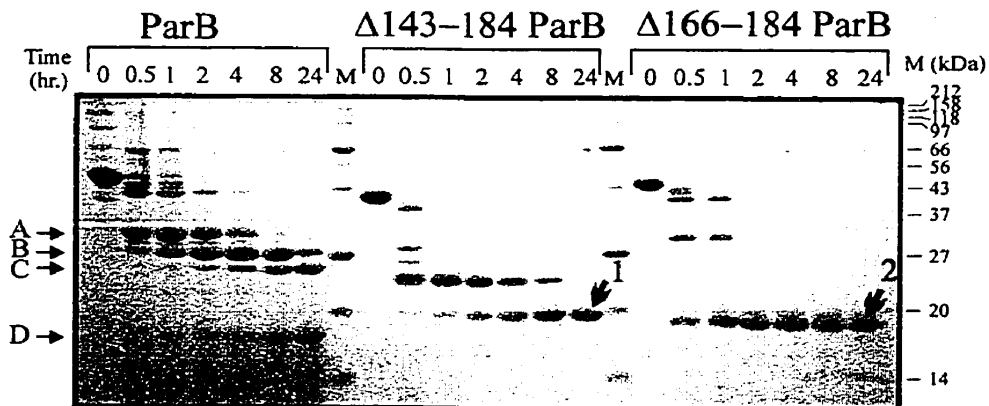
B



C



D



correspond to Bands A to D (with the last 8 residues missing) were produced. These fragments persisted for most of the time course, although they were less stable than those produced by His-ParB and His-1-330 ParB. Fragments with mobilities similar to those produced by His-1-317 were also observed (e.g. bands a and b in Fig. 5-1C). This second set of fragments may be generated as a result of a somewhat destabilized C-terminus. This result suggests that although His-1-325 dimerizes, the C-terminal dimerization domain of this ParB fragment is less stably folded as a result of the missing residues. Therefore, while proteolysis continues to proceed from the N-terminus, in some cases the weakened dimerization interface allows access of trypsin to the C-terminus of His-1-325.

Limited proteolysis of His-1-330 ParB and His-1-325 ParB indicates that the overall domain structure of these ParB fragments is not significantly altered. This is consistent with their *in vitro* DNA binding activities, which are similar to those of His-ParB. Both fragments bound *parS* in an IHF-stimulated manner (Fig. 4-4) and protected the *parS* site from digestion by DNaseI (Fig. 4-6). That the C-terminus of His-1-325 ParB may be destabilized may explain its somewhat lower affinity for *parS* (e.g. Fig. 4-6). In contrast, the domain structure of His-1-317 ParB was altered and was less stable in the presence of trypsin. The susceptibility to protease correlates with this protein's inability to dimerize (Fig. 4-3). This in turn correlates with the specific, but IHF-independent *parS* binding activity of His-1-317 ParB (Chapter 4, Fig. 4-4).

The two proteins that lack the HTH, His- Δ 166-184 ParB and His- Δ 143-184 ParB, were also examined by proteolytic digestion (Fig. 5-1D). His- Δ 143-184 ParB is missing the entire region between tryptic cleavage sites C and D (Fig. 5-1A and Chapter 4). Following removal of the histidine tag, His- Δ 143-184 ParB generated a pattern of tryptic fragments that was similar to Bands A, B and C of His-ParB, given that 40 residues are missing from the centre of the protein.

The smallest of these bands was sent for N-terminal sequencing (see Table 5-1). The sequence confirmed that this ParB fragment starts at residue 142 and therefore corresponds to an internally deleted Band C. Because the region between residues 142 and 185 has been removed, this fragment essentially represents Band D as well. In contrast, tryptic digestion of His- Δ 166-184, missing only the putative HTH motif, generated only two major proteolytic fragments. The larger fragment had a mobility that may correspond to Band A (which starts at residue 83) missing 17 residues. The next major fragment was much smaller and migrated between Bands C and D (starting at residues 142 and 185, respectively). This fragment was also sequenced and starts at residue 161, resulting from tryptic cleavage on the C-terminal side of R160 (Table 5-1). Therefore the absence of only the putative helix-turn-helix motif alters the position of the cleavage site, although cleavage still occurs within the vicinity of the HTH. Therefore this region of the protein is accessible to the protease, as would be expected given its role in DNA binding. Further, removal of this exposed region does not prevent stable folding of the C-terminal half of ParB, since the smallest fragment persisted throughout a 24 hour time course. I showed in Chapter 4 that the C-terminal DRS in both proteins is still able to interact with the box B site (Fig. 4-7), indicating that these ParB fragments are partially functional.

His-142-333 ParB corresponds to a stable tryptic fragment (Chapter 2; Surtees and Funnell, 1999) and contains all the information required for DNA binding (Chapter 4). When this protein was treated with trypsin (Fig. 5-1A), the tag was removed and the resulting fragment was relatively stable. At later time points, a band that migrated with 185-333 ParB (Band D) was produced. No additional fragments were generated. Therefore, although His-142-333 ParB is missing a substantial portion of the N-terminus of ParB, the remaining protein folds like the C-

TABLE 5-1. N-terminal sequences of proteolytic fragments generated by trypsin

<u>Band^a</u>	<u>N-terminal sequence^b</u>	<u>Starts at #</u>
1	Asp-Ser-Ser-Ala-Leu-Gln	142
2	Met-Lys-Asn-Asp-Gly-Ser	161

a. The bands refer to those indicated in Figure 5-1.

b. The sequences were determined by Edman degradation and the first 5 residues are shown.

terminal half of His-ParB. This native-like domain structure of His-142-333 ParB correlates with its native-like *in vitro parS* binding activity (Figs. 4-4 and 4-6).

DNA binding alters the conformation of His-ParB. I examined the tryptic fragments produced by His-ParB in the presence and absence of DNA (Fig. 5-2). His-ParB was mixed with a 270 base pair DNA fragment containing either *parS* or non-specific sequence at a 1:2 molar ratio of DNA to His-ParB dimer. The mixtures were then treated with trypsin in a 24 hour time course. In the presence of DNA, a substantial proportion of full-length His-ParB (minus the histidine tag) persisted throughout the 24 hours. Some fraction of ParB was cleaved by trypsin in the presence of DNA, producing a pattern of fragments very similar that observed in the absence of DNA. The amount of Band A, however, was reduced. These results suggest that the N-terminus of ParB became more stably folded and therefore less accessible to trypsin upon DNA binding. One additional fragment was also observed. The extra fragment had a slightly lower mobility than the fragment starting at residue 185 (Band D) and appeared at the later time points.

Tryptic digestions of His-ParB performed in the presence of specific (*parS*) and non-specific DNA fragments produced very similar results. In both cases the N-terminus of ParB was stabilized and a significant amount of undigested protein (minus the tag) remained at the end of the experiment. At these high protein ParB concentrations (~ 5 μ M), specific and non-specific DNA-binding by ParB are approximately equally favourable, particularly in the absence of IHF (Funnell, 1991). It did appear, however, that a larger proportion of intact protein persisted in the presence of *parS* than in the presence of non-specific DNA. The significance of this observation is not clear. One possibility is that ParB spends more time bound to the *parS* DNA than to the non-specific DNA and therefore the former affords more protection from the protease.

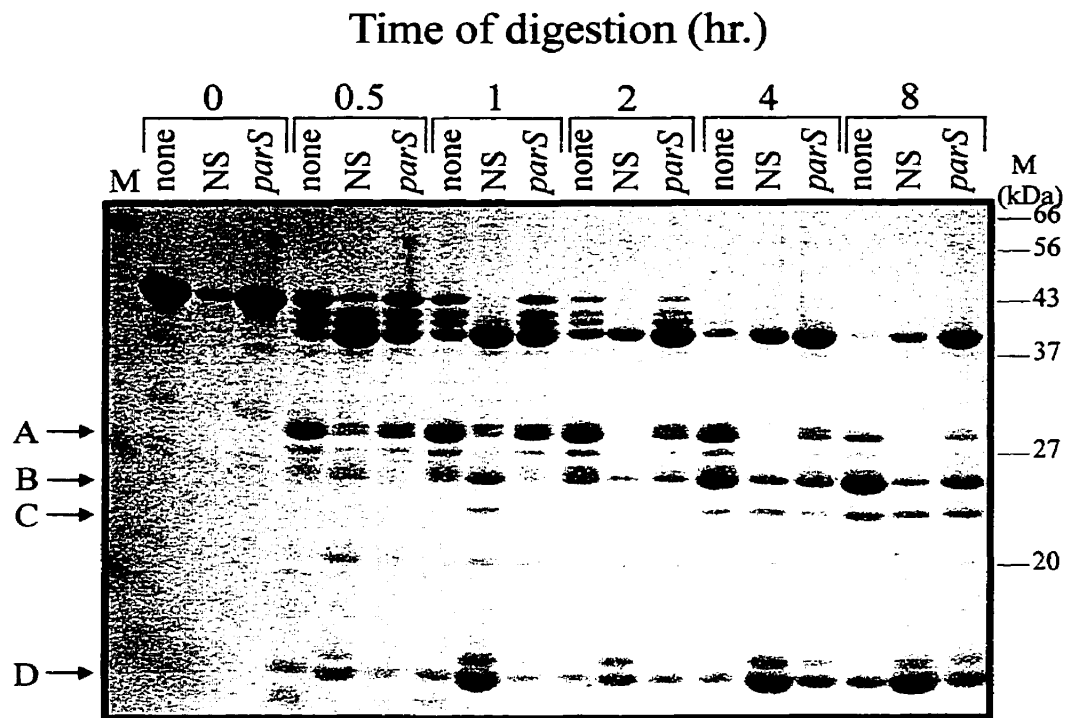


Figure 5-2. Tryptic digestion of His-ParB in the absence and presence of *parS* or non-specific DNA fragments. The DNA fragments were 270 bp in length. The DNA:protein dimer ratio was 1:2 in these reactions. For each time course, the protein-to-protease ratio was 1000:1 (w/w) and the digestions were performed at 20 C for the indicated times. The proteolytic products were separated by electrophoresis on a 15% SDS polyacrylamide gel. The arrows on the left indicate the stable proteolytic fragments of His-ParB (see Figure 5-1). M, size markers. NS, non-specific fragment.

I also performed these proteolysis experiments in the presence of IHF, both in the presence and absence of *parS* (Fig. 5-3). IHF binds its specific site in the centre of *parS* (Fig. 1-2) and brings the two sides of the site into close proximity. This increases ParB's affinity for *parS* (Funnell, 1991). In these experiments, ParB and IHF were present at approximately equimolar concentrations. I observed no differences in the proteolytic pattern of ParB in the presence of *parS* +/- IHF. The same proteolytic patterns were observed in the presence of non-specific DNA, although again somewhat less intact ParB appeared to remain in the presence of the non-specific DNA (data not shown). This result indicates that there are no ParB-IHF interactions that alter ParB's domain structure (as measured by sensitivity to proteolysis) in either the presence or absence of DNA.

The results indicate that ParB is altered upon DNA-binding. In particular, the N-terminus of ParB becomes significantly more resistant to proteolysis in the presence of DNA. It is possible that the presence of DNA blocks accessibility of the protease to this region of ParB. Remember, however, that the N-terminus of ParB is completely dispensable for ParB's specific DNA binding activity (Chapter 4). Therefore any direct contact between the N-terminus of ParB and the DNA would presumably be non-specific. Alternatively, the N-terminus of ParB may undergo a conformational change in the presence of DNA. One possibility is that DNA-binding promotes a ParB conformation that permits N-terminal oligomerization, as I suggested in Chapter 2 (Surtees and Funnell, 1999). The resulting N-terminal protein-protein interactions might then protect this region of the protein from proteolysis. These changes may, in turn, facilitate the ParA-ParB interactions that are required for plasmid partition (Bouet and Funnell, 1999; Erdmann *et al.*, 1999).

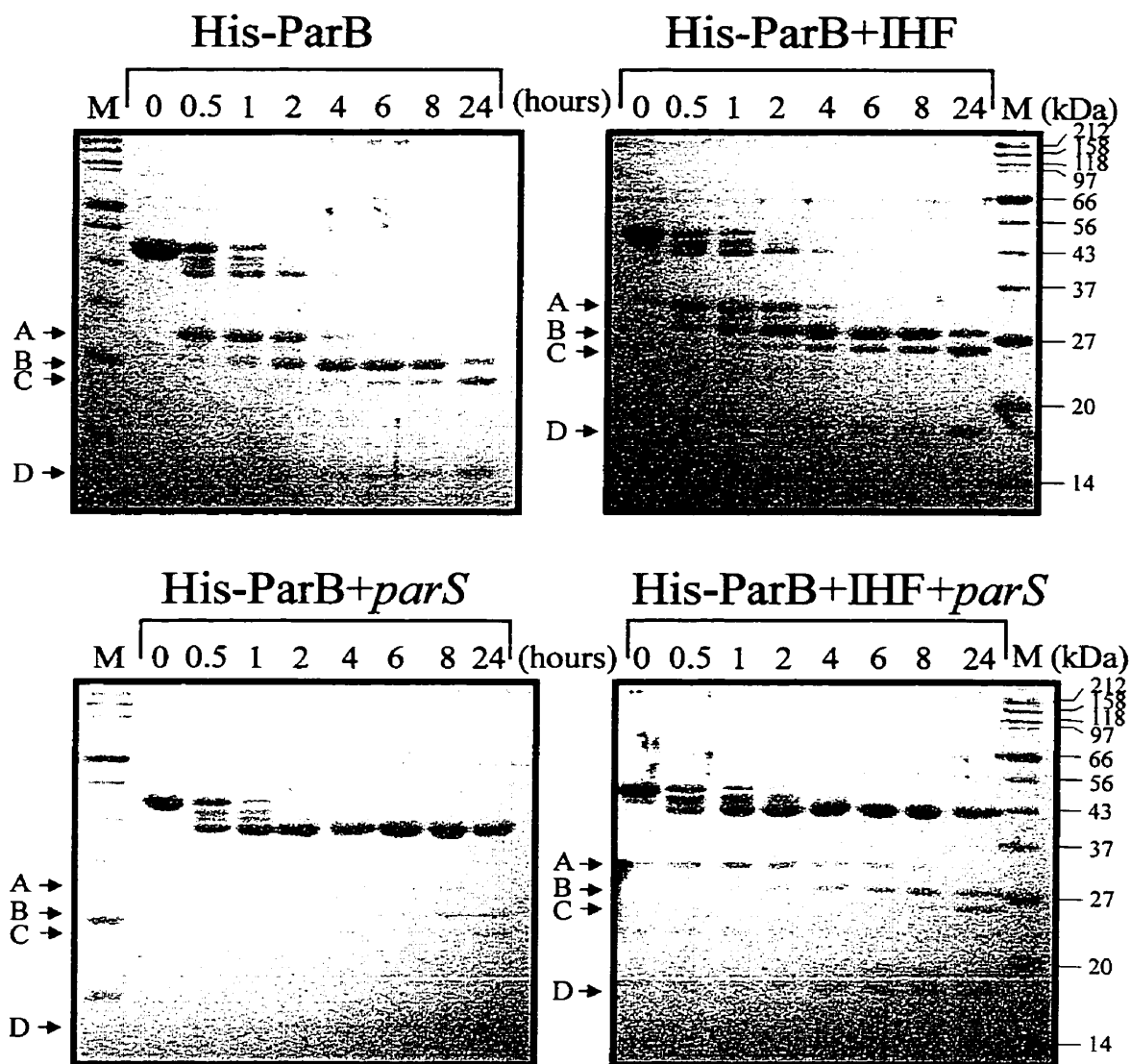


Figure 5-3. Comparison of tryptic digestions of His-ParB +/- *parS* in the presence and absence of IHF. In reactions containing IHF, ParB dimers and IHF heterodimers were present at equimolar concentrations. The ParB-to-*parS* fragment ratio was 2:1. Each time course was performed at 20 C and trypsin was present at a 1000:1 ration of protein:protease. The arrows indicate the tryptic fragments of His-ParB (see Figure 5-1). M, size markers.

Thesis Summary

In this thesis I have undertaken the molecular dissection of P1 ParB. I have used limited proteolytic digestion and deletion analyses to determine the structural and functional domains of ParB. In particular, I have identified two independent multimerization domains in ParB, one at the C-terminus and the other at the N-terminus (Chapter 2). My data indicate that the C-terminal half of ParB folds into a very stable domain around a dimerized core. The N-terminus of ParB does not appear to oligomerize, however, unless the protein has undergone some form of conformational change (Chapter 2), perhaps the one observed upon DNA binding (Chapter 5). Binding to *parS* might stimulate ParB dimer-dimer interactions to occur through the N-terminus. These interactions would stabilize additional ParB dimers that load onto the partition complex (Chapter 3) to form a large nucleoprotein structure (see Fig. 5-5). Since specific *parS* DNA is not required to induce the appropriate conformational change at the N-terminus of ParB (Chapter 5), ParB dimers could continue loading onto non-specific DNA, as is observed in gene silencing (Rodionov *et al.*, 1999).

N-terminal oligomerization of ParB upon DNA binding could also mediate plasmid pairing (Fig. 5-5). Partition models suggest that sister plasmids pair via their partition complexes and are then separated and positioned prior to cell division (section I-4). Pairing of R1 plasmids has been observed *in vitro* and was mediated by the ParR-*parC* partition complex of this plasmid (Jensen *et al.*, 1998). P1 pairing could similarly occur by N-terminal oligomerization of ParB dimers in separate partition complexes.

Dimerization is a fundamental characteristic of ParB and a single ParB dimer binds an IHF-*parS* complex to initiate formation of the partition complex (Chapter 3). The DNA binding data have particular implications regarding the architecture of the partition complex (Figs. 4-9

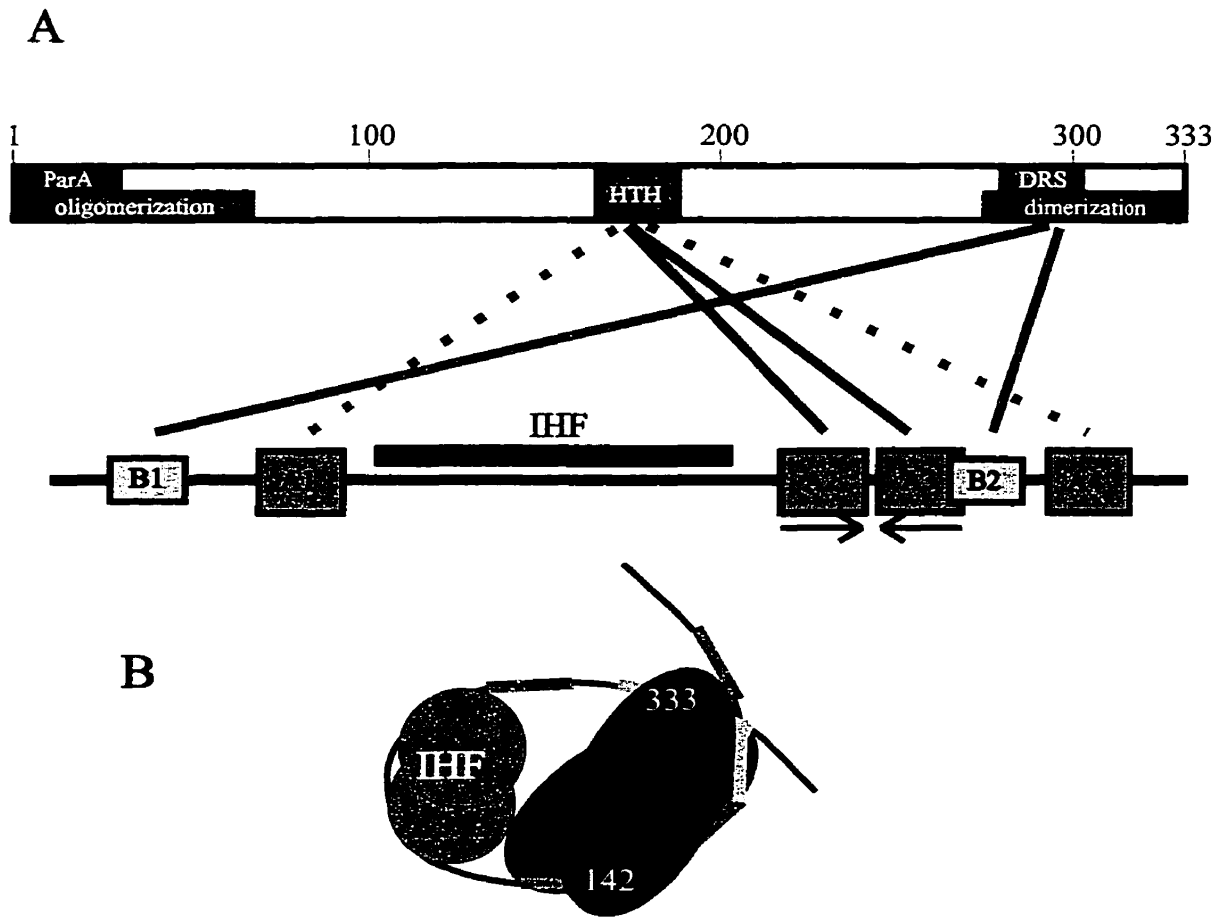


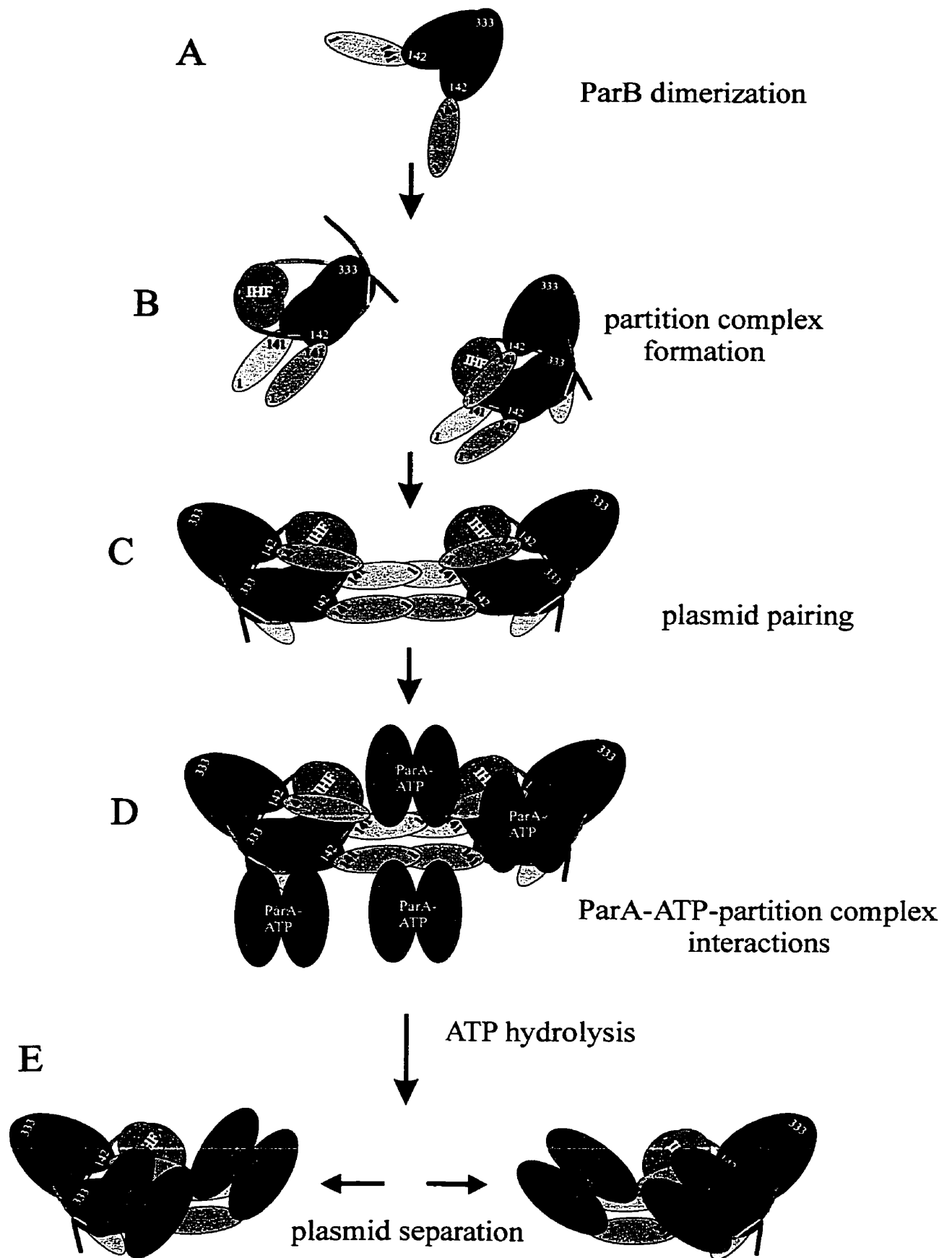
Figure 5-4. Model of ParB DNA binding. **A.** Schematic of the specific regions of ParB that interact with the box A and box B sequences within *parS*. The solid lines represent interactions that occur when a single dimer binds *parS* (Chapters 3 and 4) to form the minimal partition complex. The broken lines indicate interactions that occur when additional ParB dimers are loaded into the minimal partition complex. **B.** A drawing of how IHF and a ParB dimer interact with *parS*. The N-terminus has been left out because it is not required for specific interactions with the DNA (Chapter 4). The N-terminus would, however, be available to mediate additional protein-protein and/or protein-DNA interactions (see also Figure 5-5).

and 5-4). *In vitro* DNA binding assays performed with ParB fragments have shown that His-142-333 ParB contains all the dimerization and DNA-binding information required for wild-type binding of at least a dimer to *parS* (Chapter 4). Furthermore, the central putative helix-turn-helix motif is required to bind a box A inverted repeat (i.e. box A2-A3) on the right side of *parS*. The C-terminal DRS interacts with a box B sequence (Chapter 4) and the dimerized C-termini of a ParB dimer likely interact simultaneously with the two box B sites within *parS* (Fig. 5-4).

It has recently been shown that ParA interacts with ParB assembled in the partition complex (see section I-2.2) (Bouet and Funnell, 1999). The nature of this interaction is dependent on ParB concentration. At high ParB concentrations, ParA is recruited to the partition complex, whereas at low ParB concentrations, ParA interfered with ParB binding to *parS*. It is possible that ParA is recruited only to a partition complex that contains two or more ParB dimers (complex I+B2 or higher, Chapter 3) (Bouet *et al.*, 2000), perhaps explaining a requirement for high ParB concentrations *in vitro*, as well as in the bacterial cell. It is tempting to speculate that the destabilization of ParB binding to *parS* is a manifestation of ParA's role in separating paired plasmids (Fig. 5-5). As more ParA-ATP binds the partition complexes, the ParA:ParB ratio changes, perhaps providing a signal to initiate plasmid separation and/or positioning at the cell quarter positions. The process of separation presumably requires ATP hydrolysis, generating ParA-ADP dimers. This form of ParA has little or no affinity for ParB in the partition complex, at least *in vitro* (Bouet and Funnell, 1999), and so would likely dissociate from the partition complexes.

ParB also interacts with ParA in the absence of *parS* DNA (section I-2) (Davis *et al.*, 1992; Davey and Funnell, 1997). The region of ParB that interacts with ParA is at its extreme N-terminus (Chapter 2) (Radnedge *et al.*, 1998; Surtees and Funnell, 1999). It is possible that the

Figure 5-5. A model of P1 plasmid partition at the level of the partition complex. **A.** ParB exists as a dimer in solution (Funnell, 1991). Dimerization is mediated through the C-terminal domain (Chapter 2) (Surtees and Funnell, 1999). The N-termini are not able to self-associate in solution, either because they are occluded by the C-termini or because the conformation of ParB holds the N-termini away from each other (Chapter 2) (Surtees and Funnell, 1999). **B.** ParB binds *parS* in the presence of IHF. DNA binding alters the conformation of the N-termini of a dimer, allowing them to interact with each other and/or with the N-termini of other ParB dimers. **C.** N-terminal oligomerization may also mediate plasmid pairing. **D.** ParA-ATP interacts with ParB assembled in the partition complex. This interaction only occurs when large amounts of ParB have bound the partition complexes. **E.** As more ParA-ATP binds the partition complexes, the ParA:ParB ratio changes, ATP hydrolysis is stimulated and plasmid separation is initiated. ParA-ADP presumably dissociates from the separated and/or positioned partition complexes.



DNA-induced conformational change at the N-terminus of ParB (Fig. 5-2) modulates the ParA-ParB interaction to specify plasmid positioning.

Future Directions

Structural studies

It is intriguing that 142-333 ParB is sufficient for both IHF-stimulated *parS* binding (Fig. 4-4) and full protection of the minimal *parS* site from DNaseI (Fig. 4-6). The protein fragment is very stably folded and retains the domain structure of the C-terminus of the intact protein (Fig. 5-1). All of these characteristics indicate that 142-333 ParB is a good candidate for X-ray crystallography. It could be crystallized on its own or in the presence of a DNA site such as the minimal *parS* site, box A2-A3 and box B2 (Fig. 1-2). It may be possible to crystallize the entire partition complex, but formation of IHF-DNA co-crystals has proven to be complicated (Rice *et al.*, 1996).

An alternative way to visualize the intact partition complex (*i.e.* *parS*-ParB-IHF) is by atomic, or scanning force microscopy (SFM) (reviewed in (Bustamante and Rivette, 1996). SFM is high-resolution microscopy in which a sharply pointed sensor, or “tip”, scans the surface of a sample. Interactions with the sample cause deflections of the tip, and reveal the topography of the sample. The technique is ideal for large nucleoprotein complexes and has been used to characterize transcription complexes of *E. coli* RNA polymerase (Rees *et al.*, 1993), λ Cro dimers bound to operator regions (Erie *et al.*, 1994) and enhancer-bound NtrC (Wyman *et al.*, 1997).

ParA-ParB interactions

ParA and ParB interact at various stages of partition. ParB stimulates ParA's repressor and ATPase activities (Davis *et al.*, 1992) and ParA interacts with the partition complex in an

ATP-dependent manner (Bouet and Funnell, 1999). The extreme N-terminus of ParB is required for an interaction with ParA (Chapter 2; Radnedge *et al.*, 1996; Surtees and Funnell, 1999). Are other regions of ParB also required for this interaction? For example, does ParB have to be dimerized to interact with ParA? Does the C-terminus of ParB inhibit ParA-ParB interactions in the way that it inhibits ParB N-terminal oligomerization? I propose that ParA and ParB may have different requirements for their protein-protein interactions at *parOP* and at *parS*. The ParB fragments that I have constructed and characterized could be used to answer these questions.

First, an *in vivo* system to test ParA's repressor activity was established by Emma Fung. In this assay it would be possible to test the ability of different ParB fragments to act as a co-repressor of transcription. The effect of ParB fragments on ParA's *in vitro* ATPase activity could also be tested.

Second, it would be interesting to see if ParA is able to interact with ParB-*parS* complexes containing ParB fragments lacking the C-terminus, i.e. those that bind *parS* in an IHF-independent manner. If ParB has to be in a particular conformation on the DNA in order for ParA to bind, fragments such as His-1-317 ParB might not be able to support a ParA interaction, as determined by gel mobility shift assay. Alternatively, ParA may only require the N-terminus of ParB for an interaction. Certainly ParB need not be bound to DNA to stimulate ParA's ATPase activity, for example (Davis *et al.*, 1992) and therefore this ParA-ParB interaction does not necessarily require that the N-terminus of ParB be dimerized (see above). Therefore small N-terminal fragments that do not bind DNA might compete away the ParA-partition complex shift. If ParB N-terminal self-association inhibits ParA-ParB interactions by occluding the necessary region of ParB, then N-terminal fragments that do not dimerize (e.g. His-1-61 ParB)

might compete with intact ParB in the partition complex for ParA interactions, while N-terminal fragments capable of self-association (e.g. His-1-177 ParB) might not.

Immunofluorescence microscopy

Endogenous ParB has been visualized in fixed *E. coli* cells by immunofluorescence microscopy (Erdmann *et al.*, 1999). ParB was found to converge on *parS* which generated large, bright foci. Localization of the foci was dependent on ParA. Visualization of ParB fragments in this system could define the requirements for each step. For instance, 142-333 ParB is sufficient to form a minimal partition complex, but would it be able to recruit a sufficient number of additional dimers to form the large foci observed with the intact protein? If the N-terminus of ParB is required to mediate dimer-dimer interactions that support formation of the nucleoprotein complex, then 142-333 ParB would likely not be able to form large foci. Similarly, would ParB fragments lacking the C-terminal dimerization domain converge on *parS*? Presumably very high protein levels would be required for stable binding, given the low affinity of these ParB fragments for *parS* (Chapter 4). And if these fragments form complexes, would they be substrates for ParA localization? The protein retains the ParA interaction domain, but may not adopt a conformation that is recognized by ParA.

P1 partition complex formation is a crucial early step in partition. These unique nucleoprotein structures are thought to be involved in plasmid pairing (Austin and Abeles, 1983b; Austin and Nordstrom, 1990; Gerdes *et al.*, 2000) and are specifically localized during the cell cycle (Erdmann *et al.*, 1999). ParA interacts with ParB in the partition complex in an ATP-dependent manner (Bouet and Funnell, 1999) and this interaction is required for proper plasmid positioning. In this thesis I have examined the roles of ParB dimerization and ParB DNA binding activities in forming and maintaining the architecture of the P1 partition complex.

My model of this complex emphasizes the importance of both the central putative HTH domain and the dimerized DRS regions of ParB within the complex and allows for additional protein-protein interactions to occur through the N-terminus. Further details of the interactions required for the formation of the partition complex await structural analysis. In the meantime, we have a clearer picture of the partition complex and its potential role(s) in partition.

REFERENCES

- Abeles, A. L. (1986). P1 plasmid replication. Purification and DNA-binding activity of the replication protein RepA. *J. Biol. Chem.* *261*, 3548-3555.
- Abeles, A. L., Friedman, S. A., and Austin, S. J. (1985). Partition of unit-copy miniplasmids to daughter cells. III. The DNA sequence and functional organization of the P1 partition region. *J. Mol. Biol.* *185*, 261-272.
- Adams, D. E., Shekhtman, E. L., Zechiedrich, E. L., Schmid, M. B., and Cozzarelli, N. R. (1992). The role of topoisomerase IV in partitioning bacterial replicons and the structure of catenated intermediates in DNA replication. *Cell* *71*, 277-288.
- Aizenman, E., Engelberg-Kulka, H., and Glaser, G. (1996). An *Escherichia coli* chromosomal "addiction module" regulated by guanosine 3',5'-bispyrophosphate: a model for programmed bacterial cell death. *Proc. Natl. Acad. Sci. USA* *93*, 6059-6063.
- Austin, S., and Abeles, A. (1983a). Partition of unit-copy miniplasmids to daughter cells. I. P1 and F miniplasmids contain discrete, interchangeable sequences sufficient to promote equipartition. *J. Mol. Biol.* *169*, 353-372.
- Austin, S., and Abeles, A. (1983b). Partition of unit-copy miniplasmids to daughter cells. II. The partition region of miniplasmid P1 encodes an essential protein and a centromere-like site at which it acts. *J. Mol. Biol.* *169*, 373-387.
- Austin, S., and Nordstrom, K. (1990). Partition-mediated incompatibility of bacterial plasmids. *Cell* *60*, 351-354.
- Austin, S., Ziese, M., and Sternberg, N. (1981). A novel role for site-specific recombination in maintenance of bacterial replicons. *Cell* *25*, 729-736.
- Bahloul, A., Meury, J., Kern, R., Garwood, J., Guha, S., and Kohiyama, M. (1996). Coordination between membrane *oriC* sequestration factors and a chromosome partitioning protein, TolC (MukA). *Mol. Microbiol.* *22*, 275-282.
- Bernard, P., and Couturier, M. (1992). Cell killing by the F plasmid CcdB protein involves poisoning of DNA-topoisomerase II complexes. *J. Mol. Biol.* *226*, 735-745.
- Biek, D. P., and Shi, J. P. (1994). A single 43-bp *sopC* repeat of plasmid mini-F is sufficient to allow assembly of a functional nucleoprotein partition complex. *Proc. Natl. Acad. Sci. USA* *91*, 8027-8031.
- Biek, D. P., and Strings, J. (1995). Partition functions of mini-F affect plasmid DNA topology in *Escherichia coli*. *J. Mol. Biol.* *246*, 388-400.

- Blakely, G., Colloms, S., May, G., Burke, M., and Sherratt, D. (1991). *Escherichia coli* XerC recombinase is required for chromosomal segregation at cell division. *New Biol.* 3, 789-798.
- Blakely, G., May, G., McCulloch, R., Arciszewska, L. K., Burke, M., Lovett, S. T., and Sherratt, D. J. (1993). Two related recombinases are required for site-specific recombination at dif and cer in *E. coli* K12. *Cell* 75, 351-361.
- Bouet, J.-Y., and Funnell, B. E. (1999). P1 ParA interacts with the P1 partition complex at *parS* and an ATP-ADP switch controls ParA activities. *EMBO J.* 18, 1415-1424.
- Bouet, J.-Y., Surtees, J. A., and Funnell, B. E. (2000). Stoichiometry of P1 plasmid partition complexes. *J. Biol. Chem.* 275, 8213-8219.
- Bowie, J. U., and Sauer, R. T. (1989). Identification of C-terminal extensions that protect proteins from intracellular proteolysis. *J. Biol. Chem.* 264, 7596-7602.
- Boye, E., Stokke, T., Kleckner, N., and Skarstad, K. (1996). Coordinating DNA replication initiation with cell growth: differential roles for DnaA and SeqA proteins. *Proc. Natl. Acad. Sci. USA* 93, 12206-12211.
- Bradford, M. M. (1976). A rapid and sensitive method for the quantitation of microgram quantities of protein utilizing the principle of protein-dye binding. *Anal. Biochem.* 72, 248-254.
- Breuner, A., Jensen, R. B., M. Dam, S. P., and Gerdes, K. (1996). The centromere-like *parC* locus of plasmid R1. *Mol. Microbiol.* 20, 581-592.
- Britton, R. A., Lin, D. C.-H., and Grossman, A. D. (1998). Characterization of a prokaryotic SMC protein involved in chromosome partitioning. *Genes & Dev.* 12, 1254-1259.
- Bustamante, C., and Rivette, C. (1996). Visualizing protein-nucleic acid interactions on a large scale with the scanning force microscope. *Annu. Rev. Biophys. Biomol. Struct.* 25, 395-429.
- Cervin, M. A., Spiegelman, G. B., Raether, B., Ohlsen, K., Perego, M., and Hoch, J. A. (1998). A negative regulator linking chromosome segregation to developmental transcription in *Bacillus subtilis*. *Mol. Microbiol.* 29, 85-95.
- Chattoraj, D. K., Mason, R. J., and Wickner, S. H. (1988). Mini-P1 plasmid replication: the autoregulation-sequestration paradox. *Cell* 52, 551-557.
- Chattoraj, D. K., Snyder, K. M., and Abeles, A. L. (1985). P1 plasmid replication: multiple functions of RepA protein at the origin. *Proc. Natl. Acad. Sci. USA* 82, 2588-2592.
- Chen, J., and Matthews, K. S. (1994a). Subunit dissociation affects DNA binding in a dimeric Lac repressor produced by C-terminal deletion. *Biochem.* 33, 8728-8735.

- Chen, J., Suredran, R., Lee, J. C., and Matthews, K. S. (1994b). Construction of a dimeric repressor: Dissection of subunit interfaces in Lac repressor. *Biochem.* *33*, 1234-1241.
- Clerget, M. (1991). Site-specific recombination promoted by a short DNA segment of plasmid R1 and by a homologous segment in the terminus region of the *Escherichia coli* chromosome. *New Biol.* *3*, 780-788.
- Cole, S. T. (1998). Comparative mycobacterial genomics. *Curr. Opin. Microbiol.* *1*, 567-571.
- Colloms, S. D., Bath, J., and Sherratt, D. J. (1997). Topological selectivity in Xer site-specific recombination. *Cell* *88*, 855-864.
- Colloms, S. D., McCulloch, R., Grant, K., and Neilson, L. (1996). Xer-mediated site-specific recombination *in vitro*. *EMBO J.* *15*, 1172-1181.
- Colloms, S. D., Sykora, P., Szatmari, G., and Sherratt, D. J. (1990). Recombination at ColE1 *cer* requires the *Escherichia coli xerC* gene product, a member of the lambda integrase family of site-specific recombinases. *J. Bacteriol.* *172*, 6973-6980.
- Copeland, J. W., Nasaidka, A., Dietrich, B. H., and Krause, H. M. (1996). Patterning of the *Drosophila* embryo by a homeodomain-deleted Ftz polypeptide. *Nature* *379*, 162-165.
- Creasy, C. L., Ambrose, D. M., and Chernoff, J. (1996). The Ste20-like protein kinase, Mst1, dimerizes and contains an inhibitory domain. *J. Biol. Chem.* *271*, 21049-21053.
- Dam, M., and Gerdes, K. (1994). Partitioning of R1: Ten direct repeats flanking the promoter constitute a centromere-like partition site *parC*, that expresses incompatibility. *J. Mol. Biol.* *236*, 1289-1298.
- Davey, M. J., and Funnell, B. E. (1994). The P1 plasmid partition protein ParA. A role for ATP in site-specific DNA binding. *J. Biol. Chem.* *269*, 29908-29913.
- Davey, M. J., and Funnell, B. E. (1997). Modulation of the P1 plasmid partition protein ParA by ATP, ADP and P1 ParB. *J. Biol. Chem.* *272*, 15286-15292.
- Davis, M. A., and Austin, S. J. (1988). Recognition of the P1 plasmid centromere analog involves binding of the ParB protein and is modified by a specific host factor. *EMBO J.* *7*, 1881-1888.
- Davis, M. A., Martin, K. A., and Austin, S. J. (1990). Specificity switching of the P1 plasmid centromere-like site. *EMBO J.* *9*, 991-998.
- Davis, M. A., Martin, K. A., and Austin, S. J. (1992). Biochemical activities of the ParA partition protein of the P1 plasmid. *Mol. Microbiol.* *6*, 1141-1147.

- Davis, M. A., Radnedge, L., Martin, K. A., Hayes, F., Youngren, B., and Austin, S. J. (1996). The P1 ParA protein and its ATPase activity play a direct role in the segregation of plasmid copies to daughter cells. *Mol. Microbiol.* *21*, 1029-1036.
- Demczuk, S., Harbers, M., and Vennstrom, B. (1993). Identification and analysis of all components of a gel retardation assay by combination with immunoblotting. *Proc. Natl. Acad. Sci. USA* *90*, 2574-2578.
- Derbyshire, V., Kowalski, J. C., Dansereau, J. T., Hauer, C. R., and Belfort, M. (1997). Two-domain structure of the *td* intron-encoded endonuclease I-*TevI* correlates with the two-domain configuration of the homing site. *J.Mol.Biol.* *265*, 494-506.
- Dodd, I. B., and Egan, J. B. (1990). Improved detection of helix-turn-helix DNA-binding motifs in protein sequences. *Nucl. Acids Res.* *18*, 5019-5026.
- Donachie, W. D., and Begg, K. J. (1989). Cell length, nucleoid separation, and cell division of rod-shaped and spherical cells of *Escherichia coli*. *J. Bacteriol.* *171*, 4633-4639.
- Durfee, T., Becherer, K., Chen, P.-L., Yeh, S.-H., Yang, Y., Kilburn, A. E., Lee, W.-H., and Elledge, S. J. (1993). The retinoblastoma protein associates with the protein phosphatase type 1 catalytic subunit. *Genes & Dev.* *7*, 555-569.
- Erdmann, N. (1998). Identification of high-copy-number inhibitors of P1 plasmid stability. In *Molecular and Medical Genetics* (Toronto: University of Toronto), pp. 80.
- Erdmann, N., Petroff, T., and Funnell, B. E. (1999). Intracellular localization of P1 ParB protein depends on ParA and *parS*. *Proc. Natl. Acad. Sci. USA* *96*, 14905-14910.
- Erie, D. A., Yang, G., Schultz, H. C., and Bustamante, C. (1994). DNA bending by Cro protein in specific and nonspecific complexes: implications for protein site recognition and site specificity. *Science* *266*, 1562-1566.
- Ezaki, B., Ogura, T., Niki, H., and Hiraga, S. (1991). Partitioning of a mini-F plasmid into anucleate cells of the *mukB* null mutant. *J. Bacteriol.* *173*, 6643-6646.
- Fiedler, U., and Weiss, V. (1995). A common switch in activation of the response regulators NtrC and PhoB: phosphorylation induces dimerization of the receiver modules. *EMBO J.* *14*, 3696-3705.
- Fields, S., and Song, O.-k. (1989). A novel genetic system to detect protein-protein interactions. *Nature* *340*, 245-246.
- Fields, S., and Sternglanz, R. (1994). The two-hybrid system: An assay for protein-protein interactions. *Trends Genet.* *10*, 286-292.

- Fraser, C. M., Casjens, S., Huang, W. M., Hutton, G. G., Clayton, R., and al, e. (1997). Genomic sequence of a Lyme disease spirochaete, *Borrelia burgdorferi*. *Nature* 390, 580-586.
- Friedman, D. I. (1988). Integration host factor: A protein for all reasons. *Cell* 55, 545-554.
- Friedman, S. A., and Austin, S. J. (1988). The P1 plasmid-partition system synthesizes two essential proteins from an autoregulated operon. *Plasmid* 19, 103-112.
- Fung, E. (2000). Dissecting the roles of ParA ATP binding and hydrolysis in P1 plasmid partition. In *Molecular and Medical Genetics* (Toronto: University of Toronto), pp. 113.
- Funnell, B. E. (1988a). Mini-P1 plasmid partitioning: excess ParB protein destabilizes plasmids containing the centromere *parS*. *J. Bacteriol.* 170, 954-958.
- Funnell, B. E. (1988b). Participation of *Escherichia coli* integration host factor in the P1 plasmid partition system. *Proc. Natl. Acad. Sci. USA* 85, 6657-6661.
- Funnell, B. E. (1991). The P1 partition complex at *parS*: the influence of *Escherichia coli* integration host factor and of substrate topology. *J. Biol. Chem.* 266, 14328-14337.
- Funnell, B. E., and Gagnier, L. (1993). The P1 plasmid partition complex at *parS*: II. Analysis of ParB protein binding activity and specificity. *J. Biol. Chem.* 268, 3616-3624.
- Funnell, B. E., and Gagnier, L. (1994). P1 plasmid partition: Binding of P1 ParB protein and *Escherichia coli* integration host factor to altered *parS* sites. *Biochimie* 76, 924-932.
- Funnell, B. E., and Gagnier, L. (1995). Partition of P1 plasmids in *Escherichia coli mukB* chromosomal partition mutants. *J. Bacteriol.* 177, 2381-2386.
- Gal-Mor, O., Borovok, I., Av-Gay, Y., Cohen, G., and Aharonowitz, Y. (1998). Gene organization in the *trxA/B-oriC* region of the *Streptomyces coelicolor* chromosome and comparison with other eubacteria. *Gene* 217, 83-90.
- Gazit, E., and Sauer, R. T. (1999). The Doc toxin and Phd antidote proteins of the bacteriophage P1 plasmid addiction system form a heterotrimeric complex. *Journal of Biological Chemistry* 274, 16813-16818.
- Gerdes, K., Moller-Jensen, J., and Jensen, R. B. (2000). Plasmid and chromosome partitioning: surprises from phylogeny. *Mol. Microbiol.* 37, 455-466.
- Gerdes, K., Poulsen, L. K., Thisted, T., Nielsen, A. K., Martinussen, J., and Andreasen, P. H. (1990). The *hok* killer gene family in gram-negative bacteria. *New Biol.* 2, 946-956.
- Gerdes, K., Rasmussen, P. B., and Molin, S. (1986). Unique type of plasmid maintenance function: postsegregational killing of plasmid-free cells. *Proc. Natl. Acad. Sci. USA* 83, 3116-3120.

- Gietz, D., Jean, A. S., Woods, R. A., and Schiestl, R. H. (1992). Improved method for high efficiency transformation of intact yeast cells. *Nucl. Acids Res.* *20*, 1425.
- Glaser, P., Sharpe, M. E., Raether, B., Perego, M., Ohlsen, K., and Errington, J. (1997). Dynamic, mitotic-like behavior of a bacterial protein required for accurate chromosome partitioning. *Genes & Dev.* *11*, 1160-1168.
- Gordon, G. S., Sitnikov, D., Webb, C. D., Teleman, A., Straight, A., Losick, R., Murray, A. W., and Wright, A. (1997). Chromosome and low copy plasmid segregation in E-coli: Visual evidence for distinct mechanisms. *Cell* *90*, 1113-1121.
- Graumann, P. L., Losick, R., and Strunnikov, A. V. (1998). Subcellular localization of *Bacillus subtilis* SMC, a protein involved in chromosome condensation and segregation. *J. Bacteriol.* *180*, 5749-5755.
- Guacci, V., Koshland, D., and Strunnikov, A. (1997). A direct link between sister chromatid cohesion and chromosome condensation revealed through the analysis of *MCD1* in *S. cerevisiae*. *Cell* *91*, 47-57.
- Hanai, R., Liu, R. P., Benedetti, P., Caron, P. R., Lynch, A. S., and Wang, J. C. (1996). Molecular dissection of a protein SopB essential for *Escherichia coli* F plasmid partition. *J. Biol. Chem.* *271*, 17469-17475.
- Harrington, E. W., and Trun, N. J. (1997). Unfolding of the bacterial nucleoid both *in vivo* and *in vitro* as a result of exposure to camphor. *J. Bacteriol.* *179*, 2435-2439.
- Hayakawa, Y., Murotsu, T., and Matsubara, K. (1985). Mini-F protein that binds to a unique region for partition of plasmid DNA. *J. Bacteriol.* *163*, 349-354.
- Hayes, F., and Austin, S. (1994). Topological scanning of the P1 plasmid partition site. *J. Mol. Biol.* *243*, 190-198.
- Hayes, F., and Austin, S. J. (1993). Specificity determinants of the P1 and P7 plasmid centromere analogs. *Proc. Natl. Acad. Sci. USA* *90*, 9228-9232.
- Hayes, F., Davis, M. A., and Austin, S. J. (1993). Fine-structure analysis of the P7 plasmid partition site. *J. Bacteriol.* *175*, 3443-3451.
- Hayes, F., Radnedge, L., Davis, M. A., and Austin, S. J. (1994). The homologous operons for P1 and P7 plasmid partition are autoregulated from dissimilar operator sites. *Mol. Microbiol.* *11*, 249-260.
- Hiraga, S., Ichinose, C., Niki, H., and Yamazoe, M. (1998). Cell cycle-dependent duplication and bidirectional migration of SeqA-associated DNA-protein complexes in *E. coli*. *Mol. Cell* *1*, 381-387.

- Hiraga, S., Jaffe, A., Ogura, T., Mori, H., and Takahashi, H. (1986). F plasmid *ccd* mechanism in *Escherichia coli*. *J. Bacteriol.* *166*, 100-104.
- Hiraga, S., Niki, H., Ogura, T., Ichinose, C., Mori, H., Ezaki, B., and Jaffe, A. (1989). Chromosome partitioning in *Escherichia coli*: novel mutants producing anucleate cells. *J. Bacteriol.* *171*, 1496-1505.
- Hiraga, S., Ogura, T., Niki, H., Ichinose, C., and Mori, H. (1990). Positioning of replicated chromosomes in *Escherichia coli*. *J. Bacteriol.* *172*, 31-39.
- Hirano, M., and Hirano, T. (1998). ATP-dependent aggregation of single-stranded DNA by a bacterial SMC homodimer. *EMBO J.* *17*, 7139-7148.
- Hirano, M., Mori, H., Onogi, T., Yamazoe, M., Niki, H., Ogura, T., and Hiraga, S. (1998). Autoregulation of the partition genes of the mini-F plasmid and the intracellular localization of their products in *Escherichia coli*. *Mol. Gen. Genet.* *257*, 392-403.
- Hirano, T., Kobayashi, R., and Hirano, M. (1997). Condensins, chromosome condensation protein complexes containing XCAP-C, XCAP-E and a *Xenopus* homolog of the *Drosophila* Barren protein. *Cell* *89*, 511-521.
- Holmes, V. F., and Cozzarelli, N. R. (2000). Closing the ring: Links between SMC proteins and chromosome partitioning, condensation, and supercoiling. *Proc. Natl. Acad. Sci. USA* *97*, 1322-1324.
- Hu, K. H., Lin, E., Dean, K., Gingras, M., DeGraff, W., and Trun, N. J. (1996). Overproduction of three genes leads to camphor resistance and chromosome condensation in *Escherichia coli*. *Genetics* *143*, 1521-1532.
- Hu, P., Elliott, J., McCready, P., Skowronski, E., Games, J., Kobayashi, A., Brubaker, R. R., and Garcia, E. (1998). Structural organization of the virulence-associated plasmids of *Yersinia pestis*. *J. Bacteriol.* *180*, 5192-5202.
- Huang, H., Cao, C., and Lutkenhaus, J. (1996). Interaction between FtsZ and inhibitors of cell division. *J. Bacteriol.* *178*, 5080-5085.
- Ireton, K., Gunther, N. W., and Grossman, A. D. (1994). *spoOJ* is required for normal chromosome segregation as well as the initiation of sporulation in *Bacillus subtilis*. *J. Bacteriol.* *176*, 5320-5329.
- Jensen, R. B., Dam, M., and Gerdes, K. (1994). Partitioning of plasmid R1: The *parA* operon is autoregulated by ParR and its transcription is highly stimulated by a downstream activating element. *J. Mol. Biol.* *136*, 1299-1309.

- Jensen, R. B., and Gerdes, K. (1997). Partitioning of plasmid R1. The ParM protein exhibits ATPase activity and interacts with the centromere-like ParR-*parC* complex. *J. Mol. Biol.* *269*, 505-513.
- Jensen, R. B., and Gerdes, K. (1999). Mechanism of DNA segregation in prokaryotes: ParM partitioning protein of plasmid R1 co-localizes with its replicon during the cell cycle. *EMBO J.* *18*, 4076-4084.
- Jensen, R. B., Lurz, R., and Gerdes, K. (1998). Mechanism of DNA segregation in prokaryotes: Replicon pairing by *parC* of plasmid R1. *Proc. Natl. Acad. Sci. USA* *95*, 8550-8555.
- Jensen, R. B., and Shapiro, L. (1999). The *Caulobacter crescentus smc* gene is required for cell cycle progression and chromosome segregation. *Proc. Natl. Acad. Sci. USA* *96*, 10661-10666.
- Jessberger, R., Riwar, B., Baechtold, H., and Akhmedov, A. T. (1996). SMC proteins constitute two subunits of the mammalian recombination complex RC-1. *EMBO J.* *15*, 4061-4068.
- Kato, J., Nishimura, Y., Imamura, R., Niki, H., Hiraga, S., and Suzuki, H. (1990). New topoisomerase essential for chromosome segregation in *E. coli*. *Cell* *63*, 393-404.
- Kiesau, P., Eikmanns, U., Gutowski-Eckel, Z., Weber, S., Hammelmann, M., and Entian, K.-D. (1997). Evidence for a multimeric subtilin synthase complex. *J. Bacteriol.* *179*, 1475-1481.
- Kim, H.-J., Calcutt, M. J., Schmidt, F. J., and Chater, K. F. (2000). Partitioning of the linear chromosome during sporulation of *Streptomyces coelicolor* A3(2) involves an *oriC*-linked *parAB* locus. *J. Bacteriol.* *182*, 1313-1320.
- Kim, S. K., and Wang, J. C. (1998). Localization of F plasmid SopB protein to positions near the poles of *Escherichia coli* cells. *Proc. Natl. Acad. Sci. USA* *95*, 1523-1527.
- Kim, S.-K., and Shim, J. (1999). Interactions between F plasmid partition proteins SopA and SopB. *Biochem. Biophys. Res. Comm.* *263*, 113-117.
- Kim, S.-K., and Wang, J. C. (1999). Gene silencing via protein-mediated subcellular localization of DNA. *Proc. Natl. Acad. Sci. USA* *96*, 8557-8561.
- Kimura, K., and Hirano, T. (1997). ATP-dependent positive supercoiling of DNA by 13S Condensin: A biochemical implication for chromosome condensation. *Cell* *90*, 625-634.
- Kishore, G. M., and Shah, D. M. (1988). Amino acid biosynthesis inhibitors as herbicides. *Annu. Rev. Biochem.* *57*, 627-663.
- Konigsberg, W. H. (1995). Limited proteolysis of DNA polymerases as probe of functional domains. *Methods Enzymol.* *262*, 331-346.

- Koshland, D., and Strunnikov, A. (1996). Mitotic chromosome condensation. *Annu. Rev. Cell and Dev. Biol.* 12, 305-333.
- Kuempel, P. L., Henson, J. M., Dircks, L., Tecklenburg, M., and Lim, D. (1991). *dif*, a *recA*-independent recombination site in the terminus of the chromosome of *Escherichia coli*. *New Biol.* 3, 799-811.
- Kunkel, T. A., Bebenek, K., and McClary, J. (1991). Efficient site-directed mutagenesis using uracil-containing DNA. *Methods Enzymol.* 204, 125-139.
- Lehnherr, H., Maguin, E., Jafri, S., and Yarmolinsky, M. B. (1993). Plasmid addiction genes of bacteriophage-P1: *doc*, which causes cell death on curing of prophage, and *phd*, which prevents host death when prophage is retained. *J. Mol. Biol.* 233, 414-428.
- Lehnherr, H., and Yarmolinsky, M. B. (1995). Addiction protein Phd of plasmid prophage P1 is a substrate of the ClpXP serine protease of *Escherichia coli*. *Proc. Natl. Acad. Sci. USA* 92, 3274-3277.
- Lemon, K. P., and Grossman, A. D. (1998). Localization of bacterial DNA polymerase: evidence for a factory model of replication. *Science* 282, 1516-1519.
- Lewis, P. J., and Errington, J. (1997). Direct evidence for active segregation of *oriC* regions of the *Bacillus subtilis* chromosome and co-localization with the Spo0J partitioning protein. *Mol. Microbiol.* 25, 945-954.
- Lieb, J. D., Albrecht, M. P., Chuang, P. T., and Meyer, B. J. (1998). MIX-1: an essential component of the *C. elegans* mitotic machinery executes X chromosome dosage compensation. *Cell* 92, 265-277.
- Lin, D. C.-H., and Grossman, A. D. (1998). Identification and characterization of a bacterial chromosome partitioning site. *Cell* 92, 675-685.
- Lin, D. C.-H., Levin, P. A., and Grossman, A. D. (1997). Bipolar localization of a chromosome partition protein in *Bacillus subtilis*. *Proc. Natl. Acad. Sci. USA* 94, 4721-4726.
- Lobocka, M., and Yarmolinsky, M. (1996). P1 plasmid partition: A mutational analysis of ParB. *J. Mol. Biol.* 259, 366-382.
- Lockhart, A., and Kendrick-Jones, J. (1998). Interaction of the N-terminal domain of MukB with the bacterial tubulin homologue FtsZ. *FEBS Lett.* 430, 278-282.
- Lu, M., Campbell, J. L., Boye, E., and Kleckner, N. (1994). SeqA: a negative modulator of replication initiation in *E. coli*. *Cell* 77, 413-426.
- Ludtke, D. N., Eichorn, B. G., and Austin, S. J. (1989). Plasmid-partition functions of the P7 prophage. *J. Mol. Biol.* 209, 393-406.

- Luttinger, A. L., Springer, A. L., and Schmid, M. B. (1991). A cluster of genes that affects nucleoid segregation in *Salmonella typhimurium*. *New Biol.* 3, 687-697.
- Lynch, A. S., and Wang, J. C. (1994). Use of an inducible site-specific recombinase to probe the structure of protein-DNA complexes involved in F plasmids in *Escherichia coli*. *J. Mol. Biol.* 236, 679-684.
- Lynch, A. S., and Wang, J. C. (1995). SopB protein-mediated silencing of genes linked to the *sopC* locus of *Escherichia coli* F plasmid. *Proc. Natl. Acad. Sci. USA* 92, 1896-1900.
- Maki, S., Takiguchi, S., Miki, T., and Horiuchi, T. (1992). Modulation of DNA supercoiling activity of *Escherichia coli* DNA gyrase by F plasmid proteins. *J. Biol. Chem.* 267, 12244-12251.
- Marston, A. L., and Errington, J. (1999). Dynamic movement of the ParA-like Soj protein of *B. subtilis* and its dual role in nucleoid organization and developmental regulation. *Mol. Cell* 4, 673-682.
- Martin, K. A., Davis, M. A., and Austin, S. (1991). Fine-structure analysis of the P1 plasmid partition site. *J. Bacteriol.* 173, 3630-3634.
- Martin, K. A., Friedman, S. A., and Austin, S. J. (1987). Partition site of the P1 plasmid. *Proc. Natl. Acad. Sci. USA* 84, 8544-8547.
- Masuda, Y., Miyakawa, K., Nishimura, Y., and Ohtsubo, E. (1993). *chpA* and *chpB*, *Escherichia coli* chromosomal homologs of the *pem* locus responsible for stable maintenance of plasmid R100. *J. Bacteriol.* 175, 6850-6856.
- Melby, T. E., Ciampaglio, C. N., Briscoe, G., and Erickson, H. P. (1998). The symmetrical structure of Structural Maintenance of Chromosomes (SMC) and MukB proteins: Long, antiparallel coiled coils, folded at a flexible hinge. *J. Cell Biol.* 142, 1595-1604.
- Metzger, S., Dror, I. B., Aizenman, E., Schreiber, G., Toone, M., Friesen, J. D., Cashel, M., and Glaser, G. (1988). The nucleotide sequence and characterization of the *relA* gene of *Escherichia coli*. *J. Biol. Chem.* 263, 15699-15704.
- Michaelis, C., Ciosk, R., and Nasmyth, K. (1997). Cohesins: Chromosomal proteins that prevent premature separation of sister chromatids. *Cell* 91, 35-45.
- Mohl, D. A., and Gober, J. W. (1997). Cell cycle-dependent polar localization of chromosome partitioning proteins in *Caulobacter crescentus*. *Cell* 88, 675-684.
- Mori, H., Kondo, A., Ohshima, A., Ogura, T., and Hiraga, S. (1986). Structure and function of the F plasmid genes essential for partitioning. *J. Mol. Biol.* 192, 1-15.

- Mori, H., Mori, Y., Ichinose, C., Niki, H., Ogura, T., Kato, A., and Hiraga, S. (1989). Purification and characterization of SopA and SopB proteins essential for F plasmid partitioning. *J. Biol. Chem.* *264*, 15535-15541.
- Moriya, S., Tsujikawa, E., Hassan, A. K. M., Asai, K., Kodama, T., and Ogasawara, N. (1998). A *Bacillus subtilis* gene-encoding protein homologous to eukaryotic SMC motor protein is necessary for chromosome partition. *Mol. Microbiol.* *29*, 179-187.
- Motallebi-Veshareh, M., Rouch, D. A., and Thomas, C. M. (1990). A family of ATPases involved in active partitioning of diverse bacterial plasmids. *Mol. Microbiol.* *4*, 1455-1463.
- Mysliwiec, T. H., Errington, J., Vaidya, A. B., and Bramucci, M. G. (1991). The *Bacillus subtilis* *spoOJ* gene: evidence for involvement in catabolite repression of sporulation. *J. Bacteriol.* *173*, 1911-1919.
- Nakagawa, N., Masui, R., Kato, R., and Kuramitsu, S. (1997). Domain structure of *Thermus thermophilus* UvrB protein. *J. Biol. Chem.* *272*, 22703-22713.
- Neilson, L., Blakely, G., and Sherratt, D. J. (1999). Site-specific recombination at *dif* by *Haemophilus influenzae* XerC. *Mol. Microbiol.* *31*, 915-926.
- Niki, H., and Hiraga, S. (1997). Subcellular distribution of actively partitioning F plasmid during the cell division cycle in *E. coli*. *Cell* *90*, 951-957.
- Niki, H., and Hiraga, S. (1998). Polar localization of the replication origin and terminus in *Escherichia coli* nucleoids during chromosome partitioning. *Genes & Dev.* *12*, 1036-1045.
- Niki, H., Imamura, R., Kitaoka, M., Yamanaka, K., Ogura, T., and Hiraga, S. (1992). *E. coli* MukB protein involved in chromosome partition forms a homodimer with a rod-and-hinge structure having DNA binding and ATP/GTP binding activities. *EMBO J.* *11*, 5101-5109.
- Niki, H., Jaffe, A., Imamura, R., Ogura, T., and Hiraga, S. (1991). The new gene *mukB* codes for a 177 kd protein with coiled-coil domains involved in chromosome partitioning of *E. coli*. *EMBO J.* *10*, 183-193.
- Niki, H., Yamaichi, Y., and Hiraga, S. (2000). Dynamic organization of chromosomal DNA in *Escherichia coli*. *Genes & Dev.* *14*, 212-223.
- Nordstrom, K., and Austin, S. J. (1989). Mechanisms that contribute to the stable segregation of plasmids. *Annu. Rev. Genet.* *23*, 37-69.
- Ogasawara, N., and Yoshokawa, H. (1992). Genes and their organization in the replication origin region of the bacterial chromosome. *Mol. Microbiol.* *6*, 629-634.
- Pabo, C. O., and Sauer, R. T. (1992). Transcription factors: Structural families and principles of DNA recognition. *Annu. Rev. Biochem.* *61*, 1053-1095.

- Pal, S. K., and Chatteraj, D. K. (1988). P1 plasmid replication: initiator sequestration is inadequate to explain control by initiator binding sites. *J. Bacteriol.* *170*, 3554-3560.
- Pal, S. K., Mason, R. J., and Chatteraj, D. K. (1986). P1 plasmid replication. Role of initiator titration in copy number control. *J. Mol. Biol.* *192*, 275-285.
- Parsell, D. A., Silber, K. R., and Sauer, R. T. (1990). Carboxy-terminal determinants of intracellular protein degradation. *Genes & Dev.* *4*, 277-286.
- Pichoff, S., Benedikt, V., Touriol, C., and Bouche, J.-P. (1995). Deletion analysis of gene *minE* which encodes the topological specificity factor of cell division in *Escherichia coli*. *Mol. Microbiol.* *18*, 321-329.
- Prentki, P., Chandler, M., and Caro, L. (1977). Replication of the prophage P1 during the cell cycle of *Escherichia coli*. *Mol. Gen. Genet.* *152*, 71-76.
- Quisel, J. D., and Grossman, A. D. (2000). Control of sporulation gene expression in *Bacillus subtilis* by the chromosome partitioning proteins Soj (ParA) and Spo0J (ParB). *J. Bacteriol.* *182*, 3446-3451.
- Quisel, J. D., Lin, D. C.-H., and Grossman, A. D. (1999). Control of development by altered localization of a transcription factor in *B. subtilis*. *Mol. Cell* *4*, 665-672.
- Radnedge, L., Davis, M. A., and Austin, S. J. (1996). P1 and P7 plasmid partition: ParB protein bound to its partition site makes a separate discriminator contact with the DNA that determines species specificity. *EMBO J.* *15*, 1155-1162.
- Radnedge, L., Youngren, B., Davis, M., and Austin, S. (1998). Probing the structure of complex macromolecular interactions by homolog specificity scanning: the P1 and P7 plasmid partition systems. *EMBO J.* *17*, 6076-6085.
- Recchia, G. D., Aroyo, M., Wolf, D., Blakely, G., and Sherratt, D. J. (1999). FtsK-dependent and -independent pathways of Xer site-specific recombination. *EMBO J.* *18*, 5724-5734.
- Rees, W. A., Keller, R. W., Vesenska, J. P., Yang, G., and Bustamante, C. (1993). Evidence of DNA bending in transcription complexes imaged by scanning force microscopy. *Science* *260*, 1646-1649.
- Rice, P. A., Yang, S. W., Mizuuchi, K., and Nash, H. A. (1996). Crystal structure of an IHF-DNA complex: A protein-induced DNA u-turn. *Cell* *87*, 1295-1306.
- Robertson, C. A., and Nash, H. A. (1988). Bending of the bacteriophage λ attachment site by *Escherichia coli* integration host factor. *J. Biol. Chem.* *263*, 3554-3557.

- Rodionov, O., Lobočka, M., and Yarmolinsky, M. (1999). Silencing of genes flanking the P1 plasmid centromere. *Science* 283, 546-549.
- Rost, B., and Sander, C. (1993). Prediction of protein secondary structure at better than 70% accuracy. *J. Mol. Biol.* 232, 584-599.
- Rost, B., and Sander, C. (1994). Combining evolutionary information and neural networks to predict protein secondary structure. *Proteins* 19, 55-77.
- Saleh, A. Z. M., Yamanaka, K., Niki, H., Ogura, T., Yamazoe, M., and Hiraga, S. (1996). Carboxyl terminal region of the MukB protein in *Escherichia coli* is essential for DNA binding activity. *FEMS Microbiol. Lett.* 143, 211-216.
- Sambrook, J., Fritsch, E. F., and Maniatis, T. (1989). *Molecular Cloning: a Laboratory Manual*, Second edition Edition (Cold Spring Harbor, NY: Cold Spring Harbor Laboratory Press).
- Sawitzke, J. A., and Austin, S. (2000). Suppression of chromosome segregation defects of *Escherichia coli muk* mutants by mutations in topoisomerase I. *Proc. Natl. Acad. Sci. USA* 97, 1671-1676.
- Sedgewick, S. G., Taylor, I. A., Adam, A. C., Spanos, A., Howell, S., Morgan, B. A., Treiber, M. K., Kanuga, N., Banks, G. R., Foord, R., and Smerdon, S. J. (1998). Structural and functional architecture of the yeast cell-cycle transcription factor Swi6. *J. Mol. Biol.* 281, 763-775.
- Sharpe, M. E., and Errington, J. (1996). The *Bacillus subtilis soj-spoOJ* locus is required for a centromere-like function involved in prespore chromosome partitioning. *Mol. Microbiol.* 21, 501-509.
- Slater, S., Wold, S., Lu, M., Boye, E., Skarstad, K., and Kleckner, N. (1995). *E. coli* SeqA protein binds *oriC* in two different methyl-modulated reactions appropriate to its roles in DNA replication initiation and origin sequestration. *Cell* 82, 927-936.
- Spolar, R. S., and Record, M. T. (1994). Coupling of local folding to site-specific binding of proteins to DNA. *Science* 263, 777-784.
- Steiner, W., Liu, G., Donachie, W. D., and Kuempel, P. (1999). The cytoplasmic domain of FtsK protein is required for resolution of chromosome dimers. *Mol. Microbiol.* 31, 579-583.
- Strauss, P. R., and Holt, C. M. (1998). Domain mapping of human apurinic/apyrimidinic endonuclease. *J. Biol. Chem.* 273, 14435-14441.
- Studier, F. W., and Moffatt, B. A. (1986). Use of bacteriophage T7 RNA polymerase to direct selective high-level expression of cloned genes. *J. Mol. Biol.* 189, 113-130.

- Surtees, J. A. (1996). Search for host factors involved in P1 plasmid partition and characterization of ParB-ParB interactions using the yeast two-hybrid system. In *Molecular and Medical Genetics* (Toronto: University of Toronto), pp. 101.
- Surtees, J. A., and Funnell, B. E. (1999). P1 ParB domain structure includes two independent multimerization domains. *J. Bacteriol.* *181*, 5898-5908.
- Tasayco, M. L., and Carey, J. (1992). Ordered self-assembly of polypeptide fragments to form native-like dimeric *trp* repressor. *Science* *255*, 594-597.
- Thisted, T., and Gerdes, K. (1992). Mechanism of post-segregational killing by the *hok/sok* system of plasmid R1. Sok antisense RNA regulates *hok* gene expression indirectly through overlapping *mok* gene. *J. Mol. Biol.* *223*, 41-54.
- Thisted, T., Sorensen, N. S., Wagner, E. G., and Gerdes, K. (1994). Mechanism of post-segregational killing: Sok antisense RNA interacts with Hok mRNA via its 5'-end single-stranded leader and competes with the 3'-end of Hok mRNA for binding to the *mok* translational initiation region. *EMBO J.* *13*, 1960-1968.
- Thompson, J. F., and Landy, A. (1988). Empirical estimation of protein-induced DNA bending angles: applications to λ site-specific recombination complexes. *Nucl. Acids Res.* *16*, 9687-9705.
- Ullsperger, C., and Cozzarelli, N. R. (1996). Contrasting activities of topoisomerase IV and DNA gyrase from *Escherichia coli*. *J. Biol. Chem.* *271*, 31549-31555.
- Vale, R. D., and Goldstein, L. S. B. (1990). One motor, many tails: An expanding repertoire of force-generating enzymes. *Cell* *60*, 883-885.
- van Helvoort, J. M. L. M., and Woldringh, C. L. (1994). Nucleoid partitioning in *Escherichia coli* during steady-state growth and upon recovery from chloramphenicol treatment. *Mol. Microbiol.* *13*, 577-583.
- Walker, J. E., Saraste, M., Runswick, M. J., and Gay, N. J. (1982). Distantly related sequences in the alpha and beta-subunits of ATP synthase, myosin, kinases and other ATP-requiring enzymes and a common nucleotide binding fold. *EMBO J.* *1*, 945-951.
- Wang, X., Hiand, J., Mukherjee, A., Cao, C., and Lutkenhaus, J. (1997). Analysis of the interaction of FtsZ with itself, GTP and FtsA. *J. Bacteriol.* *179*, 5551-5559.
- Watanabe, E., Wachi, M., Yamasaki, M., and Nagai, K. (1992). ATPase activity of SopA, a protein essential for active partitioning of F-plasmid. *Mol. Gen. Genet.* *234*, 346-352.
- Webb, C. D., Graumann, P. L., Kahana, J. A., Teleman, A. A., Silver, P. A., and Losick, R. (1998). Use of time-lapse microscopy to visualize rapid movement of the replication origin

- region of the chromosome during the cell cycle in *Bacillus subtilis*. *Mol. Microbiol.* 28, 883-892.
- Webb, C. D., Teleman, A., Gordon, S., Straight, A., Belmont, A., Lin, D. C.-H., Grossman, A. D., Wright, A., and Losick, R. (1997). Bipolar localization of the replication origin regions of chromosomes in vegetative and sporulating cells of *B. subtilis*. *Cell* 88, 667-674.
- Williams, D. R., and Thomas, C. M. (1992). Active partitioning of bacterial chromosomes. *J. Gen. Microbiol.* 138, 1-16.
- Wyman, C., Rombel, I., North, A. K., Bustamante, C., and Kustu, S. (1997). Unusual oligomerization required for activity of NtrC, a bacterial enhancer-binding protein. *Science* 275, 1658-1661.
- Xu, D. (1995). Searching for high-copy-number suppressors of a *E. coli* growth defect caused by the excess of a plasmid partition protein. In *Molecular and Medical Genetics* (Toronto: University of Toronto), pp. 70.
- Yamanaka, K., Mitani, T., Ogura, T., Niki, H., and Hiraga, S. (1994). Cloning, sequencing, and characterization of multicopy suppressors of a *mukB* mutation in *Escherichia coli*. *Mol. Microbiol.* 13, 301-312.
- Yamanaka, K., Ogura, T., Niki, H., and Hiraga, S. (1996). Identification of two new genes, *mukE* and *mukF*, involved in chromosome partitioning in *Escherichia coli*. *Mol. Gen. Genet.* 250, 241-251.
- Yamazoe, M., Onogi, T., Sunako, Y., Niki, H., Yamanaka, K., Ichimura, T., and Hiraga, S. (1999). Complex formation of MukB, MukE and MukF proteins involved in chromosome partitioning in *Escherichia coli*. *EMBO J.* 18, 5873-5884.
- Yang, C.-C., and Nash, H. A. (1989). The interaction of *E. coli* IHF protein with its specific binding sites. *Cell* 57, 869-880.
- Youngren, B., and Austin, S. (1997). Altered ParA partition proteins of plasmid P1 act via the partition site to block plasmid propagation. *Mol. Microbiol.* 25, 1023-1030.
- Youngren, B., Radnedge, L., Hu, P., Garcia, E., and Austin, S. (2000). A plasmid partition system of the P1-P7*par* family from the pMT1 virulence plasmid of *Yersinia pestis*. *J. Bacteriol.* 182, 3924-3928.
- Zechiedrich, E. L., and Cozzarelli, N. R. (1995). Roles of topoisomerase IV and DNA gyrase in DNA unlinking during replication in *Escherichia coli*. *Genes & Dev.* 9, 2859-2869.
- Zelicof, A., Protopopov, V., David, D., Lin, X.-Y., Lustgarten, V., and Gerst, J. E. (1996). Two separate functions are encoded by the carboxyl-terminal domains of the yeast cyclase-associated protein and its mammalian homologs. *J. Biol. Chem.* 271, 18243-18252.